Novel [11C]CO2 radiolabelling methodologies for PET neuroimaging

Haji Dheere, Abdul Karim

Awarding institution:
King's College London

Novel [^{11}C]CO_2 radiolabelling methodologies for PET neuroimaging

Abdul Karim Haji Dheere

A thesis submitted in partial fulfilment of the requirements for the degree of Doctor of Philosophy

Supervisor: Prof. Antony Gee

Division of Imaging Sciences and Biomedical Engineering
King's College London
February 2015

Abstract

PET is a non-invasive molecular imaging technique that is increasingly being used for medical imaging and drug development. Carbon-11 (^{11}C; half-life 20.4 min) is one of the most commonly used radionuclides for PET molecular imaging. ^{11}C is usually produced in the form of [^{11}C]CO_2 and converted into more reactive secondary precursors such as [^{11}C]methyl iodide and [^{11}C]carbon monoxide for radiolabelling. Although such secondary precursors are undoubtedly useful, given the short half-life of ^{11}C, it would be advantageous to use [^{11}C]CO_2 directly from the cyclotron without additional time-consuming processing. Therefore, the development of radiochemical methods to efficiently radiolabel compounds directly with [^{11}C]CO_2 for applications in PET neuroimaging is an important goal and is the focus of this thesis.

This work includes the development of novel radiolabelling methodology utilising [^{11}C]CO_2 for the radiolabelling of molecules based on urea and carbamate scaffolds. These functional groups are found in a plethora of biologically active molecules and pharmaceuticals. As proof of concept, the utility of the developed radiochemistry methods were applied to the synthesis of novel GABA and glutamate radiotracers.

GABA and glutamate are major excitatory and inhibitory neurotransmitters in the brain. Although implicated in many diseases, the *in vivo* function of these neurotransmitter system is poorly understood. Their dysfunction are implicated in pathologies such as addiction, Alzheimer's disease, Parkinson's disease and autism. Monitoring the expression of the receptors *in vivo* and *in vitro* would enable better understanding of these diseases, their progression and treatment.

The research described in this thesis unveils new methods to radiolabel novel molecules for these targets with ^{11}C thereby enabling more opportunities to study them *in vitro* using autoradiography and *in vivo* using PET molecular imaging.

Abbreviations

µmol	micromole
$[^{11}C]CO_2$	carbon-11 carbon dioxide
$[^{11}C]CH_3OTf$	carbon-11 methyl trifluoromethansulfonate
BEMP	2-*tert*-butylimino-2-diethylamino-1,3-dimethylperhydro-1,3,2 diazaphosphorine
DBU	1,8-diazabicyclo[5.4.0]undec-7-ene
BGO	bismuth germinate
RCC	radiochemical conversion
CHI	chromatography hydrophobicity index
CHI_IAM	immobilised artificial membrane
CH_3CN	acetonitrile
CNS	central nervous system
CT	computer technology
DBAD	di-*tert*-butyl azodicarboxylate
DIAD	diisopropyl azodicarboxylate
DMF	dimethylformamide
DMSO	dimethyl sulfoxide
EOB	end of bombardment
EOS	end of synthesis
FDG	fluorodeoxyglucose
GABA	gamma Aminobutyric acid

GBq	gigabecquerels
HPLC	high-performance liquid chromatography
Hz	hertz
IC_{50}	the half maximal inhibitory concentration
IR	infrared
KeV	kiloelectron volts
Log P	partition coefficient
LSO	lutetium oxyorthosilicate
LYSO	lutetium-yttrium oxyorthosilicate
mg	milligrams
mGluR1	metabotropic glutamate receptor 1
mL	milliliter
MPa	megapascal
MRI	magnetic resonance imaging
nmol	nanomole
NMR	nuclear magnetic resonance
s	singlet
d	doublet
dd	doublet of doublets
t	triplet
^{1}H	proton-1

^{13}C	carbon-13
NSB	non-specific binding
PBu_3	tributylphosphine
PET	positron emitting tomography
$POCl_3$	phosphoryl chloride
ppm	parts per million
PPh_3	triphenylphosphine
R	organyl group
RCP	radiochemical purity
RCY	radiochemical yield
SA	specific activity
SPE	solid phase extraction
$T_{1/2}$	half-life
TBAI	tetrabutylammonium iodide
UV	ultraviolet
THF	tetrahydrofuran

Acknowledgments

I would like to begin by expressing my sincerest gratitude to Tony Gee for his supervision and encouragement. When I joined the Gee group as an MSc student 4 years ago, my knowledge of PET chemistry was minimal and now, I am able to write a thesis. Without Tony's support and contribution, this project would not have been possible.

I would like to take this opportunity to particularly thank Chloe Child, Rosie Henderson, Salvatore Bongarzone and Yolanda Hill for their unwavering support and assistance which has truly been invaluable. Cinzia, Julia, Ran and the rest of the KCL Imaging Science department have also contributed towards the writing this thesis by providing me with the right amount of social support.

I can't think of words that are strong enough to describe how grateful I am to my parents. Their consistent check-up on my welfare especially during the thesis write-up period and their regular consultation has definitely contributed towards the successful completion of this thesis, thank you.

In addition I would like to acknowledge EPSRC for their financial support in funding this project; as well as Kings' College University of London and St. Thomas' Hospital PET Centre for providing me with an enjoyable and pleasant environment in which to carry out my project.

Finally, thanks to you, reader. If you are reading this, you at least read a part of my thesis. Thank You!

Table of Contents

Abstract....1

Abbreviations....2

Acknowledgements....5

List of publications....11

Chapter 1: introduction....12

1.1 Positron Emission Tomography....13

1.2 PET applications....16

1.2.1 Disease diagnosis and progression....16

1.2.2 Drug development....17

1.2.3 Medical research....18

1.3 Radiotracers....19

1.4 Radionuclide production....20

1.5 Carbon-11....23

1.6 Summary....28

1.7 Aims and objectives....29

1.8 References....30

Chapter 2: [^{11}C]Ureas....33

2.1 Background:....34

2.1.1 Synthesis of urea *via* isocyanates....34

2.1.2 Synthesis of ureas from carbon monoxide....35

2.1.3 Synthesis of ureas from carbon dioxide....37

2.1.4 Synthesis of [^{11}C]urea *via* [^{11}C]Phosgenes....41

2.1.5 Synthesis of [^{11}C]urea *via* [^{11}C]carbon monoxide 42
2.1.6 Synthesis of [^{11}C]urea *via* [^{11}C]carbon dioxide 46
2.1.7 Summary.....50
2.2 Aim.....51
2.2 Results and discussion – Asymmetrical [^{11}C]ureas 51
2.3.1 Solvent optimisation 51
2.3.2 Mitsunobu reagents optimisation.....53
2.3.3 Temperature and reaction time optimisation. 54
2.3.4 Radiolabelling of aliphatic, aromatic and benzylic amines.....55
2.3.5 Summary.....58
2.4 Results and discussion – Symmetrical [^{11}C]ureas. 58
2.4.1 Trapping agent, solvent and base optimisation. 59
2.4.2 Temperature and concentration optimisation. 60
2.4.3 Radiolabelling of various [^{11}C]symmetrical ureas. 61
2.4.4 Reaction mechanism:.....63
2.4.5 Trapping of CO_2. 63
2.4.6 Proposed trapping mechanism.....64
2.4.7 Mitsunobu reaction mechanism.....64
2.5 Conclusion 65
2.6 Methods.....67
2.6.1 General synthesis.....67
2.6.2 Synthesis of reference compounds 68
2.6.3 [^{11}C]CO_2 Trapping 70
2.6.4 General radiolabelling procedure 71
2.7 References 72

Chapter 3: [^{11}C]Carbamates and [^{11}C]Carbonates 74

3.1 Introduction 75

3.1.1 Synthesis of carbamates *via* isocyanates 75

3.1.2 Synthesis of carbamates *via* carbon monoxide 76

3.1.3 Synthesis of carbamates *via* carbon dioxide 79

3.1.4 Synthesis of carbonates 81

3.1.5 Synthesis of carbamates and carbonates *via* CO_2 83

3.1.6 Synthesis of [^{11}C]carbonates and [^{11}C]carbamates *via* the Grignard reaction 84

3.1.7 Synthesis of [^{11}C]carbamates *via* [^{11}C]phosgenes 86

3.1.8 Synthesis of [^{11}C]carbamates *via* [^{11}C]carbon monoxide 87

3.1.9 Synthesis of [^{11}C]carbamates *via* [^{11}C]carbon dioxide 89

3.1.10 Synthesis of [^{11}C]carbonates 95

3.1.11 Summary 95

3.2 Results and Discussion 96

3.2.1 Base optimisation 96

3.2.2 Solvent, temperature and time optimisation 98

3.2.3 Concentration optimisation 100

3.2.4 HPLC analysis 101

3.2.5 Reaction mechanism 102

3.2.6 Synthesis of [^{11}C]carbamates 103

3.2.7 Synthesis of [^{11}C]carbonates 103

3.2.8 Summary 104

3.2.9 Method 2 105

3.3 Conclusion 109

3.4 Method 110
3.4.1 General 110
3.4.2 Synthesis of reference compounds 111
3.4.3 Radiolabelling procedure 112
3.5 References 114

Chapter 4: Radiotracer Development 117

4.1 Introduction 118
4.1.1 CNS radiotracer development 118
4.1.2 Low non-specific binding and lipophilicity 119
4.1.3 Ease of radiolabelling 122
4.1.4 High binding potential 122
4.1.5 Tissue permeability 123
4.1.6 Metabolism 123
4.1.7 Glutamate receptors 124
4.1.8 mGluR1 radiotracers 124
4.1.8 ^{11}C radiolabelled mGluR1 radiotracers 125
4.1.8 Summary 131
4.2 Aims 131
4.3 Development of mGluR1 radiotracer 132
4.3.1 Synthesis of compound 1 133
4.3.2 Synthesis of compound 15 137
4.3.3 The Partition Coefficient. 140
4.3.4 Radiosynthesis 143
4.4 Conclusion 147

4.5 Method 148
4.5.1 Synthesis of reference compounds 149
4.5.1 Lipophilicity 157
4.5.2 General radiolabelling procedure 158
4.6 References 161

Chapter 5: Conclusion and future work 164

5.1 Conclusions 165
5.2 Future work 168
5.2.1 mGluR1 radiotracer development 168
5.2.2 [^{11}C]CO_2 method development 172
5.3 References 172

List of publications:

Rapid and efficient synthesis of [^{11}C]ureas via *the incorporation of [^{11}C]CO_2 into aliphatic and aromatic amines.*

Abdul Karim Haji Dheere, Nadia Yusuf and Antony Gee.

Chem. Commun., 2013, **49**, 8193.

Novel [^{11}C]CO_2 Strategy For the Radio-synthesis of [^{11}C]Carbamates and [^{11}C]Carbonates.

Abdul Karim Haji Dheere, Dinah Shakir and Antony Gee.

Submitted.

Synthesis of ^{11}C-Labelled Symmetrical Ureas via the Rapid Incorporation of [^{11}C]CO_2 into Aliphatic and Aromatic Amines.

Abdul Karim Haji Dheere, Carlotta Taddei, Ran Yan, and Antony Gee.

Submitted.

Conference abstract publications:

Rapid incorporation of [^{11}C]CO_2 into [^{11}C]carbamates and [^{11}C]carbonates.

Abdul Karim Haji Dheere and Antony Gee.

J. Label. Compd. Radiopharm., 2013, 56, S17.

Novel methodology to incorporate [^{11}C]CO_2 into aliphatic and aromatic ureas.

Abdul Karim Haji Dheere and Antony Gee.

J. Label. Compd. Radiopharm., 2013, 56, P003.

Chapter 1

Introduction

1 Introduction

1.1 Positron Emission Tomography (PET)

PET is a molecular imaging technique that provides quantitative and functional data on physiological processes using molecules labelled with positron-emitting radionuclides (often referred to as radiopharmaceuticals or radiotracers).[1] The use of PET has dramatically increased in the last decade due to the high sensitivity of the technique, making it ideal for *in vivo* medical diagnosis, medical research and drug studies.[1] The ability of PET to carry out studies with tracer amounts of radiolabelled molecules enables its utility in *in vivo* research. Typically, less than 10 nmol of the radiotracer is administered to a patient, which allows highly potent and toxic compounds to be investigated in subjects without manifestation of pharmacological or toxicological effects.[2]

Positron-emitting radionuclides are inherently unstable due to their neutron deficiency. They revert to stable nuclei by emitting a positron and a neutrino. A positron is an antiparticle with an electric charge of +1e that annihilates with an electron to produce two high energy gamma rays capable of penetrating the body (Figure 1.1).[3]

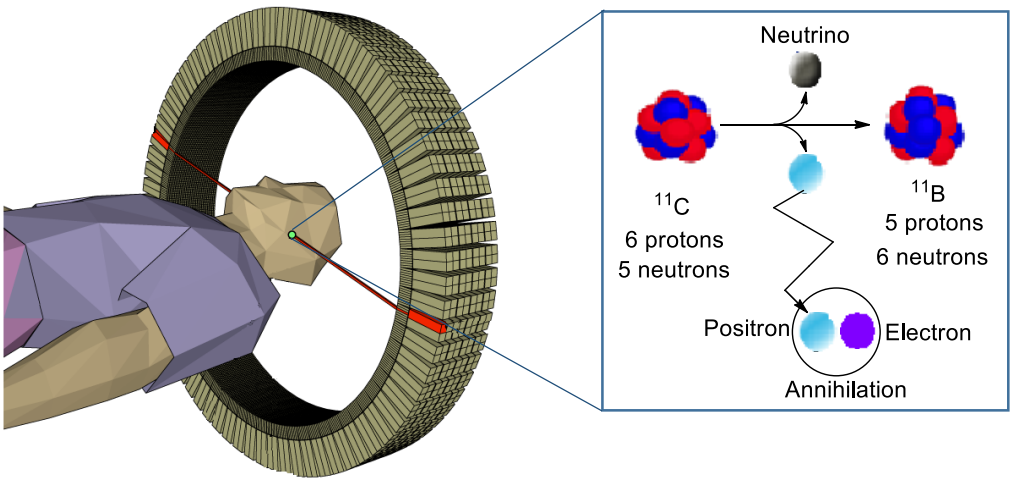

Figure 1.1 The process of positron decay and detection.

The annihilation process must satisfy the conservation laws, and as a result, a pair of gamma rays that travel in opposite directions with an energy of 511 keV are produced. The conservation laws the process must satisfy include the

conservation of electrical charge i.e. the net charge before and after must be zero, and the conservation of linear momentum and total energy (this forbids the creation of a single gamma ray, and results in slight non-collinearity of the two annihilation photons)).[4] The pair of gamma rays emitted are detected simultaneously by a ring of scintillation detectors surrounding the subject (PET scanner, Figure 1.1). Scintillators are materials that, when struck by particles such as gamma rays, they absorb the energy and re-emit in the form of light.[5] Good scintillators are transparent to their own scintillation light, and have a large light output that is proportional to the gamma ray energy. Materials, such as sodium iodide doped with thallium, bismuth germanate (BGO), lutetium oxyorthosilicate (LSO), and Lutetium-yttrium oxyorthosilicate (LYSO), display these properties.[6] Most new PET scanners have LSO/LYSO scintillators as they have faster and/or higher light output compared to other scintillators. The light emitted by the scintillators is usually detected by a photomultiplier (Figure 1.2).[7]

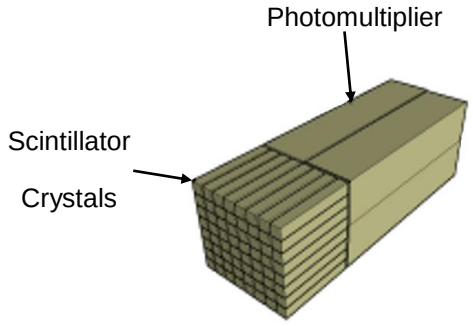

Figure 1.2 Schematic diagram of detector block.

A photomultiplier converts light into an electrical pulse and consists of a photocathode, a number of dynodes, and an anode. Firstly, the photocathode converts the light produced by the scintillators into electrons. The electrons are pulled towards a series of dynodes that in turn, multiply the number of electrons that strike them, amplifying the original signal.[8] An anode collects the electrons to produce an electronic pulse (Figure 1.3).[3]

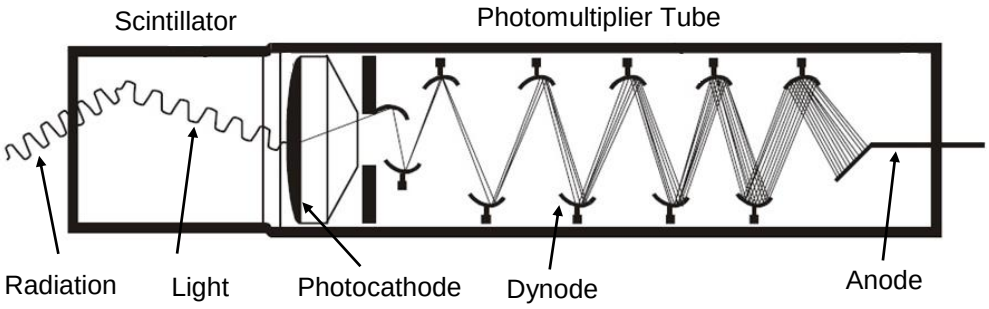

Figure 1.3 Schematic diagram of the detector block.

The electronic pulse from these detectors are deemed to be coincident if they occur within a short time interval. A coincident event joins the two relevant detectors together to assign a line of response that provides positional information from the detected radiation (Figure 1.4). The multiple coincident events and the resulting lines of response enable the creation of a map of *in vivo* regional radioactivity concentrations and dynamics (i.e. PET image).

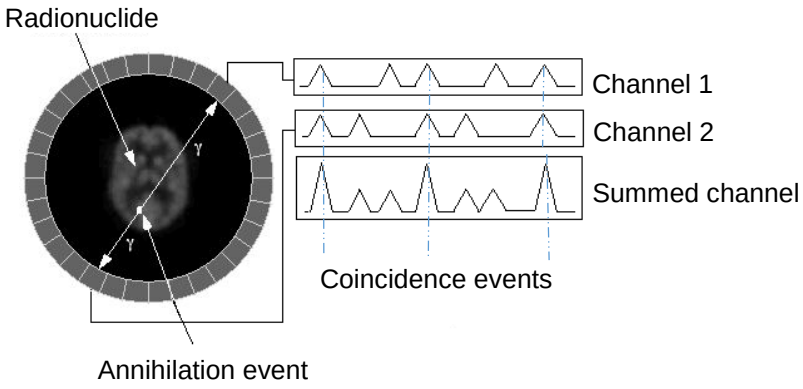

Figure 1.4 Coincidence detection in a PET scanner.

1.2 PET Applications

There are three particularly important areas in which the application of PET is becoming increasingly used: disease diagnosis and progression, drug development and medical research.

1.2.1 Disease diagnosis and progression

PET is used as a tool to help understand the molecular basis of diseases, particularly in neuroscience, cardiology and oncology.[9] A range of carbon-11 (^{11}C) and fluorine-18 (^{18}F) radiotracers have been developed to image receptors, transporters and metabolic processes *in vivo*.[10] The most common radiotracer for medical diagnosis is the ^{18}F-labelled glucose analogue, [^{18}F]fluorodeoxyglucose (FDG).[11] Although the hydroxyl group on the 2–carbon of a glucose molecule is replaced by a fluorine atom, [^{18}F]FDG enters living cells *via* facilitated transport in a similar manner to glucose. [^{18}F]FDG can be synthesised by either nucleophilic or electrophilic fluorination reactions.[12] Nucleophilic fluorination using tetra-*O*-acetyl-mannose triflate as a precursor is the most widely used [^{18}F]FDG synthesis method due to high yields and a short synthesis time (Scheme 1.1).[12] The stereoselective nucleophilic fluorination reaction involves the substitution of the trifluoromethanesulphonate (OTf) group with a nucleophilic fluoride-18 anion in an S_N2 reaction.

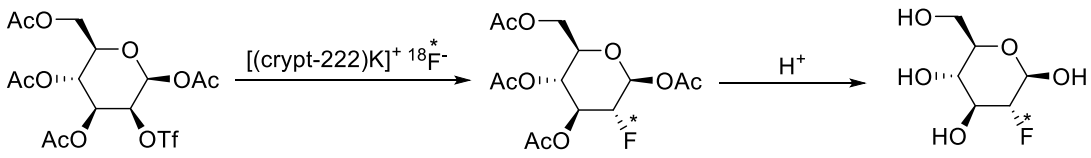

Scheme 1.1 Synthesis of [^{18}F]FDG from tetra-*O*-acetyl-mannose triflate.[12]

Following intravenous administration, [^{18}F]FDG is rapidly distributed to all organs. Inside the cell, [^{18}F]FDG is phosphorylated by hexokinase to [^{18}F]FDG-6-phosphate but unlike glucose, [^{18}F]FDG-6-phosphate is not further metabolised. This is due to the replacement of the 2–carbon hydroxyl group with ^{18}F that makes the tracer a non-substrate for the subsequent glycolysis pathway. As a result, the

^{18}F-labelled tracer accumulates within the cell and can be detected by PET. Regions of increased uptake of [^{18}F]FDG reflects elevated glucose transport and metabolism.[12]

Many cancer cells have enhanced glucose transport and metabolism which is reflected by a high uptake and accumulation of [^{18}F]FDG in these cells. Consequently, the radiotracer has numerous clinical applications such as tumour localisation, cancer staging and determining tumour response to therapy.[1]

1.2.2 Drug Development

Drug development is a lengthy and costly process with a high attrition rate. PET is being increasingly used in the selection of novel therapeutics to reduce the costs and risks associated with drug development.[13] One of the most valuable contributions that PET offers in drug development is providing enough data to establish whether a test-compound is suitable as a drug candidate in the early stages of the drug discovery process. PET can confirm whether a promising compound interacts with a drug target of interest or if it reaches the target organ in sufficient concentrations.[14] Consequently, biodistribution and drug-receptor occupancy studies are being increasingly utilised by the pharmaceutical industry, particularly in organs where it is difficult to perform biopsies to determine drug concentrations (for example, the brain).[14]

A traditional assumption in drug development has been that the concentration of a novel drug candidate in tissue is similar to that measured in the blood. However, this assumption is known to be untrue for many drugs. An error in the assumption of tissue-drug concentrations could lead to an overdosing or underdosing of the drug. PET can be used to determine both the blood/plasma and target tissue concentrations of the labelled drug candidate allowing more efficient drug dosing paradigms. Moreover, PET can also determine if sufficient concentrations of the therapeutics are attained in the organ of interest.

After a drug candidate is radiolabeled (isotopic labelling) and administrated, PET scans can demonstrate its presence in organs such as the brain, confirming blood-brain-barrier penetration.[15][16]

Receptor occupancy is another parameter in which PET is greatly utilised during the early stages of drug development.[17] Receptor occupancy refers to the percentage of a receptor population that is occupied by the drug at a specified dose or concentration in plasma.[18] The importance of determining the receptor occupancy has been elegantly demonstrated by PET studies of antipsychotic drugs acting on dopamine D2 receptors.[19] Side effects were observed at a D2 receptor occupancy higher than 80 %, increasing the incidence of extrapyramidal symptoms. However using PET, it was demonstrated that the drug-induced side effects could be avoided by reducing the D2 receptor occupancy to 65 – 80 % while retaining the beneficial anti-psychotic effect.[19]

1.2.3 Medical research

The function and expression of receptors, enzymes, transporters and other proteins are often altered in disease states and PET can help to identify them.[8] The ability of PET to monitor radiotracers that interact with proteins involved in diseases has provided a unique tool for medical research. Alzheimer's disease is one of the main diseases in which PET is being extensively utilised. Amyloid plaques and neurofibrillary tangles are pathological markers found in Alzheimer's disease brains. It is thought that these plaques are present as many as 10 years before Alzheimer's clinical symptoms appear. In the last few decades, PET radiotracers that bind to amyloid plaques have been developed (Figure 1.5).[20] Subjects with Alzheimer's disease showed a two fold increase in the retention of the amyloid PET tracer [^{11}C]PIB compared to control subjects.[21]

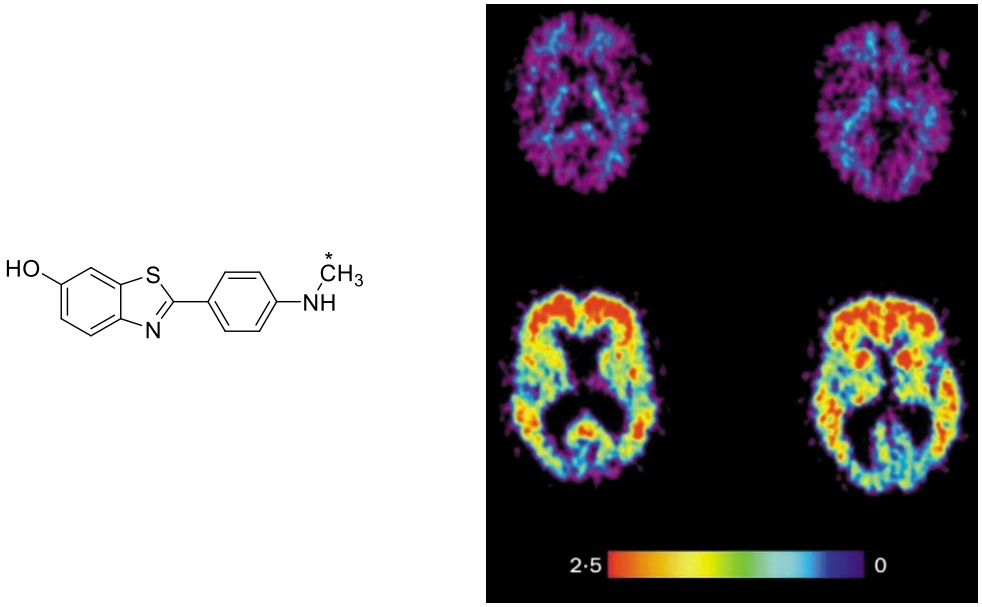

Figure 1.5 The chemical structure of [^{11}C]PIB and PET scans showing the retention of [^{11}C]PIB in the brain. Images from two control individuals are shown in the top row while bottom row shows the corresponding images from Alzheimer disease individuals. The scale bar indicates the relative levels of PIB standardised uptake values.[20]

In addition to its application in the neurosciences,[22] PET is also being actively utilised in cardiology[23] and oncology[24] research.

1.3 Radiotracers

Enzymes, receptors and metabolic substrates are some of the many biological targets/ processes that can be potentially imaged using PET.[15] To image these biological processes, a successful radiotracer that has a high signal-to-noise ratio *in vivo* must be established. There are many similarities between drug and radiotracer development, as well as many differences. In drug development, drug candidates fail for various reasons including low bioavailability, toxicology and inappropriate therapeutic windows. These are not challenges encountered when developing a radiotracer as the tracers are usually administrated intravenously in high specific activities. Specific activity is defined as the amount of radioactivity per mole of compound (GBq/µmol).[1] Radiotracers that bind to specific receptors present in finite concentrations are required to have a high specific activity, typically in the range of 50 – 500 GBq/µmol to ensure that the receptors are not

saturated. A radiotracer with a high specific activity (i.e. that does not saturate receptors) enables it to be studied in a subject without perturbing the biological system. Another challenge encountered in radiosynthesis with short-lived radionuclides is the reaction time. Whilst with traditional chemistry, the synthesis time of a drug-like molecule can range from minutes to a few days, radiolabelling reactions are generally short. Rapid and efficient purification methods are also required. Purification of radiolabelled compounds is usually performed using solid-phase extraction or semi-preparative HPLC equipped with UV and radio detectors.

1.4 Radionuclide production

The synthesis of radiotracers for PET starts with the production of the radionuclides. Cyclotrons are used to produce the majority of PET radionuclides.[25] A cyclotron is a particle accelerator invented by E. Lawrence in 1932. It functions by using a high frequency alternating voltage that is applied between two metal electrodes called “dees”. The two dees are placed in a vacuum facing each other with a narrow gap in-between (Figure 1.6). Charged particles are ejected into the centre of the gap and accelerated from the centre into the dees. A large electromagnet is located above and below the two dees which cause the particle’s path to bend in a spiral as they travel.[8]

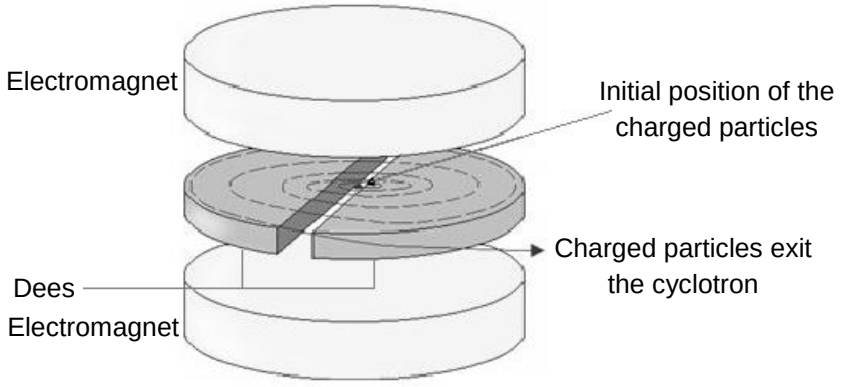

Figure 1.6 Schematic diagram of the cyclotron.

Each time the particle passes though the gap between the dees, the polarity of the alternating radiofrequency voltage reverses, accelerating the particle into the opposite dee. As a result, particles complete one circuit per frequency cycle. When the particles reach the edge of the cyclotron, they are steered out of the cyclotron toward the target where the radionuclide is to be produced. Negative-ion cyclotrons are most commonly used, due to their higher efficiency and reduced cyclotron activation. The accelerated particles in these cyclotrons are negatively charged ions (e.g. H atom with 2 electrons). When the negatively charged ions reach the end of their path, they pass through a thin carbon foil which removes electrons, leaving positively charged protons. The change of charge causes the movement of the particles to revert and travel in the opposite direction. As a result, the positively charged proton is steered out of the cyclotron to hit a target containing the material to be bombarded to produce the product PET radionuclide.[8]

The characteristics of some common positron-emitting radionuclides are shown in Table 1.1. ^{11}C is prepared by the proton bombardment of nitrogen-14 gas, fragmenting to ^{11}C and an α-particle. Similarly, ^{13}N and α-particles are produced by the cyclotron bombardment of accelerated protons onto an oxygen-16 target. ^{18}F can be produced by bombarding neon-20 (^{20}Ne) with deuterons or by bombarding ^{18}O with protons.[1, 25]

Table 1.1 The half-lives and nuclear reactions of positron-emitting radionuclides.

Radionuclide	Half-life (min)	Nuclear reaction
^{11}C	20.4	$^{14}N(p,\alpha)^{11}C$
^{13}N	9.97	$^{16}O(p,\alpha)^{13}N$
^{15}O	2.04	$^{15}N(d,n)^{15}O$
^{18}F	109.7	$^{18}O(p,n)^{18}F$ $^{20}Ne(d,\alpha)^{18}F$

These radionuclides have short half-lives and therefore must be produced at the point of use. Half-life in nuclear chemistry is the time required for half of the unstable radionuclides in a sample to undergo radioactive decay. Radioactive decay is a spontaneous process and it takes place in an exponential manner (Figure 1.7).

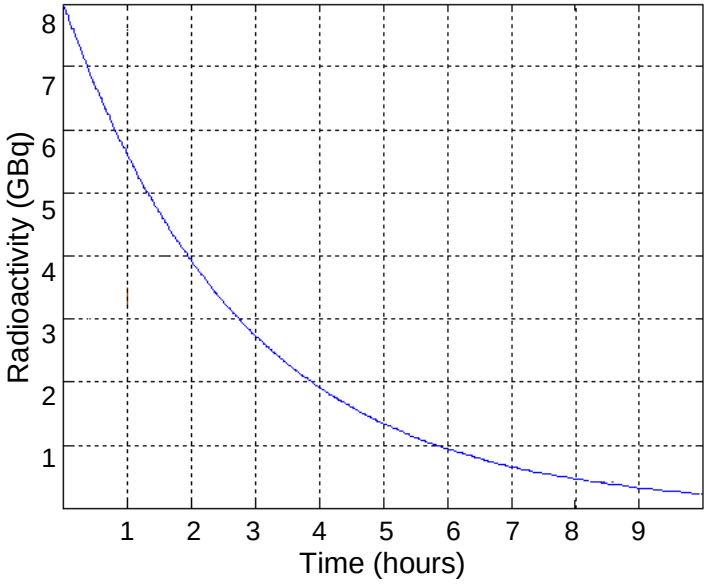

Figure 1.7 Exponential radioactivity decay curve showing a 2 hour half-life.

The number of atoms undergoing radioactive decay in a given time depends upon the number of radionuclides present at that time and the decay constant. The exponential decay process can be expressed by the differential equation (equation 1.1), where *N* is the quantity of the radionuclide, and λ is the exponential decay constant. The negative sign is inserted to indicate that *N* decreases with time.

$$\frac{dN}{dt} = -\lambda N$$

Equation 1.1 Differential equation expressing exponential decay in terms of the exponential decay constant.

Equation 1.1 can be integrated and rearranged to form equation 1.2, where *N(t)* is the quantity of the radionuclide at a given time *t*, N_0 is the quantity of the radionuclide at $t = 0$ and λ is the exponential decay constant.

$$N(t) = N_0 e^{-\lambda t}$$

Equation 1.2 The equation to determine the quantity of a radionuclide at a specific time *t*.

Half-life is defined as the time taken for the radioactivity of a radionuclide to decay to half of its original value and therefore, Nt/N_o becomes ½. To calculate the half-life, equation 1.2 can be simplified to become equation 1.3.

$$t_{1/2} = \frac{0.693}{\lambda}$$

Equation 1.3 The equation to determine half-life.

1.5 Carbon-11

^{11}C is one of the most commonly used PET radionuclides, with numerous radiotracers having been developed for imaging metabolic, enzymatic and receptor-mediated function *in vivo*.[26] The presence of carbon in all naturally occurring organic compounds makes ^{11}C an attractive positron emitter: substituting the naturally-abundant carbon-12 (^{12}C) in biologically active molecules with radioactive ^{11}C has no effect on the chemical and the biological activity of the molecule. Furthermore, the short half-life of ^{11}C ($t_{1/2}$ = 20.4 minutes) enables the collection of a sufficient amount of PET data while keeping the radiation dose to a minimum. It also permits repeated studies in the same subject on the same day.

^{11}C is produced by a cyclotron in the form of [^{11}C]carbon dioxide ([^{11}C]CO_2) or [^{11}C]methane ([^{11}C]CH_4).[25] These cyclotron-produced molecules are referred to as primary synthons. Generally, the primary synthons are converted into more reactive secondary synthons such as [^{11}C]methyl iodide ([^{11}C]CH_3I),[27] [^{11}C]methyl triflate ([^{11}C]CH_3OTf),[28] [^{11}C]carbon monoxide ([^{11}C]CO),[29] cyanide ([^{11}C]CN)[30] and phosgene ([^{11}C]$COCl_2$)[31] for further incorporation into a molecule of interest (Figure 1.8).

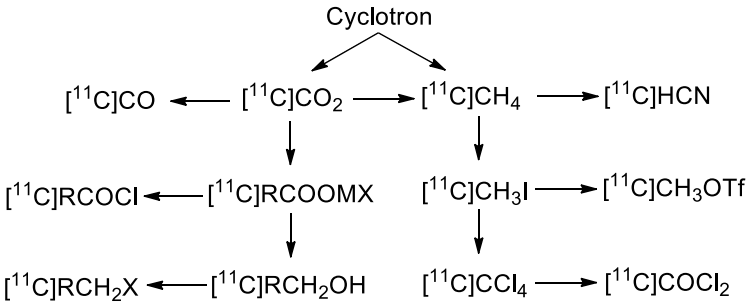

Figure 1.8 Some of the most common ^{11}C synthons.

There are a limited number of methods available that use $[^{11}C]CO_2$ directly for radiolabelling, mainly due to the chemical properties of CO_2.[32] CO_2 has an electron deficient central carbon and therefore acts as a weak electrophile. As a result, the molecule has an affinity for electron-donating reagents and nucleophiles.[33] However, due to the thermodynamic and kinetic stability of CO_2, the compound is poorly reactive. High pressures, high temperatures and catalysts (e.g. palladium) are required to activate the molecule and form a more reactive species.[34]

In traditional organic chemistry, CO_2 has been used to access compounds that contain carbonyl groups, a common structural element of biologically active molecules. Furthermore, CO_2 is widely available and therefore, it has become an attractive and challenging synthesis reagent. Various methods to incorporate stable CO_2 into target compounds have been established (Figure 1.9).[35]

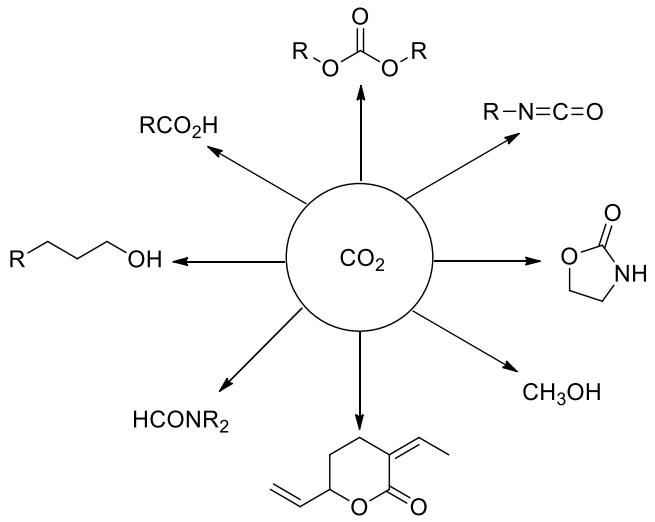

Figure 1.9 Chemical structures that can be synthesised using CO_2.[35]

The most notable of these is the Grignard reaction which involves the conversion of alkyl and aryl magnesium halides to carboxylic acids (Scheme 1.2).[36]

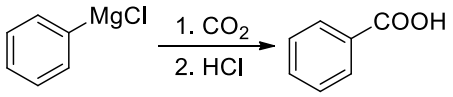

Scheme 1.2 The reaction between Grignard reagent and CO_2.

Other examples of reactions that use CO_2 for the synthesis of a target compound include the synthetic route proposed by Tran-Vu and Daugulis [37] (Scheme 1.3). The reaction incorporates CO_2 into aryl iodides sufficiently (> 50 %) by employing copper iodide/TMEDA in DMSO solvent for the synthesis of carboxylic acids.

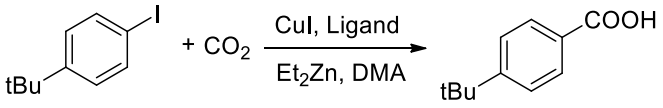

Scheme 1.3 Copper-mediated carboxylic acid synthesis *via* CO_2.[37]

Another method that uses CO_2 is reported by Tominaga *et al*.[38] The synthesis is catalysed by a Ruthenium (Ru) complex in an ionic liquid and converts alkenes into alcohols (Scheme 1.4).

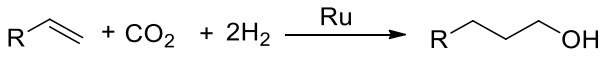

Scheme 1.4 Ruthenium-mediated alcohol synthesis *via* CO_2.[38]

A notable feature of this synthesis strategy is that it produces the target product with yields of over 70 %. However, high pressures (4.0 MPa) and temperatures (160 ^{o}C) are required.

The use of CO_2 in synthetic methods has increased over the last few years. Some examples of reactions that use CO_2 have been described above. Other reactions, particularly for the synthesis of ureas, carbamates and carbonates, will be discussed in chapter 2 and 3.[34b, 39]

1.5.1 [^{11}C]CO_2 method development

Generally, to develop a radiolabelling methodology, a traditional organic chemistry method is used as a starting point. However, when adapting the traditional method to a radiolabelling reaction, the radionuclide's half-life, reagent concentration and reaction time must be taken into account.

1. [^{11}C]CO_2 trapping: Before bubbling the [^{11}C]CO_2 into a reaction mixture, the gas is usually concentrated. There are two methods available to concentrate the [^{11}C]CO_2 that is released from the cyclotron target.[32] Cryogenic trapping consists of passing the produced gasses though a vessel cooled by liquid nitrogen. Condensable gases such as [^{11}C]CO_2 are trapped within the vessel while non-condensable gases are removed. The second method immobilises the [^{11}C]CO_2 on a solid material such as molecular sieves. The release of [^{11}C]CO_2 can be controlled thermodynamically and with a low carrier gas volume.[32]

2. Trapping reagents: Due to [^{11}C]CO_2 being produced in low concentrations and in a gaseous state, it has to be trapped within the reaction solution efficiently. To increase the trapping efficiency, a trapping reagent can be

added to the reaction mixture. DBU and BEMP have recently been developed as *in situ* [^{11}C]CO_2 trapping agents.[40]

Although traditional organic synthesis methodologies are used as a starting point when translating these methods for use in radiolabelling, the reactions require further optimisation i.e. the reaction is examined under different solvents, temperatures and concentrations. This is necessary because of the sub-stoichiometric concentration of ^{11}C used in a reaction. The [^{11}C]CO_2 radiolabelling reaction developed by Riss *et al.*[41] is an example of a radiolabelling methodology that used traditional organic chemistry as a starting point. The original organic chemistry reaction was established by Takaya *et al.*[42] The reaction incorporated CO_2 into organoboronic esters to form carboxylic acids. Optimum reaction conditions were obtained when CuI was used as catalyst, bisoxazoline was used as a ligand, CsF was used as a base and DMF as a solvent. The reaction mixture was heated at 90 ^{o}C for 10 hours (Scheme 1.5).

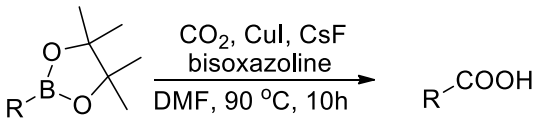

Scheme 1.5 The synthesis of carboxylic acids from boronic esters *via* CO_2.[42]

The analogous radiochemical synthesis also used CuI as a catalyst and DMF as a solvent (Scheme 1.6), however, additional reagents were required: Tetramethylethylenediamine (TMEDA) to obtain a high [^{11}C]CO_2 trapping efficiency, and potassium fluoride (KF) and 2.2.2-cryptand to increase the yield and the rate of reaction.[41]

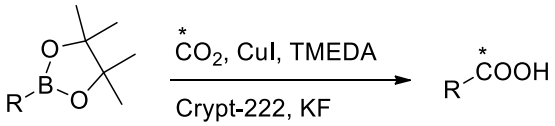

Scheme 1.6 The synthesis of [^{11}C]carboxylic acids from boronic esters *via* [^{11}C]CO_2.[41]

The reason for these modifications is that [^{11}C]CO_2 is used on a nanomolar (nmol) scale and at sub-stoichiometric concentrations while in traditional chemistry, the

CO_2 is used in excess. Other examples of traditional organic chemistry that has been translated to radiolabelling are discussed in Chapters 2 and 3.

Direct radiolabelling with [^{11}C]CO_2 has the potential advantage of avoiding the time-consuming production of secondary labelled synthons enabling the opportunity to radiolabel molecules of interest rapidly. However, the use of [^{11}C]CO_2 is limited by its stability. Further, radiolabelling with the primary synthon is prone to contamination from atmospheric CO_2.[32] Non-radioactive CO_2 competes with radioactive [^{11}C]CO_2 in labelling reactions potentially resulting in a low specific activity.

1.6 Summary

PET is a non-invasive molecular imaging technique that is used for medical diagnosis, medical research and drug development. ^{11}C is one of the most commonly used radionuclides and it is produced by a cyclotron in the form of [^{11}C]CO_2. The primary synthon is usually converted into other forms such as [^{11}C]CH_3I for incorporation into a molecule of interest. Further, [^{11}C]CO_2 is thermodynamically and kinetically stable which makes it unreactive and as a result, there are only a limited number of radiolabelling methods available that incorporates it directly into target compounds. Due to the half-life of ^{11}C, it is beneficial to incorporate the primary synthon directly. Recently, novel strategies that activate CO_2 and incorporate it into different structures have been developed.[40] These methods can be used as a starting point for developing rapid radiolabelling reactions. Developing novel [^{11}C]CO_2 reactions is of great interest as it would enable the radiolabelling of compounds that are not accessible by current radiolabelling strategies.

1.7 Aims

There are limited number of [^{11}C]CO_2 radiolabelling methodologies and therefore, the development of novel methods is of interest. Chapters 2 and 3 of this thesis focuses on the development of novel radiolabelling chemistries. This work includes the development of radiolabelling methodologies utilising [^{11}C]CO_2 for the radiolabelling of molecules based on urea and carbamate scaffolds. These functional groups are found in a plethora of biologically active molecules and pharmaceuticals. In chapter 4, the utility of the developed radiochemistry methods were applied to the synthesis of novel glutamate radiotracers. Glutamate receptors are major excitatory neurotransmitters in the brain. Although implicated in many diseases, the *in vivo* function of these neurotransmitter system is poorly understood. Their dysfunction are implicated in pathologies such as addiction, Alzheimer's disease, Parkinson's disease and autism. Monitoring the expression of the receptors *in vivo* and *in vitro* would enable better understanding of these diseases, their progression and treatment.

1.8 References

[1] P. W. Miller, N. J. Long, R. Vilar, A. D. Gee, *Angewandte Chemie International Edition* **2008**, *47*, 8998-9033.

[2] S. M. Ametamey, M. Honer, P. A. Schubiger, *Chemical Reviews* **2008**, *108*, 1501-1516.

[3] M. E. Phelps, *Proceedings of the National Academy of Sciences of the United States of America* **2000**, *97*, 9226-9233.

[4] D. Bailey, J. Karp, S. Surti, 1st edition, London, Springer, **2005**.

[5] A. Vandenbroucke, A. M. K. Foudray, P. D. Olcott, C. S. Levin, *Physics in Medicine and Biology* **2010**, *55*, 5895.

[6] R. A. Ramirez, W. Wai-Hoi, K. Soonseok, H. Baghaei, L. Hongdi, W. Yu, Z. Yuxuan, L. Shitao, L. Jiguo, in *Nuclear Science Symposium Conference Record, 2005 IEEE, Vol. 5*, **2005**, pp. 2835-2839.

[7] C. M. Pepin, P. Berard, A. L. Perrot, C. Pepin, D. Houde, R. Lecomte, C. L. Melcher, H. Dautet, *Nuclear Science, IEEE Transactions on* **2004**, *51*, 789-795.

[8] T. Theobald, C. B. Sampson, 4th edition, London, Pharmaceutical Press, **2011**.

[9] a) K. Herholz, W. D. Heiss, *Molecular Imaging and Biology* **2004**, *6*, 239-269; b) N. Oriuchi, T. Higuchi, T. Ishikita, M. Miyakubo, H. Hanaoka, Y. Iida, K. Endo, *Cancer Science* **2006**, *97*, 1291-1297.

[10] a) L. Cai, R. B. Innis, V. W. Pike, *Current Medicinal Chemistry* **2007**, *14*, 19-52; b) A. Nordberg, *The Lancet Neurology* **2004**, *3*, 519-527.

[11] P. Som, H. L. Atkins, D. Bandoypadhyay, J. S. Fowler, R. R. MacGregor, K. Matsui, Z. H. Oster, D. F. Sacker, C. Y. Shiue, H. Turner, C. N. Wan, A. P. Wolf, S. V. Zabinski, *Journal of Nuclear Medicine* **1980**, *21*, 670-675.

[12] S. Yu, *Biomedical Imaging and Intervention Journal* **2006**, *2*, e57.

[13] a) C. Halldin, B. Gulyás, L. Farde, in *From Morphological Imaging to Molecular Targeting, Vol. 48*, Springer Berlin Heidelberg, **2004**.

[14] A. D. Gee, *British Medical Bulletin* **2003**, *65*, 169-177.

[15] V. W. Pike, *Trends in pharmacological sciences* **2009**, *30*, 431-440.

[16] W. M. Pardridge, *NeuroRx* **2005**, *2*, 3-14.

[17] J. Passchier, A. Van Waarde, P. Doze, P. H. Elsinga, W. Vaalburg, *European Journal of Pharmacology* **2000**, *407*, 273-280.

[18] C. M. Lee, L. Farde, *Trends in Pharmacological Sciences* **2006**, *27*, 310-316.

[19] J. S. Fowler, N. D. Volkow, G. J. Wang, Y. S. Ding, S. L. Dewey, *Journal of Nuclear Medicine* **1999**, *40*, 1154-1163.

[20] A. Nordberg, *The Lancet Neurology* **2004**, *3*, 519-527.

[21] M. Politis, P. Piccini, *Journal of Neurology* **2012**, *259*, 1769-1780.

[22] a) A. Lingford-Hughes, A. G. Reid, J. Myers, A. Feeney, A. Hammers, L. G. Taylor, L. Rosso, F. Turkheimer, D. J. Brooks, P. Grasby, D. J. Nutt, *Journal of Psychopharmacology* **2012**, *26*, 273-281; b) D. S. Lee, S. K. Lee, M. C. Lee, *Journal of Korean Medical Science* **2001**, *16*, 689-696.

[23] M. Schwaiger, S. Ziegler, S. G. Nekolla, *Journal of Nuclear Medicine* **2005**, *46*, 1664-1678.

[24] L. G. Strauss, P. S. Conti, *Journal of Nuclear Medicine* **1991**, *32*, 623-648; discussion 649-650.

[25] P. McQuade, D. J. Rowland, J. S. Lewis, M. J. Welch, *Current Medicinal Chemistry* **2005**, *12*, 807-818.

[26] a) V. Gómez, J. D. Gispert, V. Amador, J. Llop, *Journal of Labelled Compounds and Radiopharmaceuticals* **2008**, *51*, 83-86; b) V. W. Pike, C. Halldin, C. Crouzel, L. Barré, D. J. Nutt, S. Osman, F. Shah, D. R. Turton, S. L. Waters, *Nuclear Medicine and Biology* **1993**, *20*, 503-525.

[27] B. Långström, G. Antoni, P. Gullberg, C. Halldin, P. Malmborg, K. Någren, A. Rimland, H. Svard, *Journal of Nuclear Medicine* **1987**, *28*, 1037-1040.

[28] D. M. Jewett, *International Journal of Radiation Applications and Instrumentation. Part A. Applied Radiation and Isotopes* **1992**, *43*, 1383-1385.

[29] B. Långström, O. Itsenko, O. Rahman, *Journal of Labelled Compounds and Radiopharmaceuticals* **2007**, *50*, 794-810.

[30] R. Iwata, T. Ido, T. Takahashi, H. Nakanishi, S. Iida, *International Journal of Radiation Applications and Instrumentation. Part A. Applied Radiation and Isotopes* **1987**, *38*, 97-102.

[31] a) P. Landais, C. Crouzel, *International Journal of Radiation Applications and Instrumentation. Part A. Applied Radiation and Isotopes* **1987**, *38*, 297-300; b) K.i. Nishijima, Y. Kuge, K.-i. Seki, K. Ohkura, N. Motoki, K. Nagatsu, A. Tanaka, E. Tsukamoto, N. Tamaki, *Nuclear Medicine and Biology* **2002**, *29*, 345-350.

[32] B. H. Rotstein, S. H. Liang, J. P. Holland, T. L. Collier, J. M. Hooker, A. A. Wilson, N. Vasdev, *Chemical Communications* **2013**, *49*, 5621-5629.

[33] O. Kreye, H. Mutlu, M. A. R. Meier, *Green Chemistry* **2013**, *15*, 1431-1455.

[34] a) Z. Z. Yang, L. N. He, J. Gao, A. H. Liu, B. Yu, *Energy and Environmental Science* **2012**, *5*, 6602-6639; b) R. N. Salvatore, S. I. Shin, A. S. Nagle, K. W. Jung, *Journal of Organic Chemistry* **2001**, *66*, 1035-1037.

[35] T. Sakakura, J. C. Choi, H. Yasuda, *Chemical Reviews* **2007**, *107*, 2365-2387.

[36] T. N. Sorrell, *Tetrahedron* **1989**, *45*, 3-68.

[37] H. Tran-Vu, O. Daugulis, *ACS Catalysis* **2013**, *3*, 2417-2420.

[38] K. i. Tominaga, Y. Sasaki, M. Kawai, T. Watanabe, M. Saito, *Journal of the Chemical Society, Chemical Communications* **1993**, 629-631.

[39] a) S. L. Peterson, S. M. Stucka, C. J. Dinsmore, *Organic Letters* **2010**, *12*, 1340-1343; b) T. Mizuno, Y. Ishino, *Tetrahedron* **2002**, *58*, 3155-3158.

[40] a) A. A. Wilson, A. Garcia, S. Houle, O. Sadovski, N. Vasdev, *Chemistry – A European Journal* **2011**, *17*, 259-264; b) J. M. Hooker, A. T. Reibel, S. M. Hill, M. J. Schueller, J. S. Fowler, *Angewandte Chemie International Edition* **2009**, *48*, 3482-3485.

[41] P. J. Riss, S. Lu, S. Telu, F. I. Aigbirhio, V. W. Pike, *Angewandte Chemie International Edition* **2012**, *51*, 2698-2702.

[42] J. Takaya, S. Tadami, K. Ukai, N. Iwasawa, *Organic Letters* **2008**, *10*, 2697-2700.

Chapter 2

[^{11}C]Ureas

2 Chapter 2

2.1 Background

Ureas are a stable class of compounds that contain two nitrogen atoms joined together by a carbonyl group (Figure 2.1). The functional group is found in a plethora of pharmaceutical compounds, agrochemicals and endogenous compounds. Numerous methods for the synthesis of urea have been developed.[1]

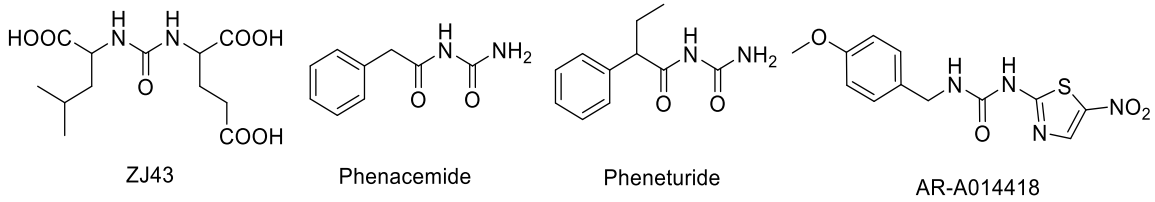

Figure 2.1 Urea-containing pharmaceutical compounds.

2.1.1 Synthesis of ureas *via* isocyanates

Isocyanates are reactive functional groups that can be synthesised from various groups such as carboxylic acids and amines. When carboxylic acids are reacted with acid chlorides in the presence of sodium azide, an isocyanate intermediate is produced *via* the Curtius rearrangement (Scheme 2.1).

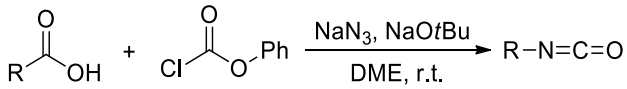

Scheme 2.1 The synthesis of isocyanates from carboxylic acids.[1]

The isocyanate intermediate is prone to nucleophilic attack from amines to form ureas (Scheme 2.2). This is one of the common methods used for the synthesis of ureas as it produces the target compound efficiently at room temperature.

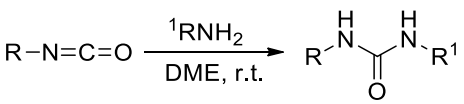

Scheme 2.2 The synthesis of ureas from carboxylic acids *via* isocyanates.[1]

2.1.2 Synthesis of ureas from carbon monoxide

Carbon monoxide (CO) gas can be used for the synthesis of ureas. In general, synthesis with CO requires specialised equipment as reactions are performed at high pressure. However, more recently, new methods for CO incorporation into ureas at lower pressure have been developed.[2]

The methods available to incorporate CO into urea molecules are usually mediated by transition metals such as palladium (Pd),[3] tungsten (W),[4] and gold (Au).[5] CO is an electron donor which enables it to act as a ligand for these metals and subsequently it can be inserted into target compounds.

Troisis *et al.*[3] developed a simple synthetic procedure that uses CO for the preparation of benzo-fused five- and six-membered heterocycles in yields of > 70 % (Scheme 2.3). The reaction is of interest as heterocyclics such as benzimidazol-2-ones and its derivatives are important pharmacophores.

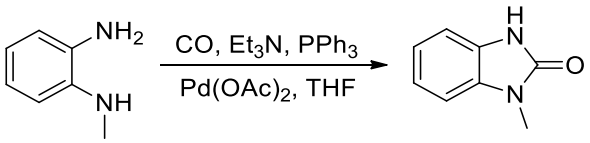

Scheme 2.3 The synthesis of benzimidazol-2-ones using CO.[3]

The palladium catalysed carbonylation reaction is performed at high pressure (2.75 MPa) and requires a base for deprotonation as shown in scheme 2.4. The starting material is believed to form a complex with Pd(0) which enables CO insertion between X and Pd to form intermediate 1 (X is either S, O or NH). Although it is reported by Troisis *et al.*[3] that the deprotonation of the YH is the next step (Y is either S, O or NH), the deprotonation is most likely to take place after the formation of the 6 membered cycle (intermediate 2, Scheme 2.4). This is due to the pKa of Et_3N being too low to deprotonate Y when it is an amine. Reductive elimination then take place to give the target cyclic product.

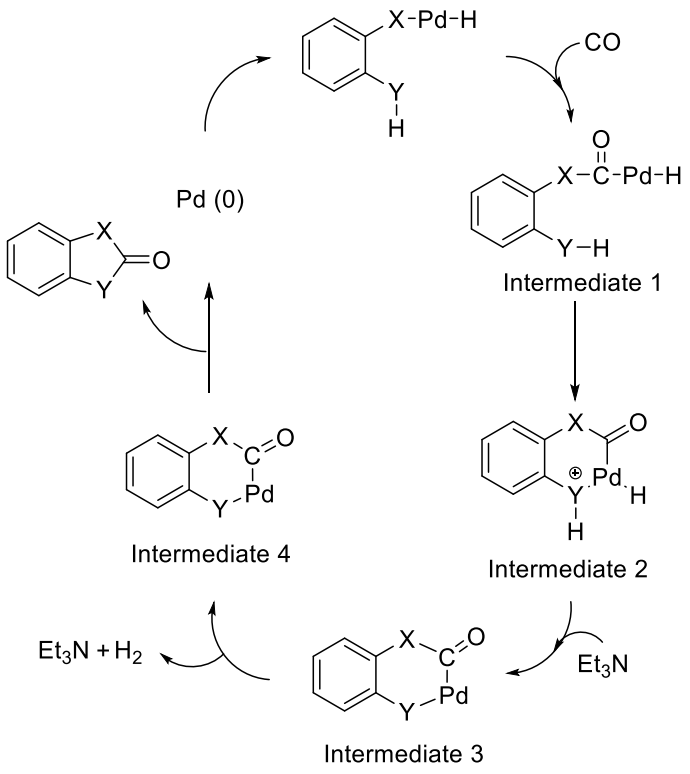

Scheme 2.4 Palladium-mediated urea synthesis.

Another method that incorporates CO into amines for the synthesis of ureas was developed by Zhang *et al.*[4] The reaction is catalysed by the tungsten hexacarbonyl [$W(CO)_6$] in the presence of 4-dimethylaminopyridine (DMAP) base, Iodine (I_2) and CO (Scheme 2.5).

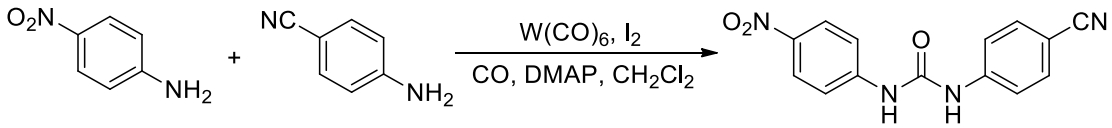

Scheme 2.5 Tungsten catalysed asymetrical urea asymmetrical by CO incorporation. [4]

The reaction is believed to proceed through isocyanate intermediate formation. It was reported that no target product was formed when carbonylation of secondary amines were attempted due to secondary amines being unable to form isocyanates.

2.1.3 Synthesis of ureas from Carbon dioxide

Peterson *et al.*[6] developed the use of 1,8-Diazabicyclo[5.4.0]undec-7-ene (DBU) and the Mitsunobu reaction with CO_2 for the synthesis of ureas. DBU was used as a CO_2-activating agent to form an unstable *in situ* intermediate (Scheme 2.6). Mitsunobu reagents were used as a dehydrating agent to form the corresponding isocyanate intermediate which reacts with a secondary amine to form the final urea product.

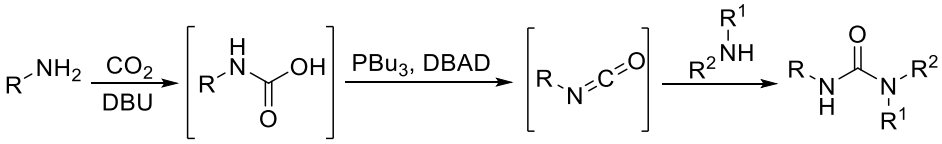

Scheme 2.6 The synthesis of ureas *via* isocynate intermediate.[6]

Table 2.1 Synthesis of ureas by the incorporation of CO_2 to amines.[6]

Entry	Product	Yield (%)
1	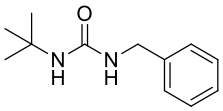	29
2	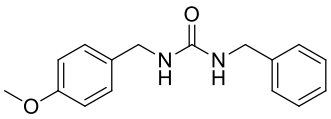	84
3	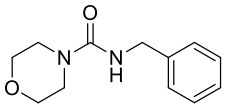	78
4	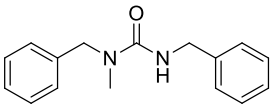	88
5	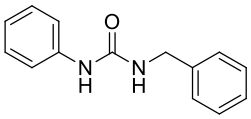	68
6	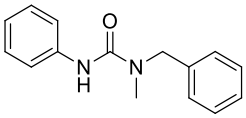	99

The reaction can be used to incorporate CO_2 into aliphatic, aromatic and benzylic amines to form ureas in high yields (Table 2.1). However, the reaction is limited by the isocyanates intermediate formation, i.e., one of the reacting amines must be a primary amine.

Mizuno *et al.*[7] also developed a method using DBU for the synthesis of quinazoline-2,4-dione (Scheme 2.7). Quinazoline-2,4-diones are key intermediates for producing pharmaceutical compounds such as Zenarestat (an aldose reductase inhibitor) and 3-ethyl-8-[2-(4-hydroxymethylpiperidino)benzylamino]-2,3-dihydro-1H-imidazo[4,5-g]quinazoline-2-thione dihydrochloride (a cyclic nucleotide phosphodiesterase 5 inhibitor).

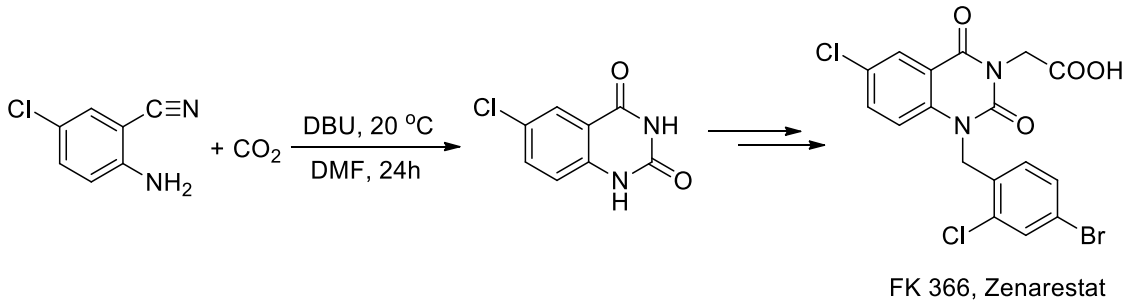

Scheme 2.7 The synthesis of Zenarestat by CO_2 incorporation.[7]

The reaction produces the corresponding product efficiently under mild conditions (Scheme 2.8). Similar results are observed when Cs_2CO_3 is used for the synthesis of quinazoline-2,4-dione.

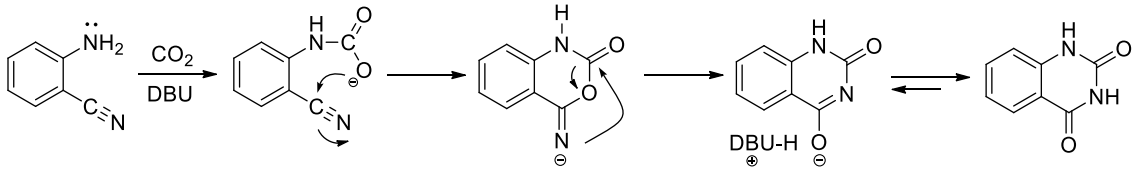

Scheme 2.8 A reaction pathway for the synthesis of quinazoline-2,4-diones as proposed by Mizuno *et al.*.[7]

In the presence of an amine, a base and carbon-14 CO_2, $POCl_3$ can also be used for the synthesis of urea.[8] The reaction proceeds through an isocyanate

intermediate when primary amines are reacted with $POCl_3$, while secondary amines proceed via a carbamyl chloride. The isocyanate intermediate was observed when the reaction was performed using [^{14}C]CO_2 at -78 ^{o}C. Good to moderate isocyanate yields were obtained when aniline bearing electron withdrawing groups were reacted (Table 2.2).

Low yields (10 %) were observed when the electron withdrawing ester group was present while nitro-containing aniline did not produce the target urea due to insufficient CO_2 trapping (Table 2.2, Entries 3 and 4). The isocyanate yield could be improved by the addition of *N*-dicyclohexyl-*N',N',N'',N*''-tetramethyl guanidine (CyTMG) and pyridine. It is believed that increased yields are obtained due to the base combination providing additional stabilization of carbamate salts (Scheme 2.9).

Table 2.2 Synthesis of isocyanates from primary and secondary amines. [a] Determined by Radio-HPLC .[8]

Entry	Amine	[^{14}C]Isocyanate yield[a] (%)
1	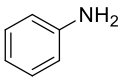	85
2	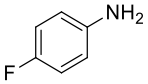	85
3	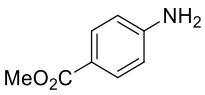	10 (35)
4	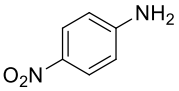	0
5		20

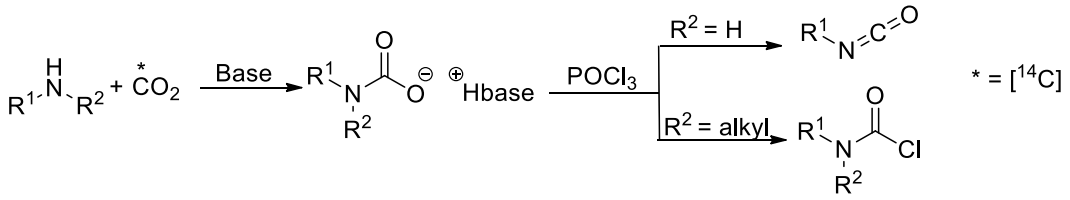

Scheme 2.9 The synthesis of ureas in the presence of $POCl_3$

In a similar method, the combination of CyTMG and pyridine allowed secondary amines to form carbamyl chlorides with moderate yields of 20 to 35 %. Warming the isocyanate species from - 78 ^{o}C to - 20 ^{o}C with the addition of further amine produced the target urea.

The method was used to label L-7400937 (a CCK B antagonist) with carbon-14 (^{14}C) with an overall yield of 70% based on the starting [^{14}C]CO_2 (Scheme 2.10).[8]

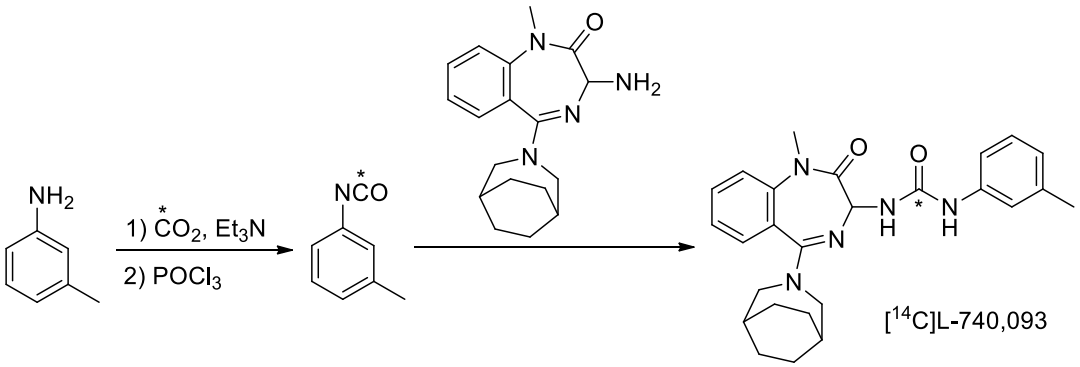

Scheme 2.10 Synthesis of carbon-14 labelled L-740,093.

Since urea structures are common motifs in biologically active molecules (see Figure 2.1) the development of methods for the radiolabelling of the functional group with PET radionuclides is of considerable interest. The urea structure has been radiolabelled previously using three different ^{11}C synthons: [^{11}C]$COCl_2$, [^{11}C]CO and [^{11}C]CO_2.

2.1.4 Synthesis of [^{11}C]ureas *via* [^{11}C]Phosgenes

[^{11}C]phosgenes ([^{11}C]$COCl_2$) are highly reactive species that can be synthesised from cyclotron-produced [^{11}C]methane *via* a [^{11}C]carbon tetrachloride intermediate or by cyclotron-produced [^{11}C]CO_2 *via* a [^{11}C]CO intermediate (Scheme 2.11).[9]

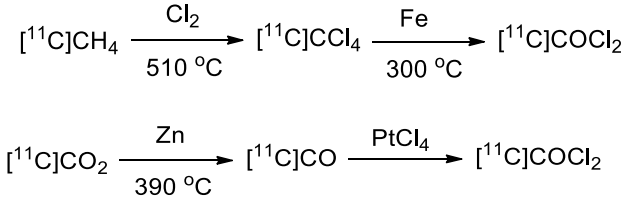

Scheme 2.11 The synthesis of [^{11}C]$COCl_2$ from [^{11}C]CH_4 *via* [^{11}C]CCl_4 and from [^{11}C]CO_2 *via* [^{11}C]CO.

Numerous compounds have been radiolabelled with [^{11}C]$COCl_2$ for *in vivo* and *in vitro* imaging. Sorafenib, a multi-kinase inhibitor used for the treatment of cancer is one such example (Scheme 2.12).[10] The reaction proceeds through the formation of an isocyanate intermediate and forms the corresponding product rapidly at room temperature.

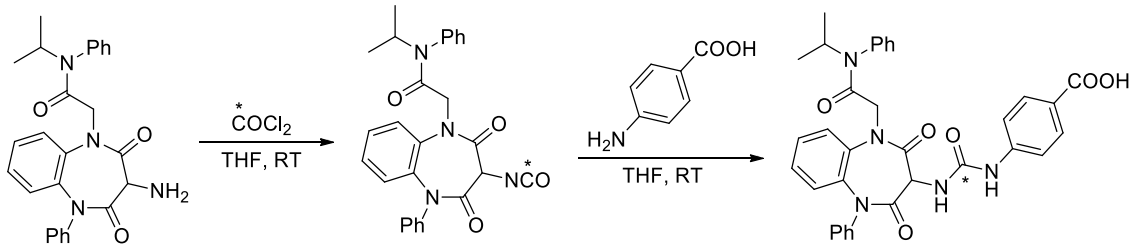

Scheme 2.12 the radiolabelling of Sorafenib with [^{11}C]$COCl_2$.[10]

Interestingly, when the aniline is reacted with [^{11}C]$COCl_2$ at room temperature, the [^{11}C]isocyanate is the major product detected by radio-HPLC (Scheme 2.13). However, heating the reaction at 50 °C results in the formation of the ^{11}C-labelled symmetrical urea in quantitative RCY.

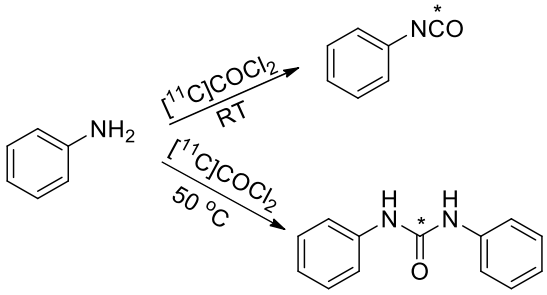

Scheme 2.13 Reaction products at different temperatures.

[^{11}C]$COCl_2$ has also been used to radiolabel Ketanserin (a serotonin antagonist) with moderate RCY of 25 to 50 % (corrected for radioactive decay from [^{11}C]$COCl_2$).[10]

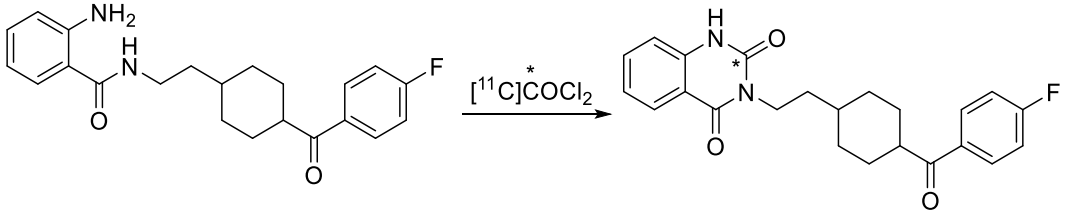

Scheme 2.14 The preparation of [^{11}C]Ketanserin

Many tracers have been radiolabelled with [^{11}C]$COCl_2$ and although radiolabelling is rapid and efficient, routine synthesis of the synthon is challenging and requires specialised equipment. Furthermore, [^{11}C]$COCl_2$ is obtained in low radiochemical yields (RCY) *via* multistep syntheses, thereby restricting its widespread use.

2.1.5 Synthesis of [^{11}C]ureas *via* [^{11}C]carbon monoxide

[^{11}C]Carbon monoxide ([^{11}C]CO) has been used to radiolabel ureas efficiently. The synthon is typically produced by passing [^{11}C]CO_2 through zinc (Zn) or molybdenum (Mo) at 290 ^{o}C and 850 ^{o}C respectively.

One of the main challenges faced when using [^{11}C]CO is its low solubility in organic solvents. This is generally counteracted by recirculation of [^{11}C]CO through the reaction or by performing the reaction under high pressure.[9, 11] More

recently, metal-ligand complexes have been used to trap [^{11}C]CO in the reaction mixture[12] and as a consequence, carbonylation is becoming a more versatile ^{11}C-labelling strategy. Several radiolabelling methodologies are available for radiolabelling ureas with [^{11}C]CO, enabling the synthesis of many different compounds. [13]

Rhodium (Rh) and Pd-mediated carbonylation reactions are the most common strategies used to radiolabel with [^{11}C]CO. Langstrom *et al.*[13a] developed a method using a Rh(l)-complex to mediate the radiolabelling of ureas with [^{11}C]CO using amines and azides (Table 2.3).

The reaction tolerates both acidic and basic substituents. However, nucleophilicity has a major effect on the RCY. As expected, high RCYs were observed for strong nucleophiles such as phenylazide (Table 2.3, Entry 2) and low RCYs were observed for weak nucleophiles such as cyanoaniline (Table 2.3, Entry 4).

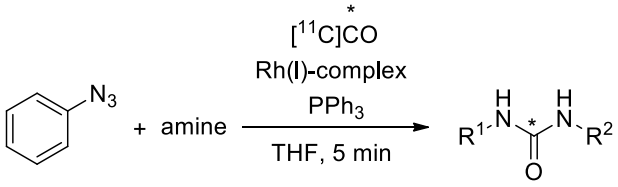

Table 2.3 The radiolabelling of asymmetrical ureas using rhodium and [^{11}C]CO.[13a]

Entry	Product	RCY[a] (%)
1	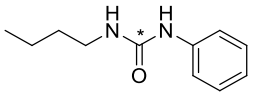	88
2	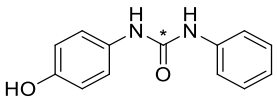	88
3	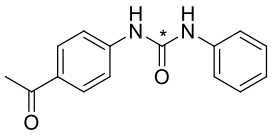	14
4	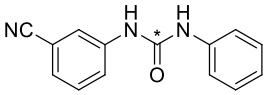	24
5	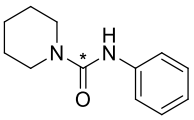	62

[a] Determined by Radio-HPLC.

This method was used for the radiolabelling of Tolbutamide (a potassium channel blocker) in RCY of 83 ± 1 % (corrected for decay from [^{11}C]CO).[13a]

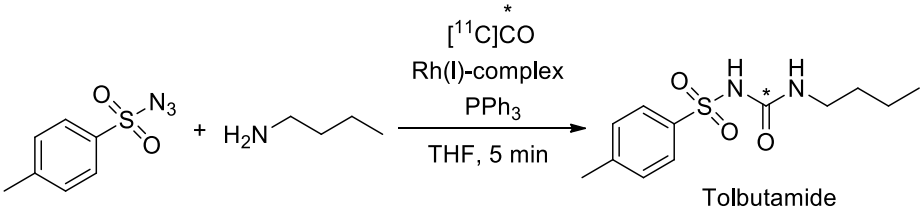

Scheme 2.15 The radiolabelling of Tolbutamide using [^{11}C]CO.[13a]

In 2014, Kealey *et al.*[13b] established a Pd-mediated oxidative carbonylation method for the synthesis of asymmetrical [^{11}C]ureas using [^{11}C]CO. Copper(I) Tris(pyrazolyl)borate complexes (CuTp(CO)) was used for trapping The [11C]CO within the reaction mixture.

High RCYs were observed when primary amines were reacted with cyclic amines while low yields were observed when aromatic amines were reacted due to their weak nucleophilicity (Table 2.4). The reaction is believed to proceed *via* the formation of [^{11}C]isocyanate intermediate and therefore, secondary amines cannot be used to form the corresponding [^{11}C]urea.

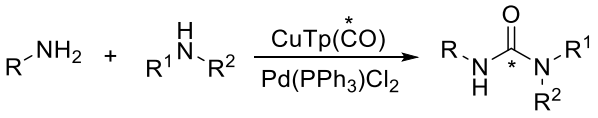

Table 2.4 The radiolabelling of ureas using copper and [^{11}C]CO.*[13b]*

Entry	Product	RCY[a] (%)
1	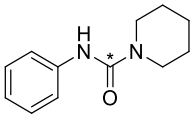	90
2	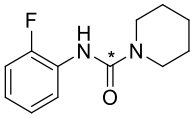	78
3	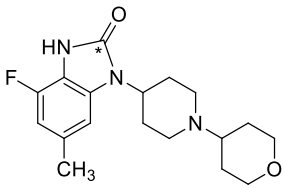	17

[a] Determined by Radio-HPLC

The attractive feature of the synthesis methodology is the simplicity of the reaction set-up compared to other [^{11}C]CO methods. The radiolabelling set-up enables the reaction to be performed in a synthesis laboratory using common apparatus. However, the reaction is limited by the use of large excess of precursor (45 - 90 µmol) in order to obtain to obtain the target product efficient.

2.1.6 Synthesis of [^{11}C]ureas *via* [^{11}C]carbon dioxide

Schirbel *et al.*[14] developed the first method to radiolabel symmetrical ureas using [^{11}C]CO_2. Similar to most other methods for urea synthesis, the reaction is believed to proceed *via* the formation of an isocyanate which undergoes nucleophilic addition with an amine to form the symmetrical urea (Scheme 2.16). The reaction temperature was found to be a critical factor. The best RCYs were observed at -20 °C.

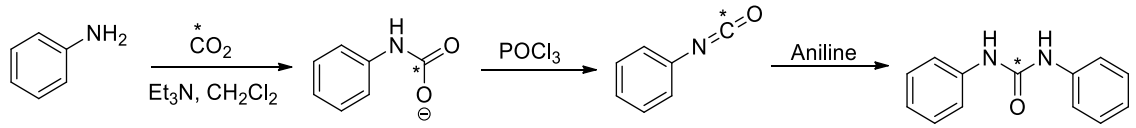

Scheme 2.16 The synthesis of [^{11}C]aromatic urea *via* [^{11}C]CO_2.

High RCYs of over 60 % were observed for aromatic and benzylic symmetrical [^{11}C]ureas (Table 2.5, Entries 1 and 2). However, low RCYs were observed when aliphatic amines were used for the synthesis of [^{11}C]ureas (Table 2.5, Entry 3).

Table 2.5 Synthesis of symmetrical ureas using [^{11}C]CO_2.

Entry	Product	RCY[a] (%)
1	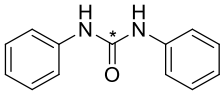	65
2	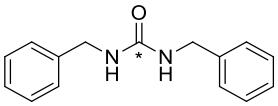	85
3	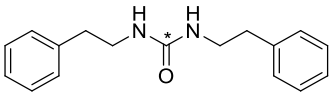	25

[a] Determined by HPLC. [14]

Wilson *et al.*[15] used a one-pot synthetic method to incorporate [^{11}C]CO_2 into urea-containing compounds using 2-*tert*-nutylimino-2-diethylamino-1,3-dimethylperhydro-1,3,2 diazaphosphorine (BEMP) as a trapping agent in the presence of $POCl_3$ (Table 2.6).

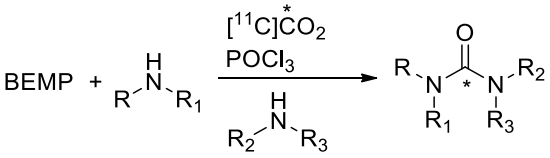

Table 2.6 BEMP-promoted [^{11}C]urea synthesis.

Entry	Product	RCY[a] (%)
1	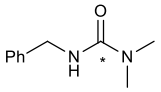	83
2	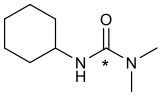	86
3	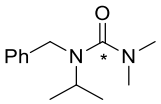	47
4	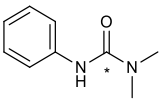	6

[a] Determined by HPLC.

A notable feature of this method is that the overall synthesis time was under five minutes. The radiolabelling procedure used cyclotron-produced [^{11}C]CO_2 directly to radiolabel aliphatic and benzylic amines to form [^{11}C]ureas in good to excellent RCY (47% - 86%).

The radiolabelling procedure was limited by low yields for anilines (6 %) due to their reduced nucleophilicity.

The reaction is believed to proceed *via* an [^{11}C]isocyanate intermediate when a primary amine is reacted with [^{11}C]CO_2. Reactions with secondary amines resulted in the formation of *N,N*-disubstituted [^{11}C]ureas. The asymmetric ureas are believed to proceed *via* an [^{11}C]carbomyl chloride intermediate (Scheme 2.17).[15]

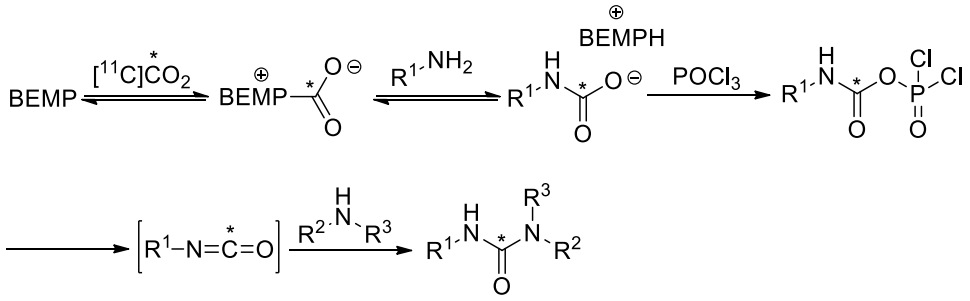

Scheme 2.17 Proposed methodology for [^{11}C]urea synthesis *via* isocyanate.[15]

The method was used for the radiolabelling of PF-04457845 (a fatty acid amide hydrolase inhibitor) to give an overall yield of 4.5 ± 1.3% based on starting [^{11}C]CO_2 (uncorrected for decay) and a radiochemical purity of > 95% with a total synthesis time of 25 ± 2 min (Scheme 2.18).[16]

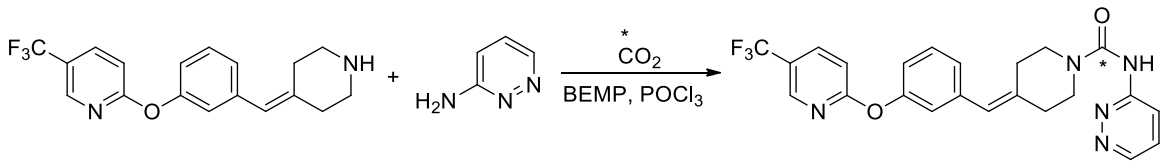

Scheme 2.18 The synthesis of [^{11}C]PF-04457845.[16]

The method has also been used to radiolabel AR-A014418 (a GSK-3 inhibitor).[17] The overall yield was 8.3 ± 3.9% based on starting [^{11}C]CO_2 (uncorrected for decay), specific activity of 150 ± 40 GBq/µmol and a radiochemical purity of > 95 % with a total synthesis time of 28 minutes including formulation (Scheme 2.19).

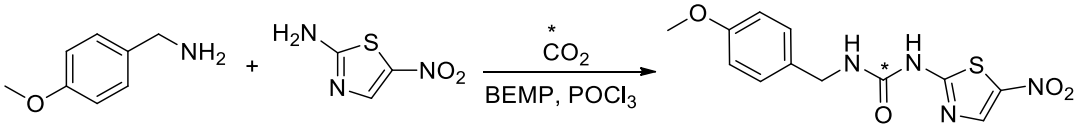

Scheme 2.19 The synthesis of [^{11}C] AR-A014418.[17]

Another reported method to radiolabel ureas was *via* the condensation of phosphinimines with [^{11}C]CO_2.[18] The method can be used to radiolabel aromatic and aliphatic amines (Scheme 2.20).

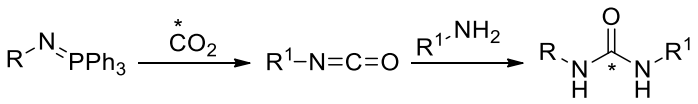

Scheme 2.20 [^{11}C]urea synthesis using triphenylphosphinimines and [^{11}C]CO_2.[18]

The [^{11}C]CO_2 was trapped in a solution of THF at – 60 ^{o}C in the presence of phosphinimine and an amine. Subsequently the solution was heated to 60 ^{o}C for six minutes and the resulting mixture was analysed by radio-HPLC. Aliphatic amines gave RCY of 45 to 49 % (determined using HPLC) while aniline gave only 8 % RCY (Table 2.7).

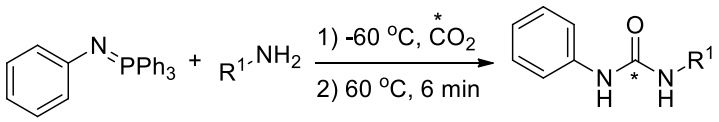

Table 2.7 Direct radiolabelling of urea with [^{11}C]CO_2.[18]

Entry	Product	RCY[a] (%)
1	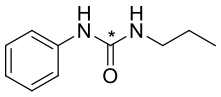	49
2	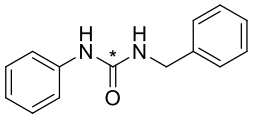	46
3	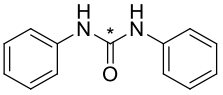	8

[a] Determined by radio-HPLC

The radiolabelling reaction is limited by the availability of phosphinime compounds. Limited numbers of phosphinime compounds are commercially available. However, they can be prepared from amines or azides.[19]

2.1.7 Summary

A plethora of molecules containing the urea functional group and possessing a wide range of pharmacological properties can be found in the literature.[20] Radiolabelling this important class of compounds with PET radionuclides may help in early diagnosis, monitoring pathophysiology and offer the opportunity to deepen our understanding of drug-receptor interactions.

[^{11}C]$COCl_2$, [^{11}C]CO and [^{11}C]CO_2 have been used to radiolabel ureas. Each synthon has its advantages and limitations. [^{11}C]$COCl_2$ reactions are rapid and efficient however, the preparation of the synthon is challenging. While [^{11}C]CO methods work well, few laboratories have the infrastructure required to produce [^{11}C]CO routinely, limiting it's widespread utility. [^{11}C]CO_2 is poorly reactive and as a result, only a limited number of methods using it directly in radiolabelling reactions are available.

In the past few years, novel methods to radiolabel compounds with [^{11}C]CO_2 have been developed. There are two methods available to radiolabel asymmetrical ureas with [^{11}C]CO_2 but both methods are limited to aliphatic and benzylic amines. Low RCYs are observed for the synthesis of aromatic ureas. Developing novel and robust methods to radiolabel aromatic ureas is of significant interest.

2.2 Aim

The aim of this chapter is to develop a one-pot radiolabelling methodology that incorporates [^{11}C]CO_2 directly into aliphatic, benzylic and aromatic ureas. It has been shown that CO_2 can be trapped within a reaction mixture by using DBU and an amine.[21] It has also been shown that Mitsunobu reaction can be used to convert nonradioactive carbamate ion to urea. The project aims to combine the trapping with DBU and Mitsunobu reaction for the synthesis of [^{11}C]ureas.

2.3 Results and discussion – Asymmetrical [^{11}C]ureas

Model reactions were initially conducted using nonradioactive CO_2. [6] Compound **1** was subsequently chosen as the initial model reaction for optimisation with [^{11}C]CO_2 (Scheme 3.21).

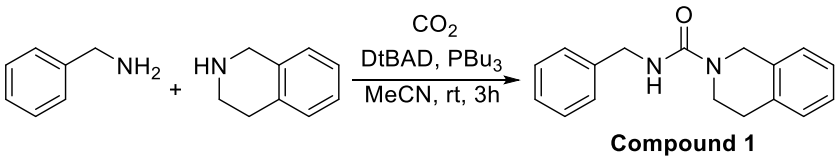

Scheme 3.21 Synthesis of the reference compound (compound 1).

2.3.1 Solvent optimisation

Initially, the radiolabelling reactions were carried out in various solvents including DMF, DMSO, dioxane and toluene at 40 ^{o}C with the aim to identify the best solvent for the reaction (Table 2.8). These solvents were selected as they have been reported to trap [^{11}C]CO_2 in the presence of DBU or possess functionalities that have previously demonstrated to trap non-radioactive CO_2. Polar solvents (DMF, DMSO and CH_3CN) trapped the [^{11}C]CO_2 more efficiently than non-polar solvents such as toluene and dioxane. The high trapping by the polar solvents is consistent with the result previously obtained by Hooker *et al.*[22] whereby CH_3CN trapping the highest radioactivity followed by DMF and DMSO. When [^{11}C]CO_2

was bubbled directly into the CH_3CN reaction mixture (Table 2.8, Entry 1), over 95 % of the produced $[^{11}C]CO_2$ was trapped, while DMSO and DMF trapped less efficiently (80 - 90 %). Dioxane and toluene trapped the $[^{11}C]CO_2$ to a lesser degree (< 20 %).

Co-elution with reference compound confirmed the synthesis of [^{11}C]compound 1 in moderate radiochemical conversions (RCC) when CH_3CN was used as solvent (46 %). The RCC was estimated by radio-HPLC and defined as the area under the [^{11}C]urea peak expressed as a percentage of the total ^{11}C labelled peak areas observed in the chromatogram. DMF and DMSO also produced the radiolabelled compound 1 but with poor RCCs of 13 % and 18 % respectively while dioxane and toluene resulted in no product formation.

Low yields for DMF and DMSO were observed presumably due to the Mitsunobu reagents not being fully soluble in these solvents leading to low yields. The highest RCCs were obtained when CH_3CN was used, and therefore it was selected as the solvent of choice for subsequent reactions.

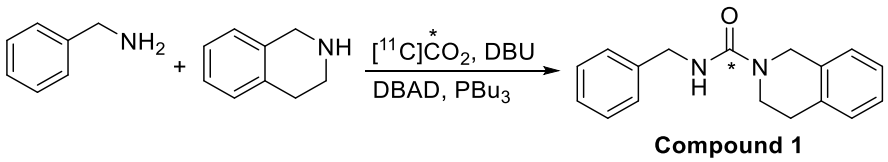

Table 2.8 Optimisation of the reaction solvent.

Entry [a]	Solvent	Trapping (%)	RCC (%)[b]
1	CH_3CN	96%	46
2	DMSO	89%	18
3	DMF	82%	13
4	Toluene	19%	0
5	Dioxane	7%	0

[a] Screening conditions: Benzylamine (18.3 µmol), tetrahydroisoquinoline (27.5 µmol), DBU (0.8 µmol), Mitsunobu reagents (36.6 µmol) in 400 µmol solvent, 40 °C, 5 min. [b] RCC values are average of 2 (n = 2), determined by radio-HPLC.

2.3.2 Mitsunobu reagents optimisation

It has been reported that BEMP traps [^{11}C]CO_2 with a similar efficiency to DBU.[22] The trapping agents were compared (Table 2.9, Entries 1 and 2) and both trapping agents trapped [^{11}C]CO_2 efficiently. However, only the reaction with DBU produced [^{11}C]compound 1 (Figure 2.2). Reactions were then performed using different combinations of Mitsunobu reagents. The highest RCCs were observed when tributylphosphine (PBu_3) with di-*tert*-butyl azodicarboxylate (DBAD) were used (Table 2.9, Entry 1) and hence, these reagents were chosen for further optimisation reactions.

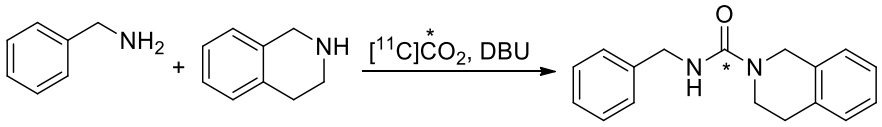

Table 2.9 Optimisation of the Mitsunobu reagents and trapping agent.

Entry [a]	Fixation agent	Mitsunobu reagents	Trapping (%)	RCC (%)[b]
1	DBU	PBu_3 and DBAD	96	46
2	BEMP	PBu_3 and DBAD	98	0
3	DBU	PPh_3 and DBAD	96	20
4	DBU	PPh_3 and DIAD	96	14
5	DBU	PBu_3 and DIAD	96	18

[a] Screening conditions: Benzylamine (18.3 µmol), tetrahydroisoquinoline (27.5 µmol), trapping reagent (0.8 µmol), Mitsunobu reagents (36.6 µmol) in 400 µmol CH_3CN, 40 °C, 5 min. n = 2. [b] RCC values are average of 2 (n = 2), determined by radio-HPLC.

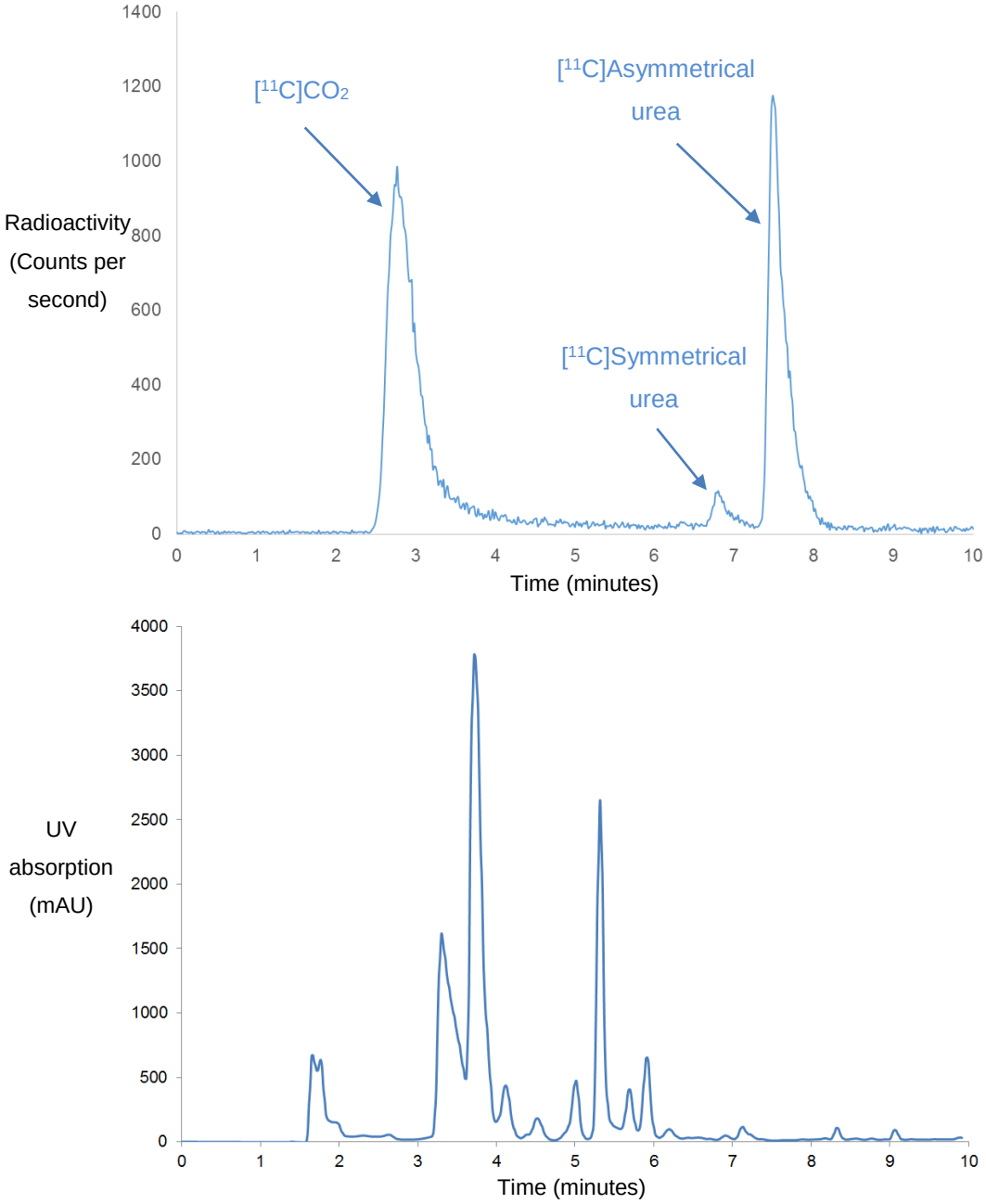

Figure 2.2 Radio-HPLC and UV chromatograms of the crude radiolabelling reaction (Table 2.9, Entry 1). The target product is eluted 7:35 minutes.

2.3.3 Temperature and reaction time optimisation

The temperature dependency of the reaction was examined (Table 2.10). Reducing the temperature from 40 °C to 25 °C reduced the RCCs. Loss of $[^{11}C]CO_2$ from the reaction vial was observed when the reactions were

performed at 60 °C. Reactions at 50 °C avoided these losses and resulted in over a 95 % incorporation of the [^{11}C]CO_2 into the target molecules. It was also observed that by reducing the reaction time to 1 minute, 96 % RCC was still observed (Table 2.10, Entry 6), which laid the foundation for the development of this rapid synthesis method for [^{11}C]CO_2 incorporation.

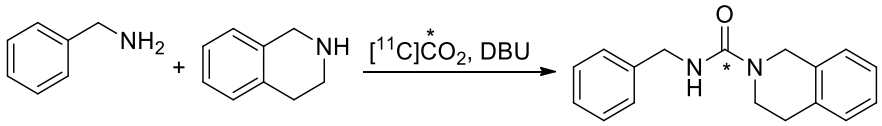

Table 2.10 Optimisation of the reaction temperature and time.

Entry [a]	T/°C	Time/min	RCC (%) [b]
1	40	5	46
2	25	5	10
3	60	5	26
4	50	5	95
5	50	20	95
6	50	1	96

[a] Screening conditions: Benzylamine (18.3 µmol), tetrahydroisoquinoline (27.5 µmol), DBU (0.8 µmol), Mitsunobu reagents (36.6 µmol) in 400 µmol CH_3CN. n = 2. [b] RCC values are average of 2 (n = 2), determined by radio-HPLC.

2.3.4 Radiolabelling of aliphatic, aromatic and benzylic amines

The reaction conditions developed using the model reaction were applied to the radiolabelling of various ureas using a range of aliphatic, benzylic and aromatic amines (Table 2.11). The reactions between a benzylic primary amine and hindered secondary amine (Table 2.11, Entry 1) resulted in a high RCC of 95 % while the reaction with a less hindered secondary amine produced [^{11}C]ureas to lesser degree (Table 2.11, Entry 2). Similarly, high RCCs were observed when less reactive compounds such as aniline and derivatives were used instead of benzylic amines to form the target radiolabelled molecules at a RCC of over 69 91 % (Table 2.11). Interestingly, the reaction favours the formation of

asymmetrical ureas rather than the symmetrical ureas even though the starting materials are available in excess. In the absence of secondary amine, the ^{11}C-labelled symmetrical urea was formed however, a low RCC of 19 % was observed (Table 2.11, Entry 3).

The effects of functional groups on aromatic amines were also studied. Reactions with the electron rich aromatic amines, *m*-toluidine and *p*-anisidine, resulted in more than 80 % RCC (Table 2.11, Entries 5 and 6). It was also seen that poor nucleophiles such as 4-nitroaniline worked efficiently, producing a high RCC of 85 % (Table 2.11, entry 7). The reaction favoured the formation of asymmetric [^{11}C]ureas despite primary amines being present in excess of [^{11}C]CO_2. In all of the radiolabelling reactions, unreacted [^{11}C]CO_2 accounts for > 80 % of the by-product which eluted at the solvent front. Small amount of symmetrical urea is also produced by the reaction which accounts for the rest of the by-product.

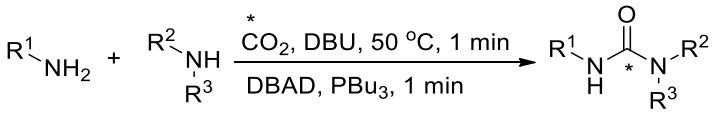

Table 2.11 Radiolabelling various aliphatic, benzylic and aromatic amines with [^{11}C]CO_2.

Entry	Product	RCC
1	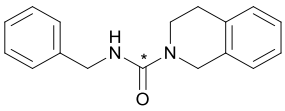	96 ± 2
2	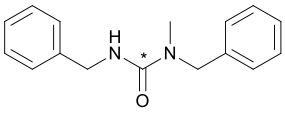	74 ± 9
3	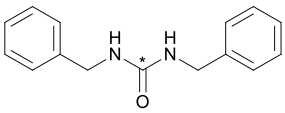	19 ± 15
4	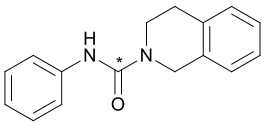	94 ± 2
5	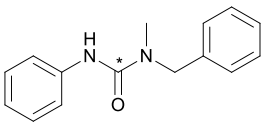	69 ± 6
6	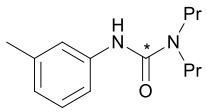	80 ± 10
7	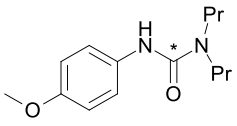	83 ± 5
8	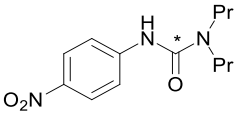	85 ± 6

[a] Screening conditions: Primary amine (18.3 µmol), secondary amine (27.5 µmol), DBU (0.8 µmol) in 300 µmol CH_3CN heated at 50 °C for 1 min, Mitsunobu reagents (36.6 µmol) in 100 µmol CH_3CN added and stirred for 1 min. [b] RCC values are mean ± (standard deviation), n = 3, determined by radio-HPLC.

2.3.5 Summary

The method developed produced high RCCs for asymmetrical ureas. However, low RCCs were observed (19 %) when synthesis of [^{11}C]symmetrical ureas was attempted. Pharmaceutical compounds that contain symmetrical ureas are not as common as compounds that contain asymmetrical ureas. Nevertheless, there are many compounds that contain a symmetrical structure such as suramin (used for treating sleeping sickness), and as a result, methods to radiolabel such structures are of interest.

[^{11}C]CO_2 has been used to radiolabel symmetrical ureas (Scheme 2.16).[14] The method produced high RCCs for aromatic and benzylic amines. However, low yields were observed for aliphatic molecules.[14] No other methods to radiolabel symmetrical ureas with [^{11}C]CO_2 have been reported in the literature and therefore developing methods to radiolabel symmetrical ureas with [^{11}C]CO_2 directly from the cyclotron is of interest.

2.4 Results and discussion – Symmetrical [^{11}C]ureas

Model reactions were initially conducted using non-radioactive CO_2. The synthesis of compound **2** produced highest yields (Scheme 3.22) and was subsequently chosen as the model reaction for optimisation with [^{11}C]CO_2.

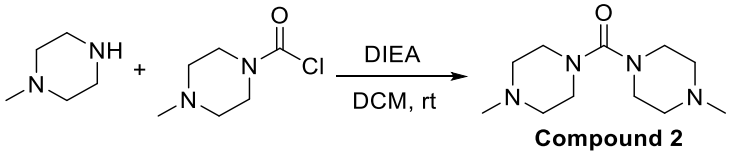

Scheme 3.22 Synthesis of the reference compound (compound 2).

2.4.1 Trapping agent, solvent and base optimisation

In order to favor the synthesis of symmetrical urea, reactions were initially assessed in the absence trapping reagents. Only 5 – 10 % of the produced [^{11}C]CO_2 was trapped within the reaction vial in the absence of trapping reagent and no [^{11}C]radiolabelled target compound was observed (Table 2.12, Entry 1). When DBU was used as a trapping agent, [^{11}C]compound 2 was formed in RCC of 31 % (Table 2.12, Entry 2). The strong base BEMP did not produce the target radiolabelled product (Table 2.12, Entry 3). Furthermore, RCCs were not improved when the reaction time was increased from 5 minutes to 15 minutes.

Optimization of the reaction then focused on screening for appropriate solvents. The target [^{11}C]ureas were not formed when DMF, THF and toluene were used as the solvent (Table 2.12, Entries 4 - 6) while DMSO (Table 2.12, Entry 7) afforded the desired product with a RCC of 24 %. The Mitsunobu reagents were prepared separately before being added to the reaction vial. As the reagents were insoluble DMSO, the process of transferring the mixture to the reaction vial may have been inaccurate, a possible reason for the large variance in product RCC (24 ± 12%). The reagent solubility issue was solved by using a mixture of DMSO and CH_3CN, however, similar RCC were observed. CH_3CN produced the highest RCC comparing it with other solvents and was therefore selected as the solvent of choice for further investigations.

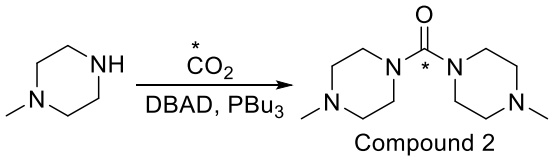

Compound 2

Table 2.12 Reaction fixing agent and solvent optimisation.

Entry [a]	Trapping agent	Solvent	RCC (%) [b]
1	-	CH_3CN	0
2	DBU	CH_3CN	31 ± 8
3	BEMP	CH_3CN	0
4	DBU	Toluene	0
5	DBU	THF	0
6	DBU	DMF	0
7	DBU	DMSO	24 ± 12

[a] Screening conditions: Amine (18.3 µmol), trapping reagent (0.8 µmol), Mitsunobu reagents (36.6 µmol) in 400 µmol solvent at 50 °C, 1 min. [b] RCC values are mean ± (standard deviation), n = 3, determined by radio-HPLC.

2.4.2 Temperature and concentration optimisation

It was previously stated that reaction temperatures below 50 °C were critical to avoid the loss of $[^{11}C]CO_2$ from the reaction vial. When reactions were performed at room temperature (Table 2.13, Entry 2), lower RCCs of the $[^{11}C]$compound 2 were observed (18 %). Increasing the concentration of the secondary amine did not improve the RCC noticeably (Table 2.13, Entry 1). When the concentration of the base, DBU, was increased from 0.8 µmol to 3.4 µmol, significant increases in RCCs were observed (Table 2.13, Entry 4). Further increasing the base concentration to 6.8 µmol reduced the RCC to 15 % (Table 2.13, Entry 5). The concentration of DBU was then examined at reduced concentrations (0.4 µmol) whereby a significant reduction in $[^{11}C]CO_2$ trapping was observed (12 %). DBU is a non-nucleophilic base and its main role in this reaction is to trap $[^{11}C]CO_2$.

However, results indicate that the basicity of the molecule has an effect on the reaction.

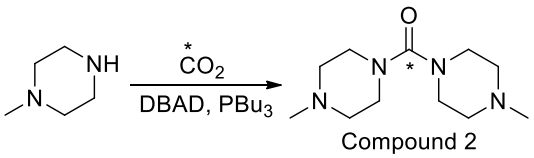

Compound 2

Table 2.13 Reaction optimisation for the synthesis of compound 2.

Entry [a]	Temperature	Amine (μmol)	DBU (μmol)	RCC (%) [b]
1	50	18.3	0.8	31 ± 8
2	25	18.3	0.8	14
3	50	36.6	0.8	35
4	50	18.3	3.4	84 ± 4
5	50	18.3	8.6	15

[a] Screening conditions: Mitsunobu reagents (36.6 μmol) in 400 μmol CH_3CN. n = 2. [b] RCC values are mean ± (standard deviation), n = 3, determined by radio-HPLC.

2.4.3 Radiolabelling of various [^{11}C]symmetrical ureas

The optimised conditions developed for the synthesis of [^{11}C]compound 2 were then applied to the radiolabelling of various symmetrical ureas using a range of aliphatic and aromatic amines (Table 2.14). High RCCs (> 80 %) of the desired [^{11}C]ureas were observed for rigid molecules such as 1-methylpiperazine and tetrahydroisoquinoline, presumably due to their low steric hindrance (Table 2.14, Entries 1 and 2). Rigid molecules are fixed and no free bond rotations are available, this property allows the molecule to be more reactive and hence the high conversions. The more flexible benzylic amine produced the target [^{11}C]1,3-dibenzyl urea but with lower RCC (29 %). Aniline and aromatic amines with electron donating and electron withdrawing groups reacted in over 70 % RCC

(Table 2.14, Entries 4 - 6). As high RCCs are observed for aromatic amines with partially available lone pairs, the reaction is expected to produce similar RCC for other weak nucleophiles.

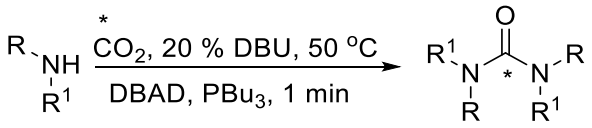

Table 2.14 Radiolabelling various aliphatic, benzylic and aromatic amines with [^{11}C]CO_2.

Entry	[^{11}C]Urea	RCC (%)
1	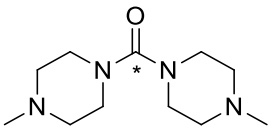	84 ± 4
2	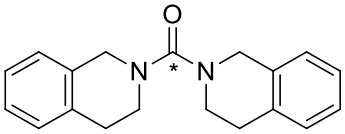	88 ± 6
3	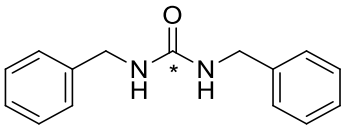	29 ± 12
4	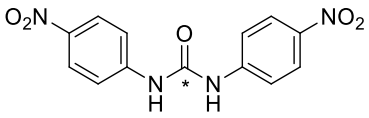	70 ± 2
5	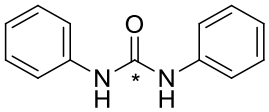	79 ± 14
6	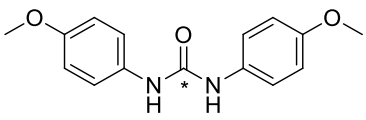	72 ± 6

[a] Screening conditions: Primary amine (18.3 µmol), DBU (3.4 µmol) in 300 µmol CH_3CN heated at 50 °C for 1 min, Mitsunobu reagents (36.6 µmol) in 100 µmol CH_3CN added and stirred for 1 min. [b] RCC values are mean ± (standard deviation), n = 3, determined by radio-HPLC.

2.4.4 Reaction mechanism

The developed synthesis methodology can be divided into two-steps: the first step is the trapping of [^{11}C]CO_2 by DBU in the presence of an amine, and the second step is the Mitsunobu reaction.

2.4.5 Trapping of CO_2

Different CO_2 trapping mechanisms have been reported:

DBU is a non-nucleophilic base due to its steric bulkiness. The steric effect prevent large groups form bonding with the base. The reaction mechanism proposed by Wilson *et al*.[15] and Hooker *et al*.[22] states that DBU is acting as a nucleophile and forming a C-N bond with [^{11}C]CO_2 (Scheme 2.23). [^{11}C]CO_2 is a small molecule and therefore, it is possible that it is forming an interaction with the base itself.[6, 22]

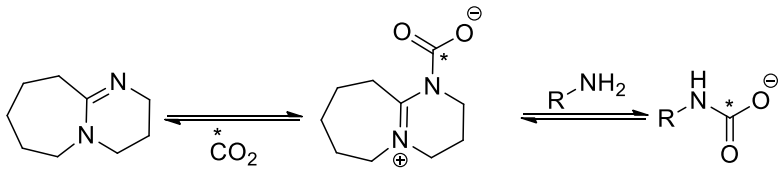

Scheme 2.23 Plausible method for the trapping [^{11}C]CO_2 by DBU.[22]

It has been reported that when CO_2 is bubbled into a reaction vial containing DBU and a small amount of water in CH_3CN, a bicarbonate salt is formed (Scheme 2.24). This traps the CO_2 within the solution.

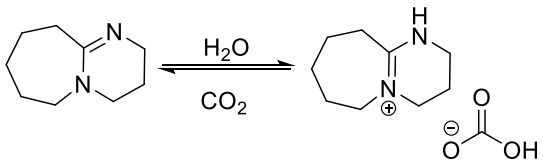

Scheme 2.24 Plausible CO_2 trapping method by DBU in the presence of H_2O.[21-23]

2.4.6 Proposed trapping mechanism

In order to determine the reaction mechanism, the trapping of the [^{11}C]CO_2 by amines and DBU was investigated. Low [^{11}C]CO_2 trapping was observed when [^{11}C]CO_2 was bubbled into a solution containing DBU and CH_3CN. Moreover, similar results were observed when [^{11}C]CO_2 was bubbled into a solution containing an amine and CH_3CN. However, high trapping efficiency was observed when [^{11}C]CO_2 was bubbled into a solution containing amine, DBU and CH_3CN (> 95 %). These results were in agreement with previously proposed methods whereby the base DBU and the amine form an interaction with the [^{11}C]CO_2 and as a result, a carbamate anion is formed (Scheme 2.25).[6]

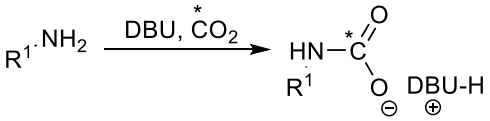

Scheme 2.25 Our proposed [^{11}C]CO_2 trapping method.

2.4.7 Mitsunobu reaction mechanism

The Mitsunobu reaction has been extensively studied. When tributylphosphine is added to a solution containing diethyl azodicarboxylate and CH_3CN, the weak azo π bond on the diethyl azodicarboxylate is attacked by the tributylphosphine producing a betaine intermediate (Intermediate 1, Scheme 2.26). Oxygen has a high affinity for phosphorus and so, the [^{11}C]carbamate anion attacks the positively charged phosphorus to form intermediates 3 and 4. The oxyphosphonium intermediate (intermediate 4) is then attacked by an amine to produce intermediate 5 which is deprotonated to form the target compound (Scheme 2.27).

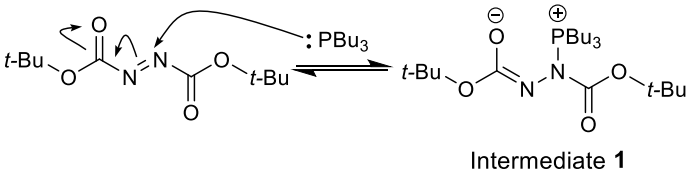

Scheme 2.26 Synthesis of betaine intermediate.

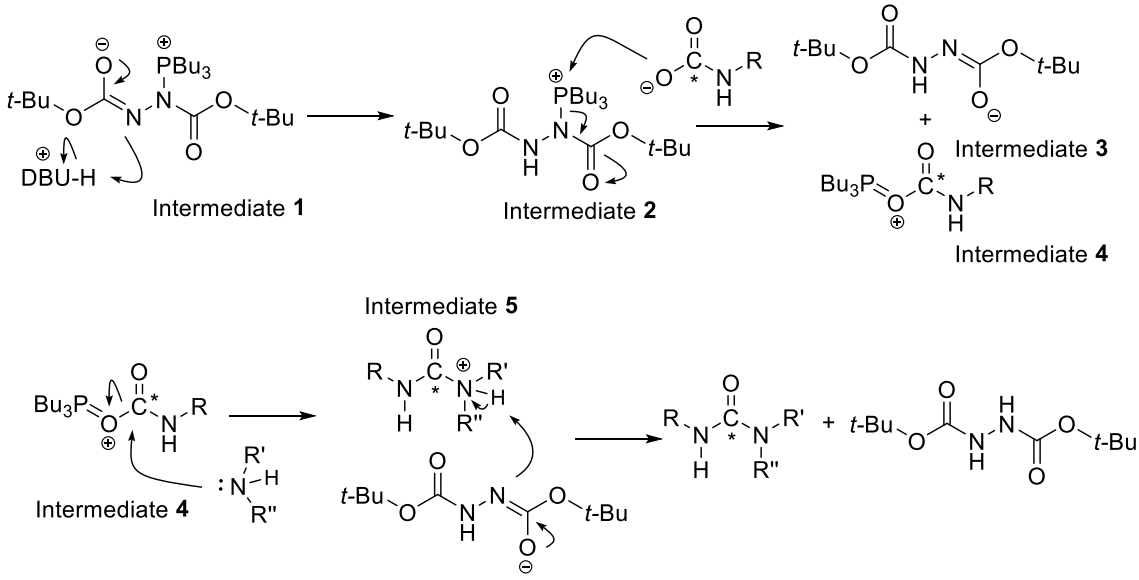

Scheme 2.27 The mechanism of Mitsunobu reaction.

2.5 Conclusion

In conclusion, a method that incorporates [^{11}C]CO_2 into aliphatic, aromatic and benzylic amines to produce target ^{11}C radiolabelled ureas has been developed. Due to the short half-life of ^{11}C, it is attractive to use primary synthons such as [^{11}C]CO_2 directly for the radiolabelling reaction rather than converting it into secondary species such as [^{11}C]CH_3I. The method developed in this work uses [^{11}C]CO_2 directly and rapidly. The synthetic method can be carried out in less than 5 minutes from the end of bombardment (excluding purification) and is highly efficient.

Although methods to radiolabel ureas with ^{11}C already exist, they are either limited by synthesis complexity or functional group tolerance. The method

developed does have some limitations such as the requirement of primary amines. However, it is a beneficial addition to the existing arsenal of ^{11}C radiolabelling techniques for *in vivo* molecular imaging.

Incorporation of stable CO_2 into amines using DBU and mitsunobu reagents has previously been developed by Petterson *et al.*[6] In traditional organic chemistry synthesis, CO_2 is available in excess however, when working at the tracer level, the $[^{11}C]CO_2$ is the limiting reagent. Due to the significant stoichiometry changes, reaction optimisation is necessary. The reaction with 'cold' CO_2 is believed to go through an isocyanate intermediate which explains why secondary amines cannot react with other secondary amines to form ureas. In this work, similar results were observed as secondary amines did not react together to form the corresponding $[^{11}C]$asymmetrical urea which suggests that the reaction mechanism is the same.

The novel method to radiolabel ureas produced high RCCs similar to that reported in literature (up to 95%) when aliphatic and benzylic amines have been used. The reaction produced much higher RCCs for unreactive amines such as aniline (up to 91%) compared to the methods described in the literature (6%). Increasing the concentration of the base 3-fold favours the formation of $[^{11}C]$symmetrical ureas.

In summary, a novel one-pot radiolabelling methodology that incorporates $[^{11}C]CO_2$ directly into aliphatic, benzylic and aromatic ureas has been developed. The synthesis bypasses the need for converting the short-lived $[^{11}C]CO_2$ into other reactive radiolabelling species. The broadly applicable ^{11}C-carbonylation strategy should enable the preparation of structurally diverse tracers.

2.6 Methods

2.6.1 General

All purchased chemicals were used without further purification. Chemicals were purchased in highest available purity from Sigma-Aldrich and Alfa Aesar and used as received (> 99 % purity). All solvents were purchased as anhydrous in highest available purity (> 99.8 % purity, water < 50 ppm, extra dry) from Sigma-Aldrich, used as received and stored under argon. Reference compounds were either purchased from Sigma-Aldrich or synthesised using reported procedures. Reactions were carried out under an atmosphere of nitrogen in heat gun dried glassware with magnetic stirring. Reactions were monitored using alumina plate thin-layer chromatography (Merck, silica gel 60, fluorescence indicator F254, or Merck, aluminium oxide neutral, fluorescence indicator F254). Silica gel chromatography was performed using 230-400 Mesh (Grade 60) silica gel. The mobile phase was a mixture of hexane : ethyl acetate in varying ratios and detected by 254 nm UV light. Infra-Red spectra were acquired on a PerkinElmer spectrum 100FTIR. ^{1}H-NMR (400 MHz) and ^{13}C-NMR (100 MHz) spectra were obtained using a BRUKER DRX 400 MHz spectrometer. Chemical shifts are reported in ppm (δ) relative to tetramethylsilane (TMS, d = 0 ppm) and calibrated using solvent residual peaks. Data are shown as follows: Chemical shift, multiplicity (s = singlet, d = doublet, t = triplet, q = quartet, m = multiplet), coupling constant (*J*, Hz) and integration. Calculated mass was determined using PerkinElmer ChemBioDraw Ultra 13.0 program. Mass spectroscopy was performed at King's College London using an Agilent 6520 Accurate-Mass Q-TOF LC/MS connected to an Agilent 1200 HPLC system with UV detector (254 nm) and auto-sampler. [^{11}C]CO_2 was produced by a Siemens RDS112 cyclotron (St Thomas' Hospital, London, United Kingdom) via the ^{14}N(p,α)^{11}C nuclear reaction. Typical irradiation times were 1 minute with a beam current of 10 μA, which yielded a [^{11}C]CO_2 amount of about 300 MBq at end of bombardment. Radiolabelling reactions were performed in a 1.5 mL screw top vial with a "V" internal shape. Analytical HPLC was performed on an Agilent 2060 Infinity HPLC system with a variable wavelength detector (254 nm was used as default

wavelength). An Agilent Eclipse XDB-C18 reverse-phase column (4.6 x 150 mm, 5 µm) was used at a flow rate of 1 mL/min and H_2O/MeOH (HPLC grade solvents and with 0.1 % TFA) gradient elution (flow rate: 1 mL/min, 0-2 min: 5% MeOH, 2-11 min: 5 to 95% MeOH linear gradient, 11-13 min: 90% MeOH, 13-14 min: 90% to 5% MeOH linear gradient, and 14-15 min:5% MeOH). The RCC was estimated by radio-HPLC and defined as the area under the [^{11}C]urea peak expressed as a percentage of the total ^{11}C labelled peak areas observed in the chromatogram. Specific radioactivity was calculated from analytical HPLC sample of 25 µL. A calibration curve of known mass quantity versus HPLC peak area (254 nm) was used to calculate the mass concentration of the 25 µL radiolabelled compound. The identity of the radiolabelled compound peak was confirmed by HPLC co-injection of a nonradioactive reference compound and yielded a single peak.

2.6.2 Synthesis of reference compounds

Reference compounds can be synthesised using reported procedures.[6] [24]

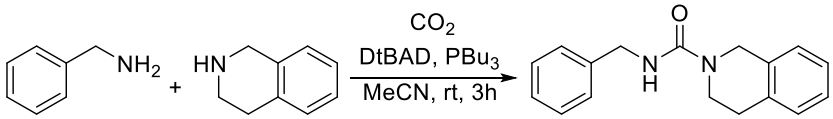

N-benzyl-3,4-dihydroisoquinoline-2(1H)-carboxamide; CO_2 gas was bubbled into a solution containing DBU (7 µL, 0.05 mmol) and benzyl amine (51 µL, 0.50 mmol) in CH_3CN (6 mL) for 1 hour at room temperature. Tetrahydroisoquinoline (89 µL, 0.70 mmol) was added to the reaction mixture and the vial was flushed with N_2. In a separate vial, PBu_3 (242 µL, 1.00 mmol) was added into a solution containing DBAD (226 mg, 1.00 mmol) in CH_3CN (2 mL) under nitrogen atmosphere. The solution was then added to the mixture dropwise and stirred at room temperature for 2 hours under nitrogen. The crude product was concentrated and purified by flash chromatography. Colourless solid; 48% yield (63 mg); IR 3316.16, 2927.85, 1620.80; ^{1}H NMR (400 MHz, $CDCl_3$) δ 7.06 – 7.55 (m, 9H), 4.55 (s, 2H), 4.40 (d, *J* = 5.7, 2H), 3.60 (t, *J*= 5.6 Hz, 2H), 2.8 (t, *J = 6.0*, 2H); ^{13}C NMR (100 MHz, $CDCl_3$) δ 157.5, 139.7, 135.2, 133.6, 128.9, 128.6,

128.3, 127.6, 126.9, 126.5, 126.7, 45.8, 45.3, 41.4, 29.4; LCMS calculated for $C_{17}H_{18}N_2O$ $[M+H]^+$ = 267.1400; found 267.1502.

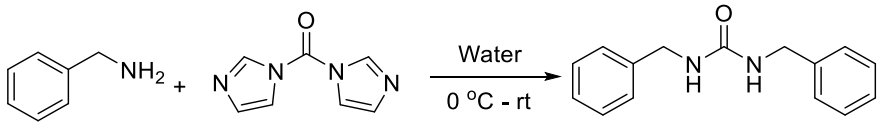

1,3-dibenzylurea; Benzylamine (51 µL, 0.50 mmol) in water was stirred at 0 °C for 10 minutes. Carbonyldiimidazole (194 mg, 1.2 mmol) was added and stirred at 0 °C for 1 hour. The reaction mixture was then warm up to room temperature and monitored by TLC. After complete conversion of amine to carbonylimidazolide, benzylamine (51 µL, 0.50 mmol) was added and the mixture stirred at room temperature for 3 hours. Reaction mixture was extracted with ethyl acetate and the organic later was dried with $MgSO_4$, concentrated, and purified by HPLC to give **3** (66 mg, 55 %); IR 3343.80, 2936.59, 1620.79 cm^{-1}; ^1H NMR (400 MHz, $CDCl_3$) δ 7.36 – 7.26 (m, 10H), 4.33 (s, 4H); HRMS calculated for $C_{15}H_{16}N_2O$ $[M+H]^+$ = 241.1335; found 241.1377.

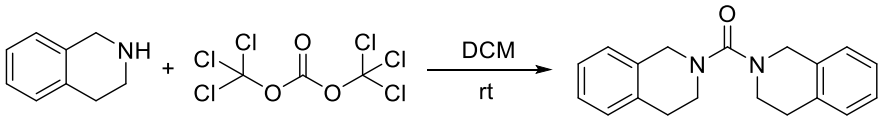

Bis(3,4-dihydroquinolin-1(2H)-yl)methanone; Tetrahydroisoquinoline (100 mg, 0.75 mmol) in CH2Cl2 (3.5 mL) was added to triphosgene (167 mg, 0.56 mmol) in CH2Cl2 (0.5 mL) at room temperature. The reaction mixture was stirred for 1 hour and 1N HCl (3.5 mL) was added. The product was extracted with CH2Cl2 (2 x 5 mL). The organic layers were dried over MgSO4. The solvent was evaporated and the residue was purified by HPLC to give 2 (32 mg, 29%); IR 3320.53, 2918.23, 1625.84 cm-1; 1H NMR (400 MHz, CD3OD) δ 7.15 (m, 6H), 7.11 (m, 2H), 4.49 (s, 4H), 3.57 (m, 4H), 2.95 (m, 4H); 13C NMR (100 MHz, CD3OD) δ 29.5, 45.8, 49.9, 127.3, 127.9, 128.8, 129.7, 133.8, 135.8, 165.8; HRMS calculated for C19H20N2O [M+H]+ = 293.1648; found 293.1598.

Bis(4-methylpiperazin-1-yl)methanone; Diisopropylethylamine (194 mg, 1.50 mmol) was added to mixture of 1-methylpiperazine (50 mg, 0.50 mmol), 4-methylpiperazin-l-ylcarbonyl chloride (122 mg, 0.75 mmol) in dichloromethane (20 mL) and the resultant mixture was stirred at room temperature for 1 hour. The mixture was concentrated and recrystallized from ethanol to give **1** (30 mg, 27 %); ^{1}H NMR (400 MHz, $CDCl_3$) δ 3.59 (m, 8H), 2.56 (m, 8H), 2.9 (s, 6H); ^{13}C NMR (100 MHz, CD_3OD) δ 163.65, 54.03, 45.04, 43.79; HRMS calculated for $C_{11}H_{22}N_4O$ $[M+H]^+$ = 227.1866; found 227.1803.

2.6.3 $[^{11}C]CO_2$ Trapping

The following set-up was chosen in order to trap and measure the radioactivity, and the trapping efficiency of the reaction (Figure 2.3).

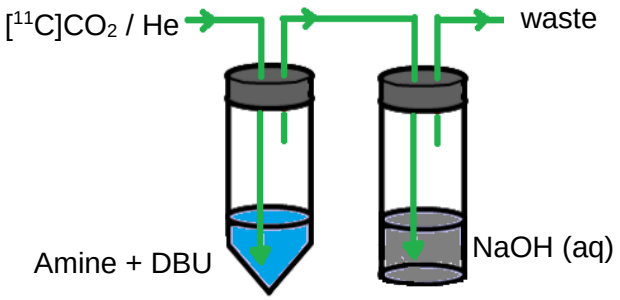

Figure 2.3 Reaction set-up.

DBU was added into a reaction vial containing an amine in CH_3CN. $[^{11}C]CO_2$ with a stream of helium gas at a flow rate of 1.4 mL/min post target depressurisation was bubbled directly into a reaction mixture. Helium and any un-trapped gases are transferred to a second vial containing concentrated NaOH solution (to measure untrapped $[^{11}C]CO_2$) prior to escaping to the waste bag.

$$\text{Trapping efficiency} = \frac{^{11}\text{C in the reaction vail}}{(^{11}\text{C in the reaction vial} + ^{11}\text{C in the NaOH solution})}$$

2.6.4 General radiolabelling procedure asymmetrical ureas

[^{11}C]CO_2 from the cyclotron target was bubbled in a stream of helium gas at a flow rate of 1.4 mL/min post target depressurisation directly into a reaction vial containing an amine (18.3 µmol), secondary amine (27.5 µmol) and DBU (0.13 µL, 0.9 µmol) in CH_3CN (300 µL). [^{11}C]CO_2 from the cyclotron was bubbled in the reaction mixture and the resulting solution was stirred, and heated at 50 ^{o}C for 1 minute. In a separate vial, tributylphosphine (9 µL, 36.6 µmol) was added to a solution containing di-*tert*-butyl azodicarboxylate (8 mg, 36.6 µmol) in CH_3CN (100 µL) under argon at room temperature. The resulting solution was transferred into the reaction mixture and stirred for one minute at 50 ^{o}C. The reaction was quenching it with water, the crude product was analysed by radio-HPLC.

2.6.5 General radiolabelling procedure symmetrical ureas

[^{11}C]CO_2 from the cyclotron target was bubbled in a stream of helium gas at a flow rate of 1.4 mL/min post target depressurisation directly into a reaction vial containing an amine (18.3 µmol) and DBU (0.13 µL, 0.9 µmol) in CH_3CN (300 µL). [^{11}C]CO_2 from the cyclotron was bubbled in the reaction mixture and the resulting solution was stirred, and heated at 50 ^{o}C for 1 minute. In a separate vial, tributylphosphine (9 µL, 36.6 µmol) was added to a solution containing di-*tert*-butyl azodicarboxylate (8 mg, 36.6 µmol) in CH_3CN (100 µL) under argon at room temperature. The resulting solution was transferred into the reaction mixture and stirred for one minute at 50 ^{o}C. The reaction was quenching it with water, the crude product was analysed by radio-HPLC.

The specific activity of the products was in the range of 20-40 GBq/µmol, similar in magnitude to other ^{11}C-labelled compounds produced at this laboratory.

2.7 Reference

[1] H. Lebel, O. Leogane, *Organic Letters* **2006**, *8*, 5717-5720.

[2] H. Zheng, X. Cao, K. Du, J. Xu, P. Zhang, *Green Chemistry* **2014**, *16*, 3142-3148.

[3] L. Troisi, C. Granito, S. Perrone, F. Rosato, *Tetrahedron Letters* **2011**, *52*, 4330-4332.

[4] L. Zhang, A. K. Darko, J. I. Johns, L. McElwee-White, *European Journal of Organic Chemistry* **2011**, *2011*, 6261-6268.

[5] F. Shi, Y. Q. Deng, *Journal of Catalysis* **2002**, *211*, 548-551.

[6] S. L. Peterson, S. M. Stucka, C. J. Dinsmore, *Organic Letters* **2010**, *12*, 1340-1343.

[7] T. Mizuno, Y. Ishino, *Tetrahedron* **2002**, *58*, 3155-3158.

[8] D. C. Dean, M. A. Wallace, T. M. Marks, D. G. Melillo, *Tetrahedron Letters* **1997**, *38*, 919-922.

[9] P. W. Miller, N. J. Long, R. Vilar, A. D. Gee, *Angewandte Chemie International Edition* **2008**, *47*, 8998-9033.

[10] C. Asakawa, M. Ogawa, K. Kumata, M. Fujinaga, K. Kato, T. Yamasaki, J. Yui, K. Kawamura, A. Hatori, T. Fukumura, M.-R. Zhang, *Bioorganic & Medicinal Chemistry Letters* **2011**, *21*, 2220-2223.

[11] E. D. Hostetler, H. D. Burns, *Nuclear Medicine and Biology* **2002**, *29*, 845-848.

[12] a) C. R. Child, S. Kealey, H. Jones, P. W. Miller, A. J. P. White, A. D. Gee, N. J. Long, *Dalton Transactions* **2011**, *40*, 6210-6215; b) S. Kealey, P. W. Miller, N. J. Long, C. Plisson, L. Martarello, A. D. Gee, *Chemical Communications* **2009**, 3696-3698; c) S. Kealey, A. J. P. White, A. D. Gee, N. J. Long, *European Journal of Inorganic Chemistry* **2014**, *2014*, 1896-1905.

[13] a) H. Doi, J. Barletta, M. Suzuki, R. Noyori, Y. Watanabe, B. Langstrom, *Organic & Biomolecular Chemistry* **2004**, *2*, 3063-3066; b) S. Kealey, S. M. Husbands, I. Bennacef, A. D. Gee, J. Passchier, *Journal of Labelled Compounds and Radiopharmaceuticals* **2014**, *57*, 202-208.

[14] A. Schirbel, M. H. Holschbach, H. H. Coenen, *Journal of Labelled Compounds and Radiopharmaceuticals* **1999**, *42*, 537-551.

[15] A. A. Wilson, A. Garcia, S. Houle, O. Sadovski, N. Vasdev, *Chemistry – A European Journal* **2011**, *17*, 259-264.

[16] J. W. Hicks, J. Parkes, O. Sadovski, J. Tong, S. Houle, N. Vasdev, A. A. Wilson, *Nuclear Medicine and Bbiology* **2013**, *40*, 740-746.

[17] J. W. Hicks, A. A. Wilson, E. A. Rubie, J. R. Woodgett, S. Houle, N. Vasdev, *Bioorganic & Medicinal Chemistry Letters* **2012**, *22*, 2099-2101.

[18] E. W. van Tilburg, A. D. Windhorst, M. van der Mey, J. D. M. Herscheid, *Journal of Labelled Compounds and Radiopharmaceuticals* **2006**, *49*, 321-330.

[19] a) P. Molina, E. Aller, Á. Lorenzo, P. López-Cremades, I. Rioja, A. Ubeda, M. C. Terencio, M. J. Alcaraz, *Journal of Medicinal Chemistry* **2001**, *44*, 1011-1014; b) L. Horner, H. Oediger, *Justus Liebigs Annalen der Chemie* **1959**, *627*, 142-162; c) H. Zimmer, M. Jayawant, P. Gutsch, *The Journal of Organic Chemistry* **1970**, *35*, 2826-2828.

[20] a) T. Sakakura, J.-C. Choi, H. Yasuda, *Chemical Review* **2007**, *107*, 2365-2387; b) B. H. Rotstein, S. H. Liang, J. P. Holland, T. L. Collier, J. M. Hooker, A. A. Wilson, N. Vasdev, *Chemical Communication* **2013**, *49*, 5621-5629.

[21] D. J. Heldebrant, P. G. Jessop, C. A. Thomas, C. A. Eckert, C. L. Liotta, *The Journal of Organic Chemistry* **2005**, *70*, 5335-5338.

[22] J. M. Hooker, A. T. Reibel, S. M. Hill, M. J. Schueller, J. S. Fowler, *Angewandte Chemie International Edition* **2009**, *48*, 3482-3485.

[23] E. R. Pérez, R. H. A. Santos, M. T. P. Gambardella, L. G. M. de Macedo, U. P. Rodrigues-Filho, J.-C. Launay, D. W. Franco, *The Journal of Organic Chemistry* **2004**, *69*, 8005-8011.

[24] K. J. Padiya, S. Gavade, B. Kardile, M. Tiwari, S. Bajare, M. Mane, V. Gaware, S. Varghese, D. Harel, S. Kurhade, *Organic Letters* **2012**, *14*, 2814-2817.

Chapter 3

[^{11}C]Carbamates and [^{11}C]Carbonates

3 Chapter 3

3.1 Introduction

Carbamates are common functional groups in biomolecules due to their stability *in vivo*, while carbonates are less common as they are less stable.[1] Nevertheless, carbamates and carbonates are found in various biologically active molecules (Figure 3.1) such as parabolan (an antiretroviral drug), zopiclone (a hypnotic agent) and physostigmine (a cholinesterase inhibitor).[2]

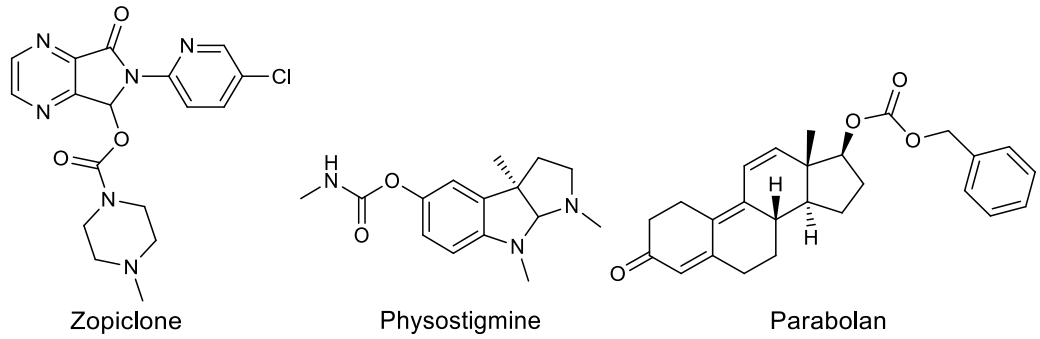

Figure 3.1 The chemical structure of zopiclone, physostigmine and parabolan.

The reaction between amines and chloroformate is one of the simplest reactions used for the synthesis of carbonates and carbamates (Scheme 3.1).[3]

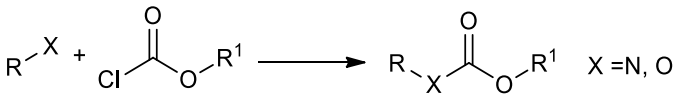

Scheme 3.1 The synthesis of carbamates using chloroformate.[3]

There are many literature reviews describing the synthesis of carbamates and carbonates.[4] Some of the main synthetic strategies include the use of isocyanates, CO and CO_2.

3.1.1 Synthesis of carbamates *via* isocyanates

One of the most commonly used synthetic methods for the synthesis of carbamates is *via* isocyanates.[5] Isocyanates are obtained through the reaction of amines with phosgene ($COCl_2$); the addition of an alcohol forms carbamates (Scheme 3.2).[1c, 6]

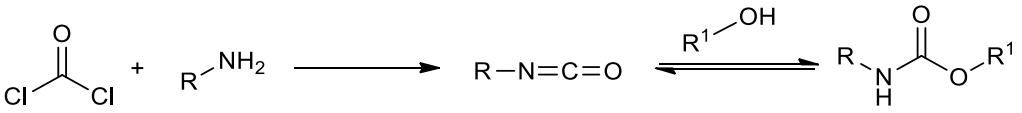

Scheme 3.2 The synthesis of carbamates *via* an isocyanate intermediate.

Isocyanates can also be synthesised using the Hoffmann rearrangement[7] (Scheme 3.3), Curtius rearrangement[8] (Scheme 3.4) or Lossen rearrangement[9] (Scheme 3.5), and subsequently converted into the carbamate.

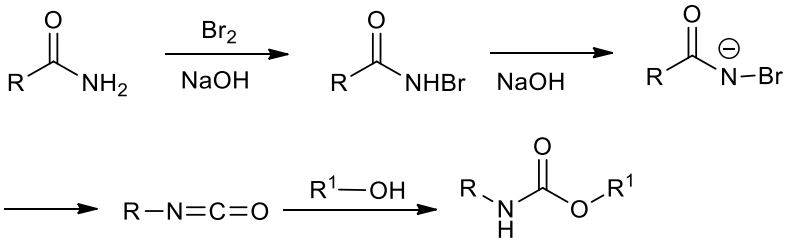

Scheme 3.3 The synthesis of carbamates *via* the Hoffmann rearrangement.[7]

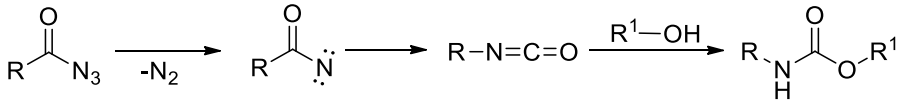

Scheme 3.4 The synthesis of carbamates *via* the Curtius rearrangement.[8]

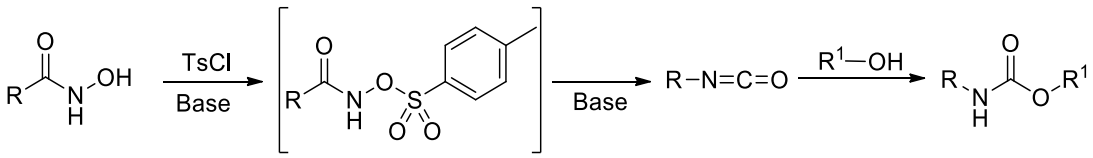

Scheme 3.5 The synthesis of carbamates *via* the Lossen rearrangement.[9]

3.1.2 Synthesis of carbamates from carbon monoxide

Carbon monoxide (CO) has been used for the synthesis of carbamates and carbonates. High pressures, temperatures and a catalyst are generally required for reactions with CO.[10]

Leung *et al.*[11] developed one of the first methods to incorporate CO into carbamates. Different catalysts such as cobalt (Co), rhodium (Rh), palladium (Pd) and copper (Cu) macrocyclic compounds were screened during reaction optimisation. The highest yields were obtained when Co or Rh was used as a

catalyst, NaI was used as a co-catalyst and a pressure of 6.9 MPa was used (Scheme 3.6).

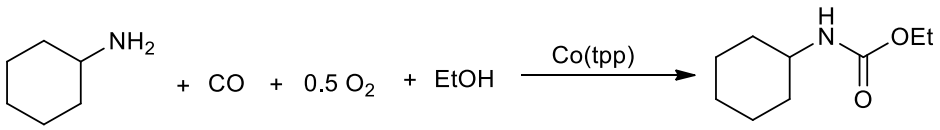

Scheme 3.6 Cobalt-catalysed carbamate synthesis.[11]

High yields were obtained when aromatic amines (aniline) and tertiary amines (tert-butyl amine) were used. However, due to the limited number of examples provided, the scope of the reaction is not clear.

Reactions with CO are expected to require high pressures and temperatures. However, Ren and Jiao[12] developed an attractive novel method to incorporate CO into carbamates at ambient pressure. Ligand-free palladium (ll) chloride ($PdCl_2$) salt was used as a catalyst and CO was introduced into the system *via* a balloon (Scheme 3.7).

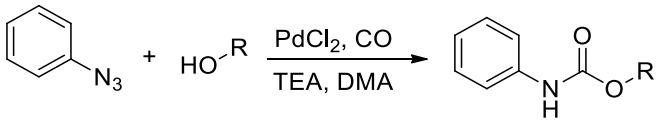

Scheme 3.7 Palladium-catalysed carbamate synthesis.[12]

During reaction optimisation, high yields were observed when polar solvents such as dimethylacetamide (DMA) were used, while no product or only trace amounts of product were detected when non-polar solvents were used. Interestingly, reduced yields (35 %) were observed when the ligand triphenylphosphine (PPh_3) was added to the reaction mixture. The scope of the reaction was investigated using different alcohols and azides (Table 3.1). Aryl azides with electron donating and electron withdrawing groups produced the target product at yields of over 80 %. High yields were also observed when primary and secondary azides were used. However, low yields of 14 % were observed when tertiary azides were used, most likely due to steric hindrance.

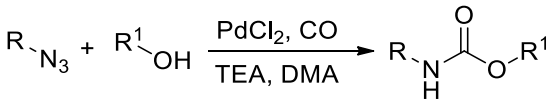

Table 3.1 Palladium-catalysed carbamate synthesis.[12]

Entry	Product	Yield (%)
1	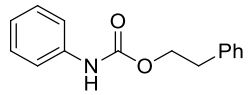	37
2	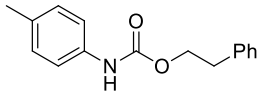	80
3	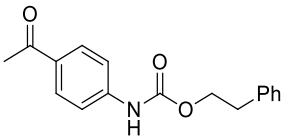	93
4	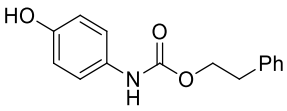	78
5	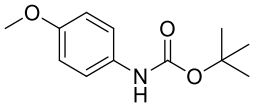	15
6	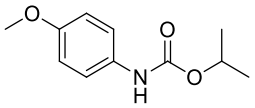	76

When the azide and $PdCl_2$ were added to the reaction mixture, an intermediate (Complex A) was formed with the release of N_2 (Scheme 3.8). CO was then inserted into the Pd Complex A to form the 3-membered ring intermediate, Complex B. A reductive elimination process then took place to form the isocyanate and the Pd-catalyst was subsequently regenerated. When alcohol was added to the mixture, nucleophilic addition took place to form the corresponding carbamate.

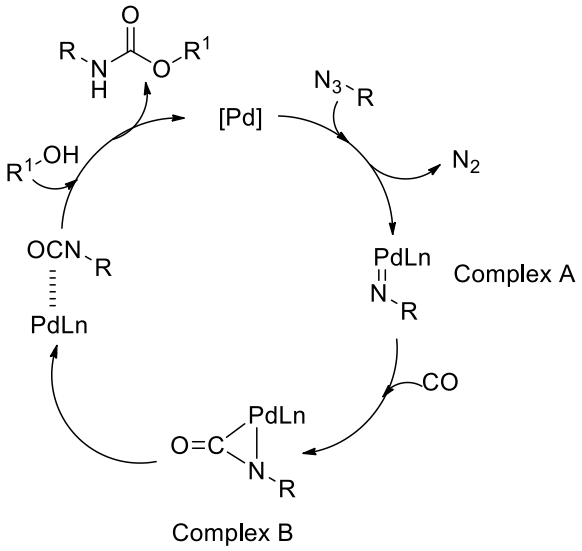

Scheme 3.8 The proposed reaction mechanism for the Pd-mediated synthesis of Pd.[12]

3.1.3 Synthesis of carbamates from carbon dioxide

CO_2 has been used extensively for the synthesis of carbamates. Many methods for the synthesis of carbamate derivatives such as oxazolidinone and polyurethane have been developed.

Paz *et al.*[13] used phosphorylating agents such as diphenyl phosphorochloridate (DPPCl) along with 1,1-amino alcohol and CO_2 to form cyclic carbamates with high yields. Other dehydrogenation reagents such as thionyl chloride ($SOCl_2$) and methanesulfonyl chloride (MsCl) can also be used. Due to the reagents reactivity, the reaction mixture has to be cooled to - 40 ^oC in order to obtain efficient yields. When the CO_2 is trapped within the solution, a carbamate anion is formed followed by two possible intermediates (Scheme 3.9). The intermediates subsequently cyclise to form the target compound.

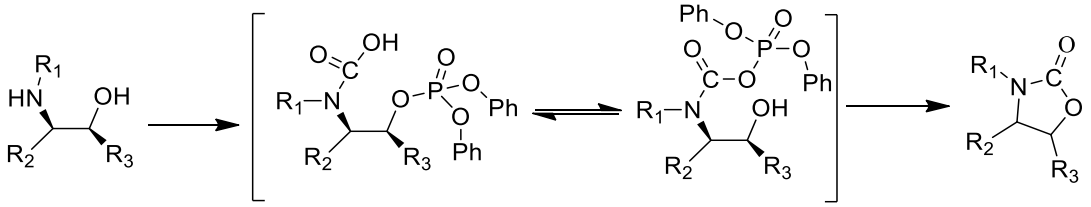

Scheme 3.9 The proposed reaction mechanism for the cyclization of 1,1-amino alcohols.[13]

Another strategy for the synthesis of carbamates *via* CO_2 was developed by Miller and Nguyen.[14] (Salen)chromium(III)/DMAP was found to be an ideal catalyst for inserting CO_2 into aziridines to form oxazolidinones. The reaction scope was examined with compounds containing various *N*-substituted and 1,2-disubstituted aziridines (Table 3.2). The reaction is efficient as it produces high yields for all of the assessed compounds including compounds with bulky *N*-substituted groups. The rates of reaction for different compounds were also explored and as expected, reactions with sterically hindered groups had low rates of reaction. Bulky azides coordinate poorly to the Cr centre, slowing their conversion to oxazolidinones.

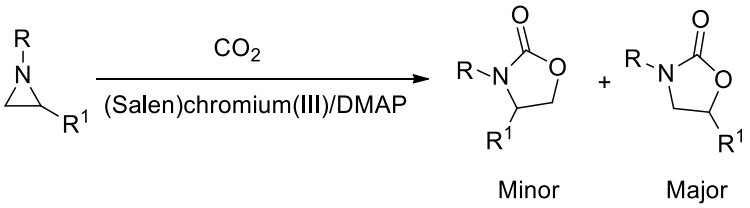

Table 3.2 The synthesis of cyclic carbamates.[14]

Entry	Product	Time (min)	Yield (%)
1	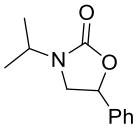	12	92
2	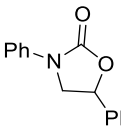	28	89
3	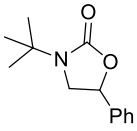	120	92
4	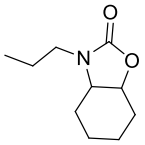	18	94

3.1.4 Synthesis of carbonates

Carbonates are generally synthesised using either carbonochloridate or CO_2. Kim and Jang[3] showed that carbonochloridate can be used for the synthesis of carbamates when it is added to alcohols and indium (Scheme 3.10).

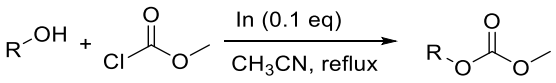

Scheme 3.10 Indium-catalysed carbonate synthesis.[3]

High yields of over 70 % were observed for aliphatic and aromatic alcohols. High yields were also observed for compounds with electron withdrawing groups such as nitrophenol (72 %). However, low yields were observed for satirically hindered tertiary alcohols such as tetra-butyl alcohol (41 %).

Another method for the synthesis of carbonates is *via* mesyl carbonates.[15] Mesyl compounds are frequently used to make hydroxyl groups a good leaving groups, due to theirs low costs and ease of handling (Scheme 3.11).

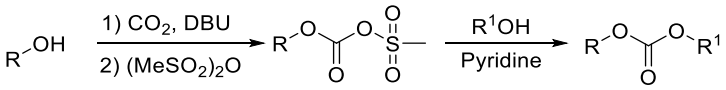

Scheme 3.11 The synthesis of carbamates *via* mesyl carbonates.[15]

The reaction is useful as it produces the target compound but in low yields (Table 3.3). The expected product was not observed when bulky alcohols such as isobutyl alcohol were used (Table 3.3, Entry 4).

Table 3.3 The synthesis of carbonates *via* mesyl carbonates.[15]

Entry	Product	Yield (%)
1	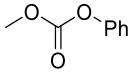	26
2	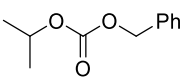	26
3	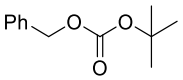	0

Calo *et al.*[16] developed a method for the synthesis of cyclic carbonates by coupling CO_2 and epoxides (Scheme 3.12). Many similar methods are available [17] however; this method is interesting due to the simplicity of the reaction and the high yields of the product produced. The product is formed when epoxides are dissolved in tetrabutylammonium bromide, in the presence of CO_2.

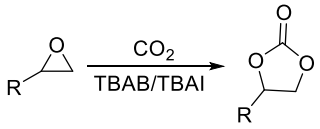

Scheme 3.12 The reaction between epoxides and CO_2.[16]

High yields are observed when aliphatic, aromatic and benzylic amine R-groups are used (Table 3.4).

Table 3.4 Synthesis of cynclic carbonate compounds.[16]

Entry	Product	Yield (%)
1	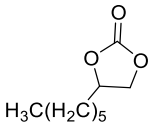	80
2	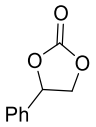	83
3	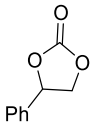	90

The reaction uses CO_2 which is a readily available reagent, and is performed under atmospheric pressure which makes it attractive. The translation of this strategy to radiochemistry is therefore appealing.

3.1.5 Synthesis of carbamates and carbonates *via* CO_2

Salvatore *et al.*[18] developed a method to incorporate CO_2 into carbamates and carbonates (Scheme 3.13) using caesium carbonate (Cs_2CO_3) as a base in the presence of tetrabutylammonium iodide (TBAI).

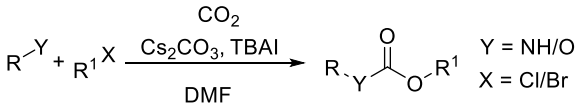

Scheme 3.13 The developed method for the synthesis of carbamates and carbonates.[18]

Caesium (Cs) plays an important role in the reaction as it is involved in charge stabilisation by forming a weak conjugate with the alkoxides generated *in situ* (Scheme 3.14).

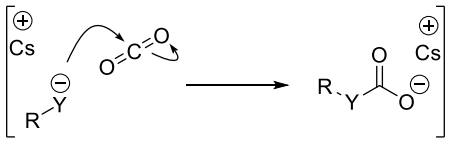

Scheme 3.14 The trapping of CO_2 by amine/alcohol and Cs_2CO_3.[18]

TBAI was found to be an essential additive. In absence of TBAI, *N*-alkylation is observed (Scheme 3.15) rather than the generation of carbamates and carbonates.

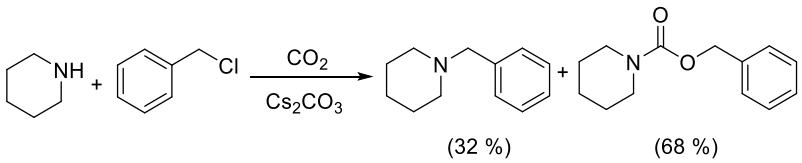

Scheme 3.15 The reaction in the absence of TBAI.[18]

The methodology was used for the synthesis of several carbamate and carbonate compounds. The reaction produced high yields for both chemical structures when aliphatic, aromatic and benzylic nucleophiles were used (Table 3.5).

Table 3.5 Synthesis of carbamates and carbonates using Cs_2CO_3 and CO_2.[18]

Entry	Product	Time (h)	Yield (%)
1	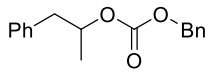	3	98
2	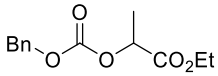	3	85
3	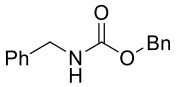	3	96
4	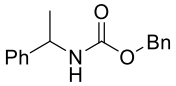	7	97
5	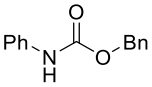	5	98

The reaction is one of the few methods available that has been shown to work to synthesise both carbonates and carbonates. Translating the reaction into a radioactive synthesis (using $[^{11}C]CO_2$) would enhance the portfolio of available molecules that can be radiolabeled with ^{11}C.

Since carbamates are common in biologically active molecules, the development of methods to radiolabel the functional group with PET radionuclide is of considerable interest. The structure has been radiolabelled previously using Grignard reactions as well as $[^{11}C]COCl_2$, $[^{11}C]CO$ and $[^{11}C]CO_2$.

3.1.6 Synthesis of $[^{11}C]$carbonates and $[^{11}C]$carbamates *via* the Grignard reaction

The Grignard reaction is one of the most well studied reactions used for C – C bond formation. When $[^{11}C]CO_2$ is treated with Grignard reagents, $[^{11}C]$carboxylmagnesium halide is formed. With the addition of phthaloyl dichloride, the corresponding acid halide is formed (Scheme 3.16).

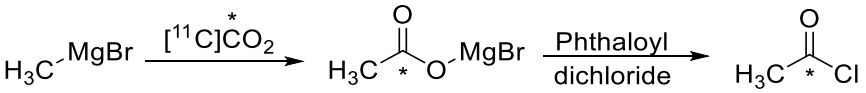

Scheme 3.16 Synthesis of acid halides using the Grignard reaction.[19]

When Bu_4NN_3 was added to the acid halide, the corresponding isocyanate compound was formed (Scheme 3.17).

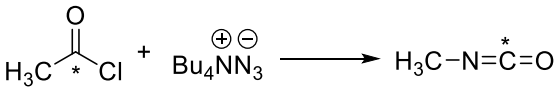

Scheme 3.17 Synthesis of [^{11}C]isocynates from [^{11}C]acid halide.[19]

One of the main disadvantages of using the Grignard reaction is the high reactivity of the reagents. The Grignard reagents readily absorb CO_2 from the atmosphere and are moisture-sensitive. Therefore, they have to be freshly prepared under inert atmosphere to obtain high specific activity.

This reaction has not been used for the radiolabelling of biomolecules that contain carbonates, however it has been used for the radiolabelling of carbamates such as heptylphysostigmine and physostigmine.[20]

Physostigmine is a reversible cholinesterase inhibitor that is found in the Calabar bean.[21] The reaction is a multi-step synthesis (Scheme 3.18) and includes the trapping of [^{11}C]CO_2, the Grignard reaction, synthesis of [^{11}C]acyl halide, synthesis of [^{11}C]isocyanate and finally the formation of the [^{11}C]physostigmine (Table 3.6).[20] The overall reaction time, including formulation, was approximately 60 minutes (Table 3.6) and the RCY 14 ± 3 % (decay corrected).

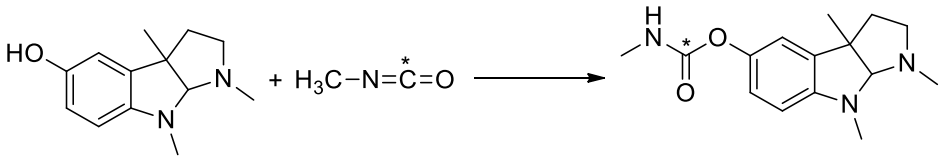

Scheme 3.18 The radiosynthesis of [^{11}C] physostigmine.[20]

Table 3.6 Overview of the synthesis of [^{11}C]physostigmine.[20]

		Radioactivity (GBq)	RCY % (decay corrected)
Time (min)	EOB	55.5	100
0 to 5	[^{11}C]CO_2	46	98
5 to 20	[^{11}C]CH_3OCl	15	52
20 to 37	[^{11}C]$CONCH_3$	3.7	23.5
37 to 52	[^{11}C]physostigmine	1.42	15.5
52 to 57	Formulation	1.19	14.5

The radiolabelling reaction is useful and produces the target compound. However, multi-step radiosynthesis and potential for isotopic dilution limits the usability of the Grignard reaction.

3.1.7 Synthesis of [^{11}C]carbamates *via* [^{11}C]phosgenes

[^{11}C]$COCl_2$, produced from [^{11}C]CO_2, is one of the most useful synthons used for radiolabelling with ^{11}C. Various compounds have been radiolabelled using the synthon due to the reaction being rapid and efficient.

Lemoucheux *et al.*[22] developed a method to radiolabel carbamates with [^{11}C]$COCl_2$. The reaction was developed for the radiosynthesis of [^{11}C]urea however, the authors demonstrated that the reaction can also be used for the radiolabelling of carbamates. Tetrahydroisoquinoline was chosen as the structure is frequently encountered in biomolecules, and the presence of an aromatic ring enables the compound to be UV active.

[^{11}C]carbamoyl chloride was initially synthesised by reacting an amine with [^{11}C]$COCl_2$ and sodium ethanolate (Scheme 3.19). A RCY of over 94 % was observed (decay corrected).

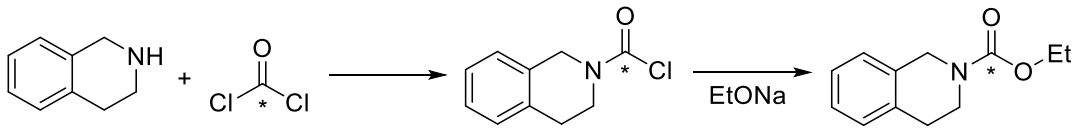

Scheme 3.19 The synthesis of a [^{11}C]carbamate *via* [^{11}C]carbamoyl chloride.[22]

Although the reaction was rapid and produced the target ^{11}C labelled carbamate efficiently, the reaction was limited by the synthesis of [^{11}C]$COCl_2$. Specialised equipment is required for its synthesis. The [^{11}C]$COCl_2$ is obtained from a multi-step reaction which affects the RCY as ^{11}C has a fairly short half-life.

3.1.8 Synthesis of [^{11}C]carbamates *via* [^{11}C]carbon monoxide

As previously stated in chapter 2, one of the main challenges encountered when radiolabelling with [^{11}C]CO is the low solubility in organic reagents. The reaction with [^{11}C]CO usually requires high pressure, high temperature and a catalyst. Nevertheless, there are methods available to radiolabel carbamates with [^{11}C]CO.

Doi *et al.*[23] developed one of the first methods to radiolabel carbamates with the [^{11}C]CO (Scheme 3.20). The reaction requires high pressure (35 MPa), high temperature (120 ^{o}C to 150 ^{o}C) and Rh complex ([RhCl(cod)]$_2$ /3 dppe).

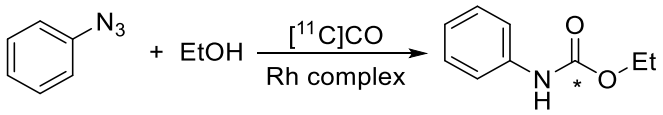

Scheme 3.20 Rhodium-mediated [^{11}C]carbamate synthesis.[23]

Different reagent concentrations were explored (Table 3.7) and high trapping efficiencies with good RCYs were observed when the lithium ethoxide (EtOLi) additive was added to the reaction.

Table 3.7 Synthesis of [^{11}C]ethyl phenylcarbamate by Rh-promoted carbonylation

Entry	Rh Complex	Additive	[^{11}C]CO trapping (%)	RCY[a] (%)
1	$RhCl(PPh_3)_3$	-	27	34
2	$[RhCl(cod)]_2$/2dppe	-	70	25
3	$[RhCl(cod)]_2$/3dppe	-	74	30
4	$[RhCl(cod)]_2$/3dppe	LiBr	81	40
5	$[RhCl(cod)]_2$/3dppe	EtOLi	90	76

[a] Determined by radio-HPLC.[23]

Similar to many other [^{11}C]CO radiolabelling methodologies, the reaction is believed to proceed *via* an isocyanate intermediate (Scheme 3.21).

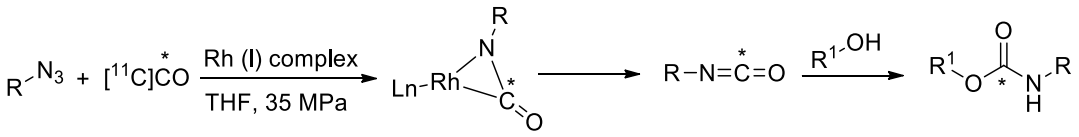

Scheme 3.21 The proposed Rhodium-mediated reaction mechanism.[23]

The radiolabelling strategy used [^{11}C]CO to radiolabel carbamates. High RCYs (> 70 %) were obtained however, high pressure and temperature was required, limiting the feasibility of the reaction.

Another method to radiolabel carbamates using [^{11}C]CO was developed by Kihlberg *et al.*[24] Sufficient trapping is observed when [^{11}C]CO is bubbled into a solution containing selenium, an amine and an alcohol in DMSO (50 - 95 %). A pressure of 0.3 – 0.4 MPa was required to obtain the target product, achieved using a microautoclave.

The reaction is believed to proceed by a similar mechanism to that with non-radioactive CO. Selenium (Se) traps the [^{11}C]CO within the solution by forming carbonylselenide. In the presence of an amine, the carbonylselenide reacts with it and forms a carbamoselenoate intermediate (Scheme 3.22).

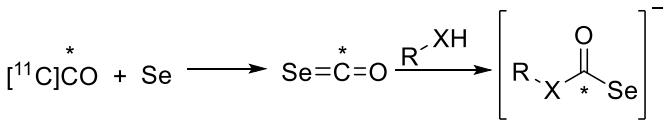

Scheme 3.22 The formation of the carbamoselenoate intermediate.[24]

When the amine added is a primary amine, the reaction is believed to form an isocyanate intermediate (Scheme 3.23), while secondary amines proceed *via* bis(carbamoyl) diselenides (Scheme 3.24).

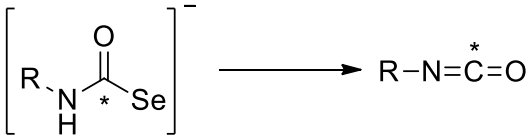

Scheme 3.23 The synthesis of [^{11}C]isocyanate with primary amine.[24]

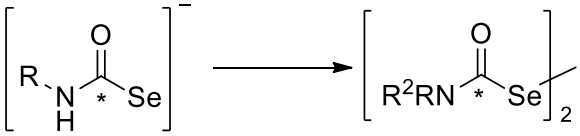

Scheme 3.24 The synthesis [^{11}C]bis(carbamoyl) diselenides with secondary amine.[24]

3.1.9 Synthesis of [^{11}C]carbamates *via* [^{11}C]carbon dioxide

[^{11}C]CO_2 is the most commonly used synthon for the radiolabelling of carbonates. Hooker *et al*.[25] developed the first one-pot synthesis to directly incorporate [^{11}C]CO_2 into a carbamate (Scheme 3.25).

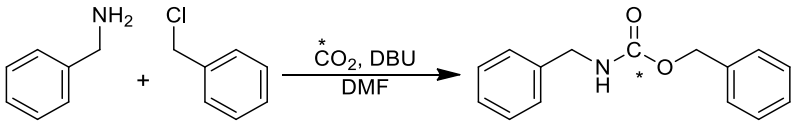

Scheme 3.25 The synthesis of [^{11}C]carbamate *via* [^{11}C]CO_2.[25]

The reaction involved the use of 1,8-diazabicyclo[5.4.0]undec-7-ene (DBU) as a trapping agent (Scheme 3.26). The authors propose that the [^{11}C]CO_2 is trapped by DBU and the resulting complex (Intermediate A) reacts with alkyl chloride to form a second complex (Intermediate B). The second complex then reacts with an amine to form the target ^{11}C labelled carbamate compound. [25]

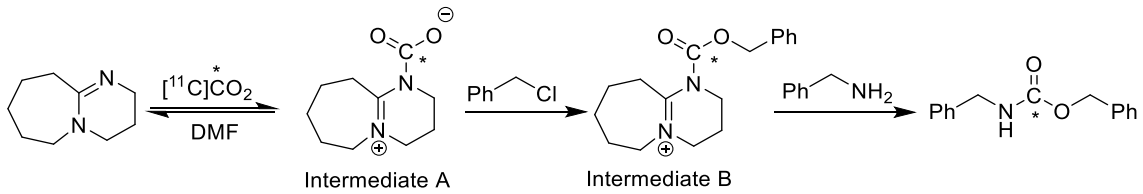

Scheme 3.26 The proposed mechanism for the synthesis of [^{11}C]carbonate.[25]

Different reaction conditions were used during the reaction optimisation process. The RCY was low when the reaction was carried out at room temperature. High RCYs were obtained with higher temperatures until a plateau was reached (75 ^{o}C, Table 3.8, Entry 2); after which the yield starts to decline (Table 3.8, Entry 3). The best results were obtained when the reaction was performed in DMF, at 75 ^{o}C and for 10 minutes.

Table 3.8 The effect of temperature on the radiosynthesis of [^{11}C]carbamates. [a] Determined by radio-HPLC.[25]

Entry	T (^{o}C)	RCY[a] (%)
1	25	17
2	75	85
3	100	75

Primary and secondary benzylic amines produced the target [^{11}C]carbamate with RCYs of over 60 % (Table 3.9, Entries 1 and 2). When aliphatic halides were used, the RCYs were reduced to less than 10 % (Table 3.9, Entries 3 and 6) and when aromatic amines (i.e. aniline) were used in the reaction, poor RCYs were observed (Table 3.9, Entries 5 and 6).

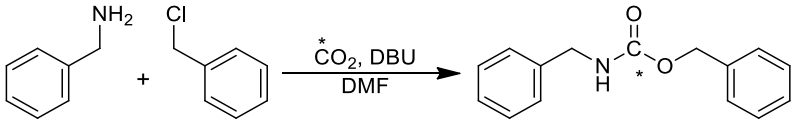

Table 3.9 The radiochemical yield of different ^{11}C radiolabeled carbamates.[25]

Entry	Product	RCY [a] (%)
1	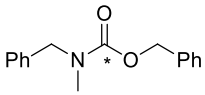	60
2	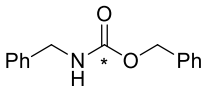	77
3	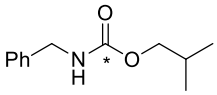	6
4	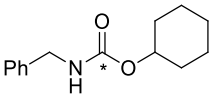	< 1
5	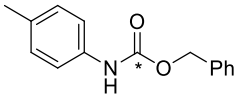	16
6	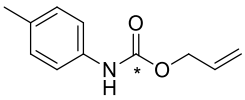	7

[a] Determined by radio-HPLC.

The reaction was rapid and attractive as it produced the [^{11}C]carbamate using [^{11}C]CO_2 directly from the cyclotron. However, the strategy was limited by the low RCYs observed for aromatic amines.

Wilson *et al.*[26] also developed a one-pot synthesis to incorporate [^{11}C]CO_2 into carbamate compounds using 2-*tert*-Butylimino-2-diethylamino-1,3-dimethylperhydro-1,3,2 diazaphosphorine (BEMP).

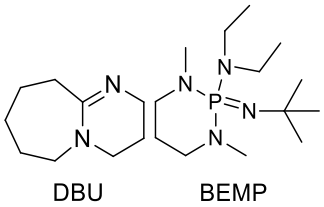

DBU BEMP

Figure 3.2 The chemical structure of DBU and BEMP.[26]

The reaction mechanism is believed to proceed *via* [^{11}C]isocyanate intermediates (Scheme 3.27), which react with amines to give carbamate compound.

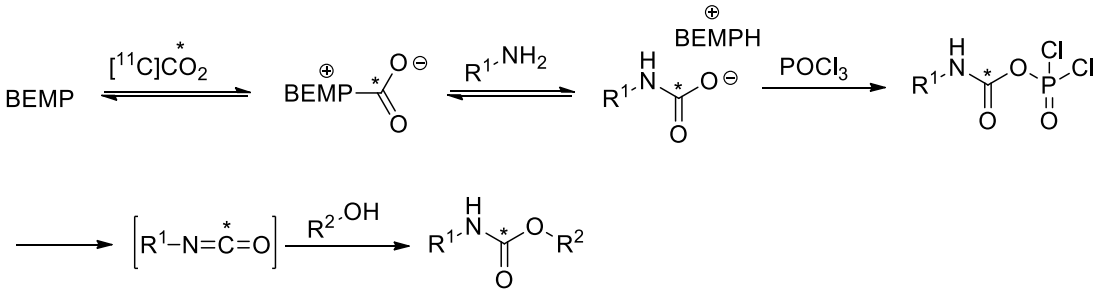

Scheme 3.27 The proposed mechanism of [^{11}C]urea synthesis *via* isocyanate.[26]

A large excess of $POCl_3$ (57 µmol) was found to favour the formation of isocyanate and when methanol was added to the reaction mixture, the target carbamate product was produced (Scheme 3.28). Reducing the $POCl_3$ (5.4 µmol) encouraged the formation of [^{11}C]symmetrical urea as the major product.

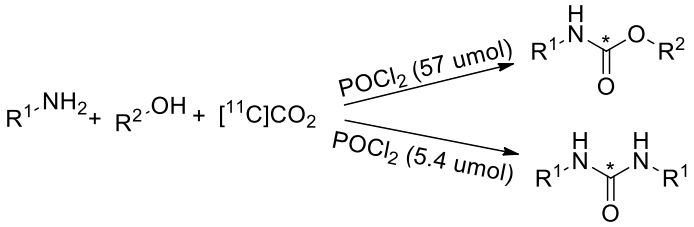

Scheme 3.28 The effect of $POCl_2$ concentration on the product.[26]

A notable feature of this method is that the overall synthesis time was under five minutes. The radiolabelling procedure used cyclotron-produced [^{11}C]CO_2 to radiolabel aliphatic and benzylic amines to form [^{11}C]carbamates.

The developed reaction was used by the group for radiolabelling various pharmaceuticals including URB694, SL25.1188, and metergoline.[27]

URB694 is a second generation phenyl carbamate fatty acid amide hydrolase inhibitor.[28] The method was used to radiolabel the compound to give an overall RCY of 0.7 ± 0.3 % based on the starting [^{11}C]CO_2 (uncorrected for decay) and a radiochemical purity of 99 % with a total synthesis time of 27 minutes (Scheme 3.29).[27b]

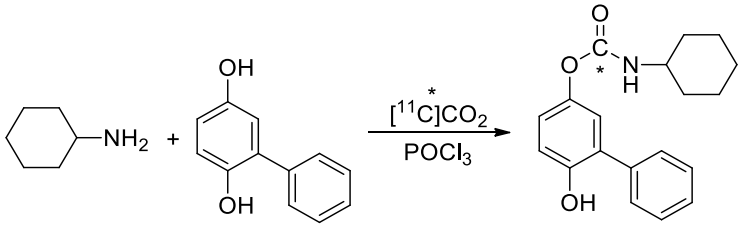

Scheme 3.29 The radiolabelling of URB694 with $[^{11}C]CO_2$.[27b]

The method has also been used to radiolabel SL25.1188, a promising monoamine oxidase B tracer. The tracer has previously been radiolabelled using $[^{11}C]COCl_2$ which limited its use due to specialised equipment and technical expertise being required.[27a] The compound was radiolabelled with $[^{11}C]CO_2$ with an overall radiochemical yield of 11.5 ± 0.9% based on the starting $[^{11}C]CO_2$ (uncorrected for decay), a radiochemical purity of > 99 % with a total synthesis time of 30 minutes and specific activity of 37.0 ± 1.7 GBq/µmol (Scheme 3.30).[29]

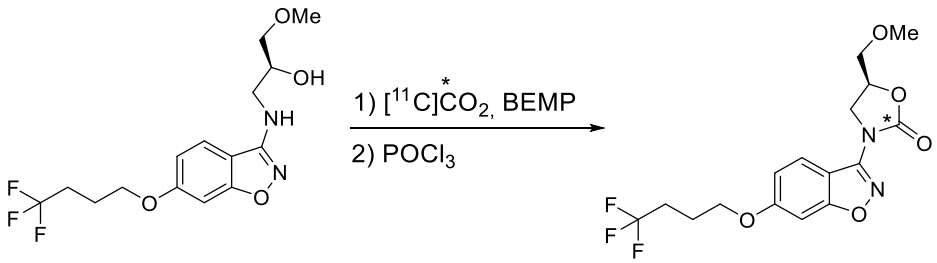

Scheme 3.30 The radiosynthesis of $[^{11}C]$SL25.1188 with $[^{11}C]CO_2$.[29]

Another method to radiolabel carbamates with $[^{11}C]CO_2$ has been described by Wilson *et al.*[30] Initially, the authors compared the trapping efficiency of $[^{11}C]CO_2$ by DBU and BEMP. Although both agents trapped 95 % of the $[^{11}C]CO_2$, the reaction using BEMP produced the target product with higher RCY (93 %) compared with 79 % RCY for DBU and therefore, BEMP was favoured (Table 3.10).

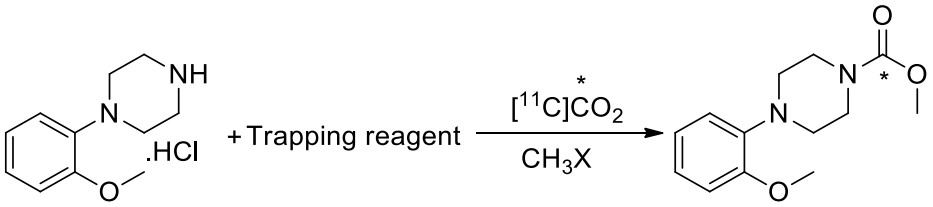

Table 3.10 The effect of DBU and BEMP on the reaction RCY. [30]

Entry	Trapping agent	RCY[a] (%)
1	DBU	79
2	BEMP	93

[a] Determined by radio-HPLC

Two possible mechanisms were proposed for trapping the $[^{11}C]CO_2$. The first method involved the trapping reagent interacting with the $[^{11}C]CO_2$ to form a zwitterion intermediate as shown in scheme 3.31. The intermediate is methylated by the DMS followed by nucleophilic substitution with the amine.

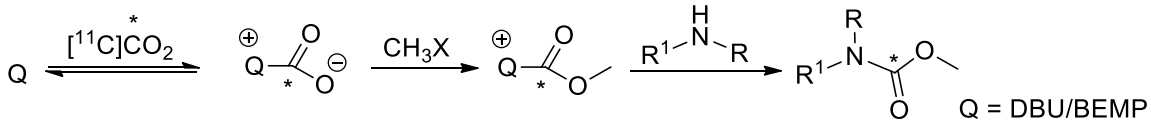

Scheme 3.31 The first proposed mechanism by Wilson *et al*.[30]

In the second proposed mechanism, nucleophilic substitution with the amine takes place before methylation with DMS (Scheme 3.32).

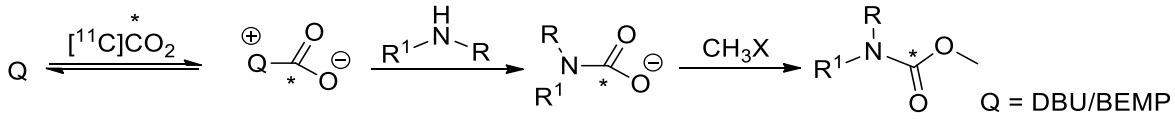

Scheme 3.32 The second proposed mechanism by Wilson *et al*.[30]

The method is used for the radiolabelling of GR 103545 (a selective kappa opioid receptor agonist).[30] The compound was radiolabelled with $[^{11}C]CO_2$ with an overall RCY of 13 % based on the starting $[^{11}C]CO_2$ (uncorrected for decay) and a total synthesis time was 23 minutes (Scheme 3.33).

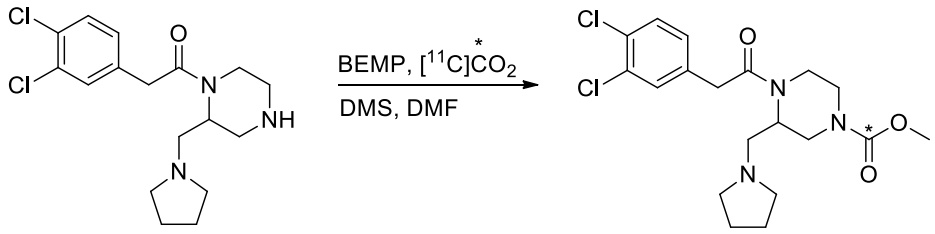

Scheme 3.33 The radiosynthesis of [^{11}C]GR 103545.[30]

3.1.10 Synthesis of [^{11}C]carbonates

There are no methods available to radiolabel carbonates with carbon-11 (^{11}C). This could be due to carbonates being less common compared to other structures such as carbamates. Carbonates are metabolised by proteins in the blood and as a result, only a limited amount of the tracer reaches the target receptor. However, radiolabelling carbonates would enable the studies of drug-protein interactions and metabolite studies. Therefore, strategies to radiolabel carbonates as well as carbamates with ^{11}C is of interest.

3.1.11 Summary

There are numerous compounds that contain carbamates and carbonates and as such, various methods have been developed for their synthesis. The carbamate structure has been radiolabelled with [^{11}C]CO and [^{11}C]CCl_4. Although the radiolabelling methods are useful and produce the target compound, they are limited by the specialised equipment required to perform the radiolabelling reactions. More recently, two new methods to radiolabel carbamates with [^{11}C]CO_2 directly from the cyclotron have been developed. The methods are efficient and have been used for the radiolabelling of SL25.1188 (Scheme 3.30) and GR 103545 (Scheme 3.33).

Although carbamates have a similar structure to carbonates, there are no methods available to radiolabel carbonates with ^{11}C and as PET imaging is becoming more widely available in clinical and research environments, the demand for more radiolabeling techniques is increasing.

The aim of this project was to develop a one-pot radiolabelling methodology that incorporates [^{11}C]CO_2 directly into alcohols/amines for the synthesis of [^{11}C]carbonates and [^{11}C]carbamates.

3.2 Results and discussion

The reaction for the radiosynthesis of [^{11}C]benzyl isopropyl carbonate (compound 1) was selected as a model reaction for optimisation due to high yields observed in non-radioactive synthesis.

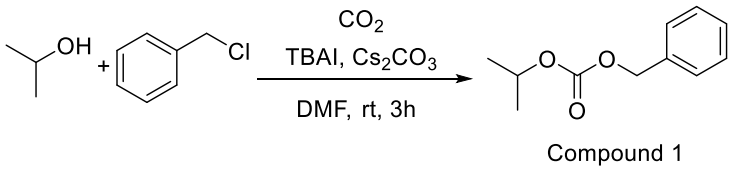

Scheme 3.34 Synthesis of reference compound.

3.2.1 Base optimisation

The initial challenge that is usually encountered when developing a novel [^{11}C]CO_2 radiolabelling strategy is the trapping of the radioactive gas within the reaction mixture. The trapping efficiencies of different caesium (Cs) bases in DMF were explored (Table 3.11). DMF was reported to work best for the synthesis of carbamates and carbonates when using non-radioactive CO_2 and therefore, it was selected as the solvent of choice.[18]

When Cs_2SO_4 and CsI were used as the trapping reagent, a minute amount of ^{11}C was detected within the solution (Table 3.11, Entries 1 and 2). The strongest bases screened, Cs_2CO_3 and CsOH, trapped the cyclotron-produced [^{11}C]CO_2 very effectively (Table 3.11, Entries 4 and 5) while CsF trapped to a lesser degree (33 %). These results indicate that the basicity of the Cs compound has an effect on the trapping efficiency.

Cs bases have low solubility in DMF and as a result, the reaction mixture is heterogeneous. Vigorous stirring of the mixture was essential for the reaction to proceed. The low solubility of Cs compounds can be explained by the size of the

ion. Large ions such as Cs have a low degree of solvation in a reaction medium. As the Cs compounds are the trapping agent, it was essential to use flat-end needles and a low carrier gas flow rate to obtain sufficient [^{11}C]CO_2 trapping.

The radiolabelling reactions with Cs_2CO_3 produced the target radiolabelled compound with a moderate RCC of 24 % (Table 3.11, Entry 4) while CsI produced the target compound at a RCC of 5 % (Table 3.11, Entry 2). Although CsOH trapped the radioactive isotope efficiently (> 98 %), the reaction did not produce the target compound (Table 3.11, Entry 5). Similarly, the radiolabeled product was not observed when Cs_2SO_4 and CsF were used.[18] The RCCs was estimated by radio-HPLC and defined as the area under the target ^{11}C-labelled target product peak expressed as a percentage of the total ^{11}C labelled peak areas observed in the chromatogram

Cs_2CO_3 was then compared with potassium carbonate and calcium carbonate (Table 3.11, Entries 6 and 7). The trapping efficiencies were extremely low for both reagents and the target product was not produced. Similar results have been reported in the literature when non-radioactive CO_2 is used.[18] These observations indicate that Cs plays a role in trapping the radioactive [^{11}C]CO_2 and the synthesis of target molecule. Cs has a large cationic radius, a low charge density and is highly polarizable. This enables Cs to be “stripped” when added to an aprotic solvent such as DMF which enables it to form a weak conjugation with CO_2 *in situ.*

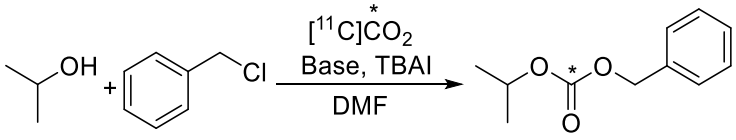

Table 3.11 The base optimisation reactions.

Entry[a]	Base	Trapping (%)	RCC[b] (%)
1	Cs_2SO_4	1.5	0
2	CsI	4.3	5
3	CsF	33.5	0
4	Cs_2CO_3	95.2	24
5	CsOH	98.7	0
6	K_2CO_3	10	0
7	$CaCO_3$	0	0

[a] Screening conditions: isopropyl alcohol (22 µmol), TBAI (66 µmol), base (66 µmol) in 400 µmol DMF. Benzyl chloride (66 µmol) 25 °C, 10 min. [b] RCC values are average of 2 (n = 2), determined by radio-HPLC.

After discovering Cs_2CO_3 was the best base for the reaction, experiments were then evaluated in different solvents, temperatures and reaction times (Table 3.12).

3.2.2 Solvent, temperature and time optimisation

DMF, CH_3CN and DMSO were selected as solvents due to their aprotic properties which enable them to polarize Cs compounds. CH_3CN and DMSO trapped $[^{11}C]CO_2$ but to a lesser extent than DMF (20 % and 65 % respectively). Only reactions conducted with DMF as the solvent produced the target radiolabeled product (Table 3.12, Entry 1) and therefore, DMF was selected as the solvent of choice for subsequent reactions.

The reaction dependency on temperature was then examined. At room temperature, 24 % RCC was observed however, when the temperature was

increased to 65 °C, the RCC increased to 33 % (Table 3.12, Entry 5). Increasing the reaction temperature further to 100 °C promoted the product formation and resulted in a RCC of 82 %.

A short reaction time is beneficial when radiolabelling with ^{11}C. Reducing the reaction time from 10 minutes to 5 minutes reduced the RCC slightly (Table 3.12, Entries 6 and 7). Doubling the reaction time to 20 minutes resulted in similar RCCs to that obtained with 10 minutes reaction time.

Reactions conducted at 100 °C for 10 minutes produced the best results, however, high reagent concentrations were used. The use of lower regent concentrations is advantageous, especially for radiolabelling complexes and precious precursors. The next experiments explored the possibilities of reducing the reagent concentrations.

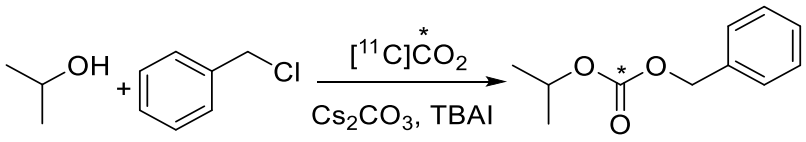

Table 3.12 The solvent, time and temperature optimisation reactions.

Entry[a]	Solvent	T (°C)	Time (min)	RCC[b] (%)
1	DMF	25	10	24
2	CH_3CN	25	10	0
3	DMSO	25	10	0
5	DMF	65	10	33
6	DMF	100	10	81
7	DMF	100	5	77
8	DMF	100	20	81

[a] Screening conditions: isopropyl alcohol (22 µmol), TBAI (66 µmol), Cs_2CO_3 (66 µmol) in 400 µmol solvent. Benzyl chloride (66 µmol). [b] RCC values are average of 2 (n = 2), determined by radio-HPLC.

3.2.3 Concentration optimisation

The results in Table 3.13 indicated that reducing the concentration of the organohalide and TBAI has a significant effect on the RCC (Table 3.13, Entries 2 and 3). TBAI was found to be essential for the reaction to proceed as the target product was not observed in its absence (Table 3.13, Entry 4). Nucleophilic addition of alcohols into organohalides was favoured in the absence of TBAI when the reaction was performed with non-radioactive CO_2 which reduces the availability of the reagents for $[^{11}C]CO_2$ incorporation.

Reducing the concentration of Cs_2CO_3 reduced the trapping efficiency to 5 – 15 % and the RCC to 4% (Table 3.13, Entry 5).

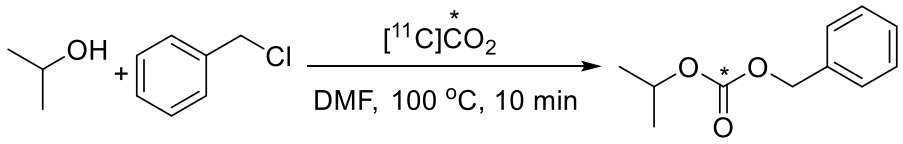

Table 3.13 The concentration (equivalence) optimisation reactions.

Entry	ROH	R-Cl	Cs_2CO_3	TBAI	RCC[b] %
1[a]	1	3	3	3	82
2	0.3	1	1	1	0
3	1	1	1	1	0
4	1	3	3	-	0
5	3	3	1	3	4

[a] Reaction conditions: alcohol (1.65 µL, 22 µmol), TBAI (24 mg, 66 µmol), Cs_2CO_3 (21 mg, 66 µmol) in 400 µmol DMF. Benzyl chloride (7.5 µL, 66 µmol), 100 °C, 10 min. n = 3. RCC values are average of 2 (n = 2), determined by radio-HPLC.

After examining the reaction with different bases, concentrations, solvents and temperatures, best results were obtained when Cs_2CO_3 and DMF were used at 100 °C.

It has been shown that in some cases, similar reaction conditions can be used for the synthesis of carbamates and carbonates when working with non-

radioactive CO_2.[18] Our optimized reaction conditions for the radiosynthesis of [^{11}C]carbonates were therefore tested for the radiolabelling of [^{11}C]carbamates.

RCCs of 90% were observed when tetrahydroisoquinoline and benzyl chloride were used for the radiosynthesis of compound 2 (Scheme 3.35). This suggested that the developed method could be used to radiolabel both carbamates and carbonates.

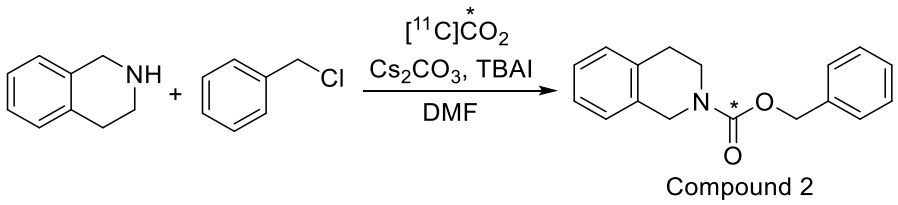

Scheme 3.35 The radiolabelling of carbamate with [^{11}C]CO_2. Reaction conditions: Amine (1.65 µL, 22 µmol), TBAI (24 mg, 66 µmol), Cs_2CO_3 (21 mg, 66 µmol) in 400 µmol DMF. Benzyl chloride (7.5 µL, 66 µmol), 100 °C, 10 min.

3.2.4 HPLC analysis

When the developed method was used for radiolabelling, the target product was the main peak observed on the radio-HPLC chromatogram (Figure 3.3, A). A small radioactive peak was observed around the solvent front which could be [^{11}C]carbonate or unreacted [^{11}C]CO_2 interacting with Cs.

Although high conversions were observed for both [^{11}C]carbonates and [^{11}C]carbamates on the radio-HPLC chromatogram, the UV-HPLC chromatogram showed a major mass peak for the reference compound suggesting a low specific activity (Figure 3.3). The typical specific activity of ^{11}C-labelled compounds produced in the laboratory is in the range of 30-50 GBq/µmol at the EOB. The specific activity produced by the Cs_2CO_3-mediated reaction was in the range of 1-10 GBq/µmol, suggesting 3 – 5 fold isotopic dilution from the Cs_2CO_3 carbonate moiety.

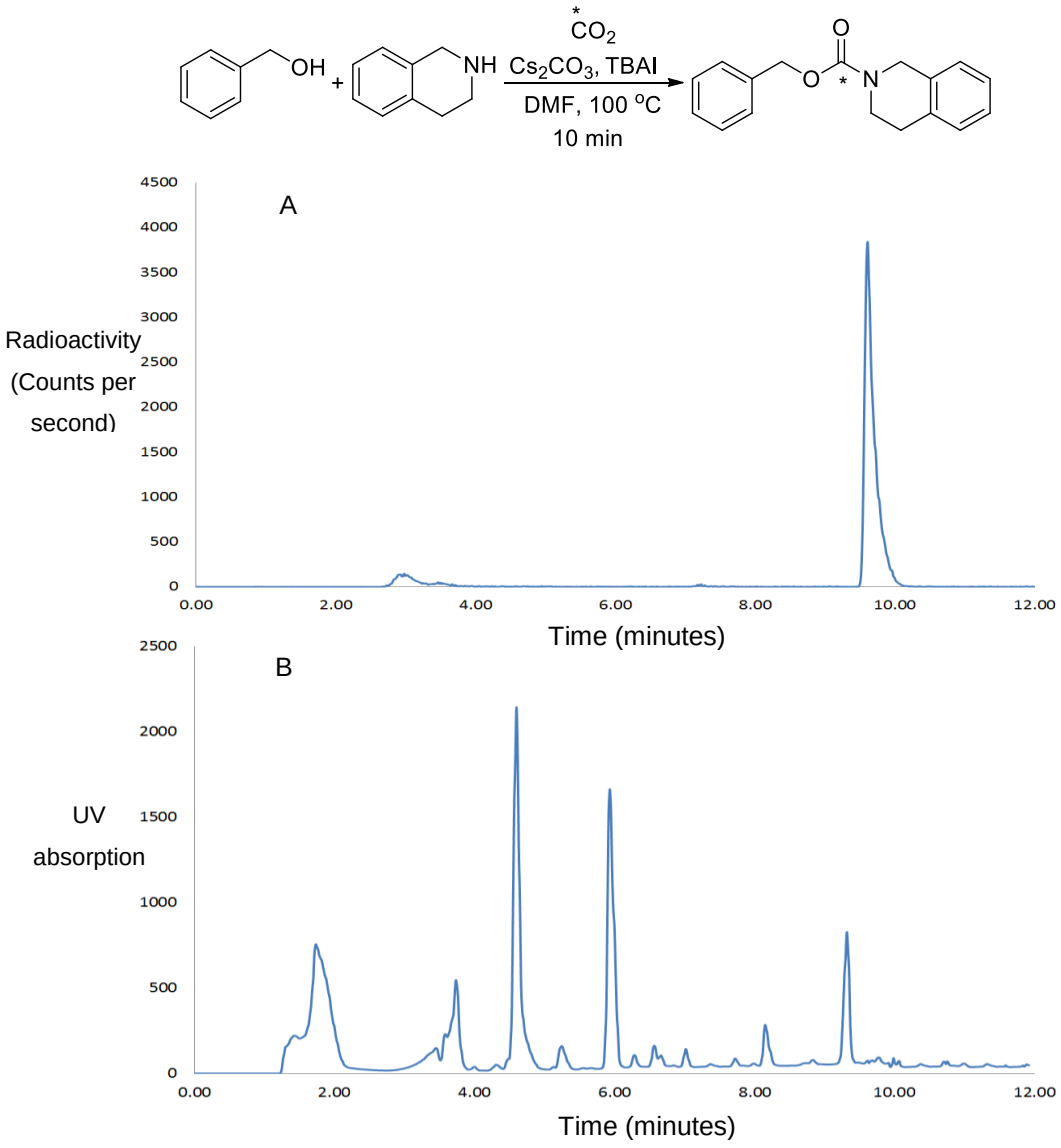

Figure 3.3 The crude radio-HPLC of compound 2. [A] Radioactivity (counts per sec.). [B] UV absorption at 254 nm.

3.2.5 Reaction mechanism

The results indicated that Cs_2CO_3 and TBAI were essential for sufficient [^{11}C]CO_2 trapping and forming the target product. Similar results were observed when the reaction was performed using non-radioactive CO_2. It was therefore reasonable to presume that the radiolabelling reaction followed a similar mechanism to that of the non-radioactive reaction.

3.2.6 Synthesis of [^{11}C]carbamates

A nucleophilic attack from the amine lone pair on the [^{11}C]CO_2 forms an ammonium salt. The ammonium salt is deprotonated by the Cs_2CO_3 base to form a Cs carbamate salt and Cs bicarbonate (Scheme 3.36).

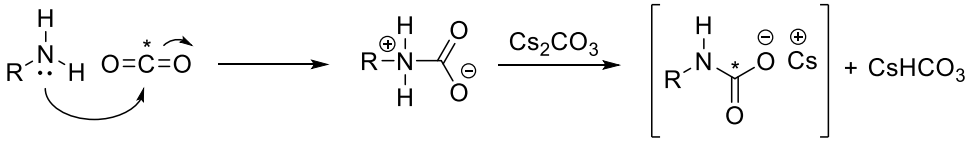

Scheme 3.36 The synthesis of Cs carbamate salt.

Organochlorides interact with TBAI to form organoiodide (Scheme 3.37).

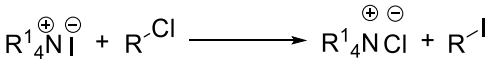

Scheme 3.37 The synthesis of organoiodide.

The organoiodide reacts with the Cs carbamate salt to form the target product (Scheme 3.38).

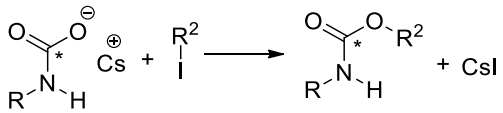

Scheme 3.38 Synthesis of [^{11}C]carbamates.

3.2.7 Synthesis of [^{11}C]carbonates

The mechanism for the synthesis of [^{11}C]carbamates is expected to be similar to that of [^{11}C]carbamates (Scheme 3.39).

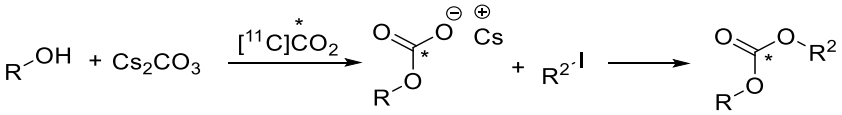

Scheme 3.39 The overall reaction scheme for the synthesis of [^{11}C]carbonates.

3.2.8 Summary

A novel radiolabelling methodology for the radiosynthesis of [^{11}C]carbamates and [^{11}C]carbonates has been developed. The method uses [^{11}C]CO_2 directly from the cyclotron and gives a high RCCs in a short reaction time. The strategy enables the radiolabelling of carbonates which were previously inaccessible for ^{11}C radiolabelling. This reaction is therefore a useful addition to the arsenal of methodologies available for ^{11}C radiolabelling.

Due to the presence of carbonate (from Cs_2CO_3), the reaction results in a low specific activity. Although this is undesirable for receptor or enzyme imaging, the method can be used for other purposes including the study of the biodistribution and kinetics of drugs *in vivo*.

Due to the low specific activity, research focus was shifted towards the development of a different methodology for radiolabelling carbamates. The Mitsunobu reaction described in chapter 2 has been reported to produce carbonates efficiently as well as urea when non-radioactive CO_2 is used.[31] The method developed in chapter 2 for radiolabelling ureas uses Mitsunobu reaction, the optimised reaction conditions can, in principle, be applied to the radiolabelling of [^{11}C]carbamates.

3.2.9 Method 2

Zopiclone (Figure 3.2) is a $GABA_A$ agonist that is used as a hypnotic agent. The compound has an affinity (K_i) value of 24 nM in the cerebral cortex and 31 nM in the cerebellum. In addition to its potential use as a PET radiotracer, it was chosen as a molecule to demonstrate proof-of-concept labelling using the method described in chapter 2.

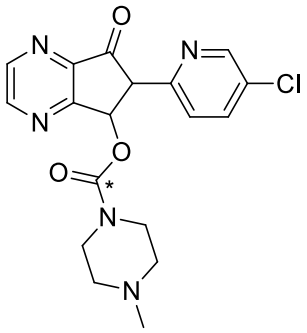

Figure 3.4 The structure of Zopiclone.

Methylation with [^{11}C]CH_3I would be an obvious labelling strategy that comes to mind when considering the radiolabelling of Zopiclone. Although that would be ideal, the compound is metabolised into desmethylzopiclone which is also an active drug (Scheme 3.40).[32]

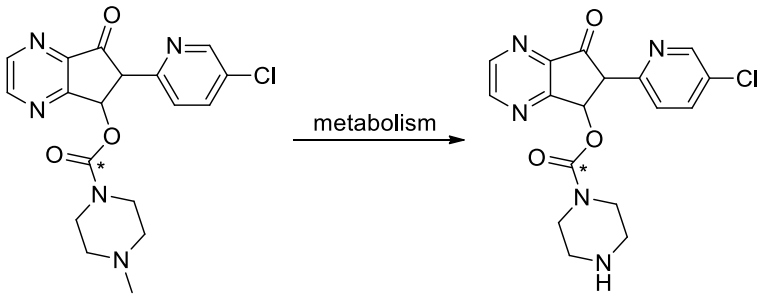

Scheme 3.40 The liver metabolism of Zopiclone to desmethylzopiclon.

Radiolabelling at the carbonyl position will enable *in vivo* assessment of both methylated and desmethylated compounds.

Initially, reactions were performed using the previously developed method (chapter 2) for the radiolabeling of ureas. The obtained chromatogram did not show the target radiolabelled compound (expected to elute at 8.15 min). However, a major peak (80 %) was observed (at 7.35 min) which corresponded

to the ^{11}C-labelled symmetrical urea (Figure 3.5). Three minor peaks were also observed; the first peak was unreacted [^{11}C]CO_2 (at 2.40 min). The labelled by-products were also observed when the reaction was performed in the absence of the alcohol and the amine compound, suggesting that the peaks were Mitsunobu reaction by-products.

Amines are more reactive than alcohols and the ratio of amine to alcohol in the first experiment was high (3: 1) which could explain the [^{11}C]symmetrical urea formation. In an attempt to prevent the synthesis of [^{11}C]symmetrical ureas, the concentration of the amine was reduced so that it matched the concentration of the alcohol. The crude product was obtained in 24 % RCC (Table 3.14, Entry 2). However, a reduced trapping efficiency (30 – 60 %) was also observed. BEMP has been reported to have a better trapping efficiency than DBU and in order to increase the trapping, the trapping reagent was changed to BEMP. High trapping efficiency of > 90 % was obtained, however, the ^{11}C-labelled product was not observed (Table 3.14, Entry 3).

To increase the trapping efficiency while using DBU, the concentration of the trapping reagent was increased (Table 3.14, Entries 4 and 5). Although this improved the trapping efficiency, the target product was not observed. The results indicated that an optimal concentration of DBU was essential for the reaction to produce the [^{11}C]zopiclone product.

The reaction was then performed using high concentrations of the alcohol compared to the amine (3:1) while keeping the concentration of the DBU constant (Table 3.14, Entry 6). A trapping efficiency of 70 % and a RCC of 28 % was observed (Figure 3.6).

In order to increase the RCC and avoid the synthesis of a [^{11}C]symmetrical urea, [^{11}C]CO_2 was bubbled into a solution containing only alcohol and DBU in CH_3CN, and the amine subsequently added (Table 3.14, Entry 7). Increase in RCC was not observed and [^{11}C]symmetrical urea was observed as the major product.

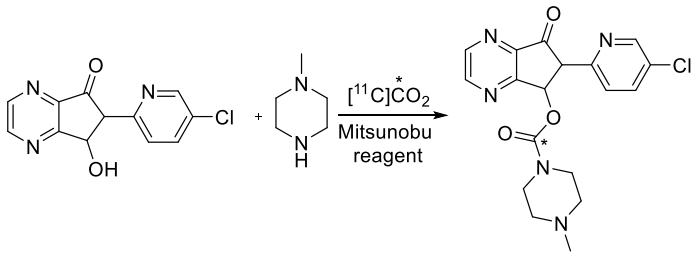

Table 3.14 Method 2 optimisation reactions.

Entry	[Base] [d]	[ROH]	[R_2NH]	RCC (%)[e]
1[a]	10%	1	3	0
2	10%	1	1	24
3[b]	10%	1	3	0
4	20%	1	1	0
5	100%	1	1	0
6	10%	3	1	28
7[c]	10%	3	1	26

[a] Reaction conditions: amine (18.3 µmol), alcohol (27.5 µmol), DBU (0.8 µmol), in 300 µmol CH_3CN heated at 50 °C for 1 min, Mitsunobu reagents (36.6 µmol) in 100 µmol CH_3CN added and stirred for 1 min. [b] BEMP was used as the base. [c] amine added after the trapping of [^{11}C]CO_2. [d] equivalence of base used. [e] RCC values are average of 2 (n = 2), determined by radio-HPLC.

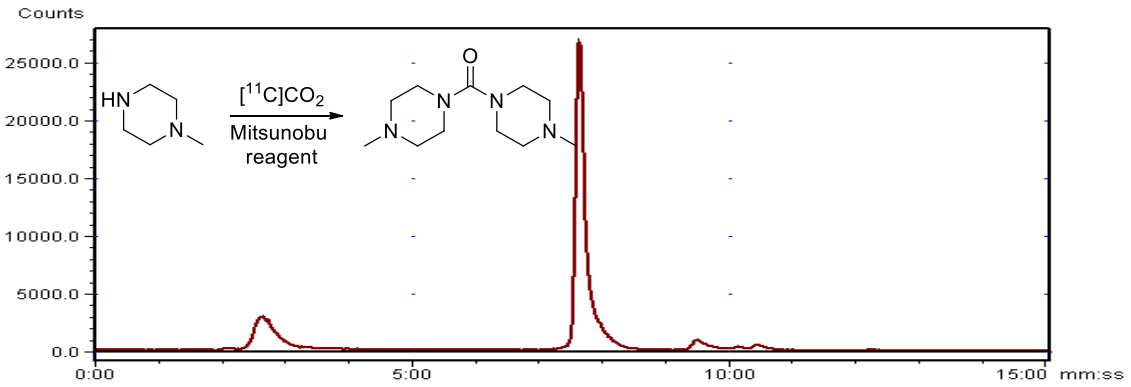

Figure 3.5 The radio-HPLC chromatogram of the synthesis of [^{11}C]symmetrical urea. The symmetrical urea t_r = 7.45 min and unreacted [^{11}C]CO_2 t_r = 2.50 min

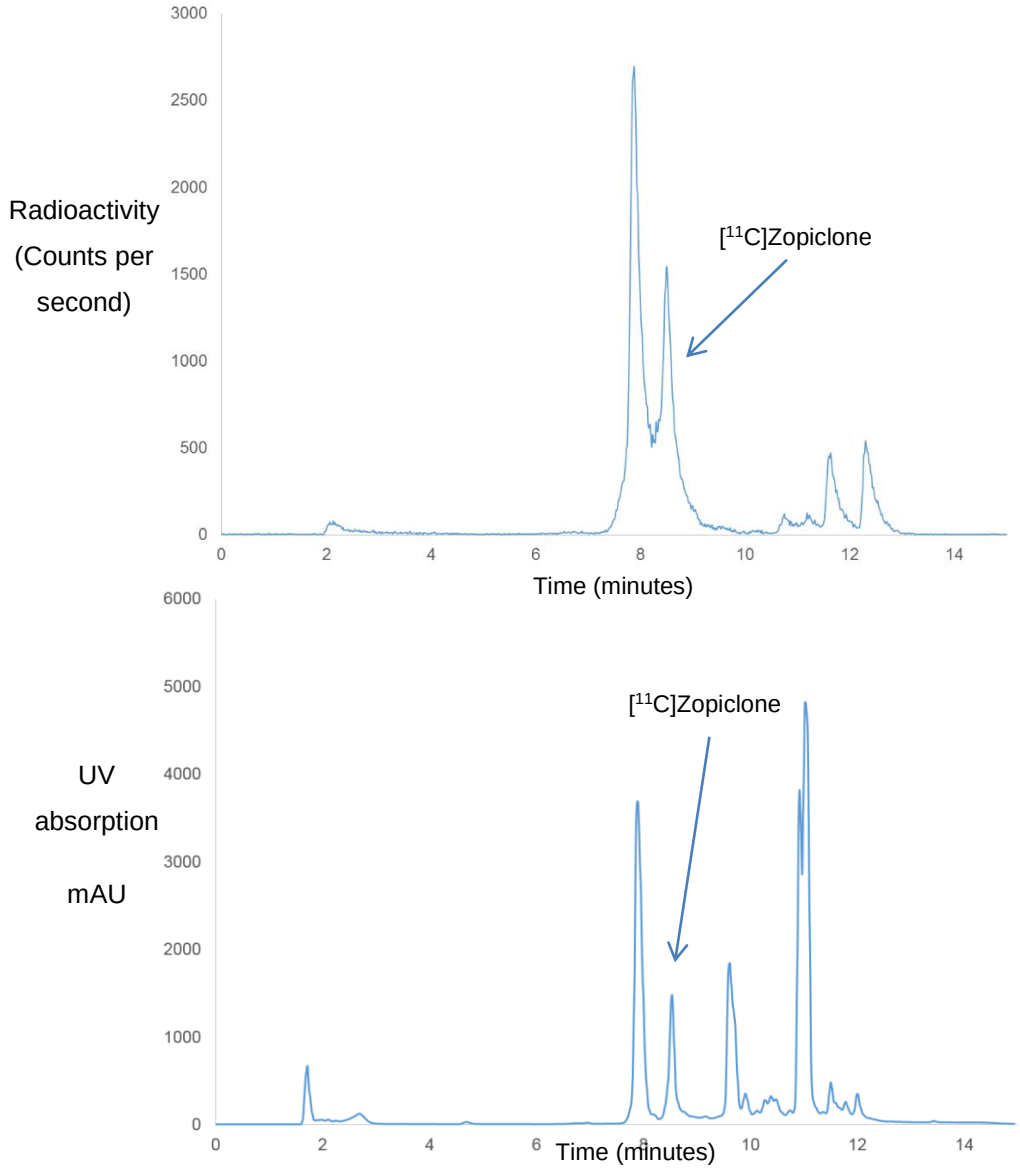

Figure 3.6 Radio-HPLC and UV chromatograms of the crude [^{11}C]Zopiclone reaction co-injected with the reference standard. The target product t_r = 8:15 minutes and the symmetrical urea t_r = 7.45 min. unreacted [^{11}C]CO_2 at 2.10 min and unknown radiolabelled by-products t_r = 10.40, 11.15, 11.45 and 12.20 min.

Further attempts to increase the RCC by performing the reaction at different temperatures (25 ^{o}C and 40 ^{o}C) were unsuccessful and frustratingly, the product formation was not always reproducible. The best purification was obtained when a gradient HPLC method (methanol and water) were used (Figure 3.6). High purity of the radiotracer is essential in order to obtain reliable autoradiography. The use of different HPLC columns and solvents for purification is currently in progress.

3.3 Conclusion

Carbamates and carbonates are common structural features of molecules acting on the GABA and glutamate receptor system. To date, there are few methods in which these structures can be radiolabeled with ^{11}C. Radiolabeling this class of molecules offers an opportunity to deepen our understanding of GABA and glutamate receptor's function by following the fate of these radiolabeled molecules *in vivo*.

There are many non-radioactive synthetic methodologies that can be translated to radioactive synthesis and an example of this is the chemistry by Salvatore *et al.*[18] The reaction is ideal as it is high yielding and it can be used for the synthesis of both carbamates and carbonates.

To date, there are no methods available for the radiolabelling of carbonate structures with ^{11}C however, carbamates have been radiolabelled. The established methods to radiolabel carbamates with ^{11}C are limited by functionality tolerance therefore, new radiolabeling reactions to incorporate ^{11}C into carbonates and carbamate molecules are required. Novel methods would increase the range of radiotracers that can be synthesised.

This work describes two methods to radiolabel carbamates with $[^{11}C]CO_2$ directly from the cyclotron. Both methods are useful additions to existing radiolabelling methods using $[^{11}C]CO_2$. The first method uses Cs_2CO_3 as a trapping reagent to produce target $[^{11}C]$carbamates in high RCCs of over 80 %. The method also works well for the radiosynthesis of $[^{11}C]$carbonates. However, products with low specific activity were obtained due to the introduction of non-radioactive carbonate into the reaction from the Cs_2CO_3. Although this is undesirable for receptor or enzyme imaging, the method can be used for other purposes including the study of the biodistribution and kinetics of drugs *in vivo*.

The second method is a further development to our previously established method to radiolabel ureas. Moderate trapping and yields were observed when the reaction was used for the radiosynthesis of $[^{11}C]$zopiclone.

3.4 **Method**

3.4.1 General

All purchased chemicals were used without further purification. Chemicals were purchased in highest available purity from Sigma-Aldrich and Alfa Aesar and used as received (> 99 % purity). All solvents were purchased as anhydrous in highest available purity (> 99.8 % purity, water < 50 ppm, extra dry) from Sigma-Aldrich, used as received and stored under argon. Reference compounds were either purchased from Sigma-Aldrich or synthesised using reported procedures. Reactions were carried out under an atmosphere of nitrogen in heat gun dried glassware with magnetic stirring. Reactions were monitored using alumina plate thin-layer chromatography (Merck, silica gel 60, fluorescence indicator F254, or Merck, aluminium oxide neutral, fluorescence indicator F254). Silica gel chromatography was performed using 230-400 Mesh (Grade 60) silica gel. The mobile phase was a mixture of hexane : ethyl acetate in varying ratios and detected by 254 nm UV light. Infra-Red spectra were acquired on a PerkinElmer spectrum 100FTIR. ^{1}H-NMR (400 MHz) and ^{13}C-NMR (100 MHz) spectra were obtained using a BRUKER DRX 400 MHz spectrometer. Chemical shifts are reported in ppm (δ) relative to tetramethylsilane (TMS, d = 0 ppm) and calibrated using solvent residual peaks. Data are shown as follows: Chemical shift, multiplicity (s = singlet, d = doublet, t = triplet, q = quartet, m = multiplet), coupling constant (*J*, Hz) and integration. Calculated mass was determined using PerkinElmer ChemBioDraw Ultra 13.0 program. Mass spectroscopy was performed at King's College London using an Agilent 6520 Accurate-Mass Q-TOF LC/MS connected to an Agilent 1200 HPLC system with UV detector (254 nm) and auto-sampler. [^{11}C]CO_2 was produced by a Siemens RDS112 cyclotron (St Thomas' Hospital, London, United Kingdom) via the ^{14}N(p,α)^{11}C nuclear reaction. Typical irradiation times were 1 minute with a beam current of 10 μA, which yielded a [^{11}C]CO_2 amount of about 300 MBq at end of bombardment. Radiolabelling reactions were performed in a 1.5 mL screw top vial with a "V" internal shape. Analytical HPLC was performed on an Agilent 2060 Infinity HPLC system with a variable wavelength detector (254 nm was used as default wavelength). An Agilent Eclipse XDB-C18 reverse-phase column (4.6 x 150 mm,

5 µm) was used at a flow rate of 1 mL/min and H_2O/MeOH (HPLC grade solvents and with 0.1 % TFA) gradient elution (flow rate: 1 mL/min, 0-2 min: 5% MeOH, 2-11 min: 5 to 95% MeOH linear gradient, 11-13 min: 90% MeOH, 13-14 min: 90% to 5% MeOH linear gradient, and 14-15 min:5% MeOH). The RCC was estimated by radio-HPLC and defined as the area under the [^{11}C]urea peak expressed as a percentage of the total ^{11}C labelled peak areas observed in the chromatogram. Specific radioactivity was calculated from analytical HPLC sample of 25 µL. A calibration curve of known mass quantity versus HPLC peak area (254 nm) was used to calculate the mass concentration of the 25 µL radiolabelled compound. The identity of the radiolabelled compound peak was confirmed by HPLC co-injection of a nonradioactive reference compound and yielded a single peak.

3.4.2 Synthesis of reference compounds

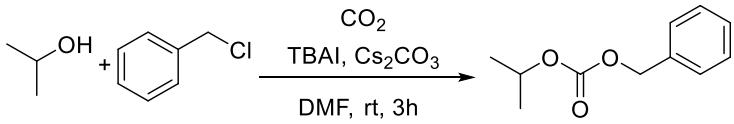

Synthesis of compound 1: CO_2 gas was bubbled into a solution containing isopropyl alcohol (61 µL, 0.8 mmol), Cs_2CO_3 (0.782 g, 2.4 mmol) and TBAI (0.887 g, 2.4 mmol) in 2.5 mL DMF for 1 hour. Benzyl chloride (276 µL, 2.4 mmol) was then added and the reaction stirred at room temperature with CO_2 gas bubbling through for another 3 hours. The reaction mixture was poured into water and extracted with ethyl acetate. The organic layer was washed with water and brine, and dried over sodium sulphate. The crude product was concentrated and purified by flash chromatography (gradient, 0% to 50%, hexane-ethyl acetate). 19 % yield (0.029 g); IR 2924.17, 1741.12, 1259.81; ^{1}H NMR (400 MHz, $CDCl_3$) δ 7.45 (m, 5H), 5.20 (s, 2H), 5.15 (m, 1H), 1.30 (d, *J* = 7.1, 6H); LCMS calculated for $C_{11}H_{14}O_3$ $[M+H]^+$ = 195.0900; found 195.1025. The spectral data of the synthesised product is consistent with reported values.[31]

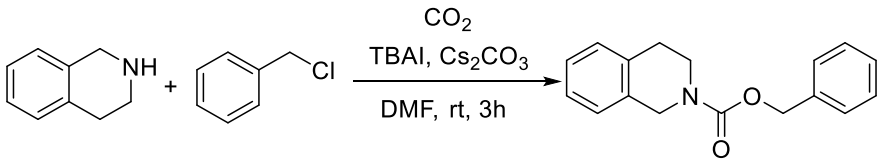

Synthesis of compound 2: CO_2 gas was bubbled into a solution containing tetrahydroisoquinoline (101 µL, 0.8 mmol), Cs_2CO_3 (0.782 g, 2.4 mmol) and TBAI (0.887 g, 2.4 mmol) in 2.5 mL DMF for 1 hour. Benzyl chloride (276 µL, 2.4 mmol) was then added and the reaction stirred at room temperature with CO_2 gas bubbling through for another 3 hours. The reaction mixture was poured into water and extracted with ethyl acetate. The organic layer was washed with water and brine, and dried over sodium sulphate. The crude product was concentrated and purified by flash chromatography (gradient, 0% to 50%, hexane-ethyl acetate. 34 % yield (0.072 g); IR 2925.08, 1702.50, 1227.06; ^{1}H NMR (400 MHz, $CDCl_3$) δ 7.30 (m, 9H), 5.90 (s, 1H), 5.10 (s, 2H), 4.23 (s, 2H), 3.60 (m, 2H), 3.10 (m, 2H); LCMS calculated for $C_{17}H_{17}N_1O_2$ $[M+H]^+$ = 268.1300; found 268.1332. The spectral data of the synthesised product is consistent with reported values.[31]

3.4.3 Radiolabelling procedure

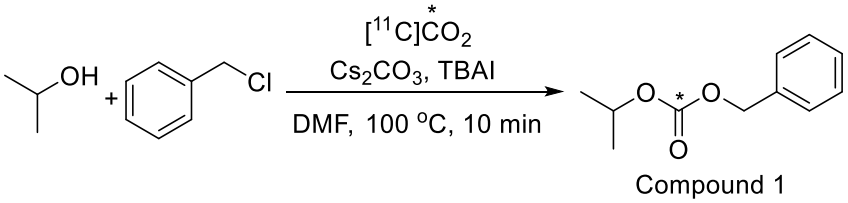

Synthesis of [^{11}C]compound 1: [^{11}C]CO_2 from the cyclotron target was bubbled in a stream of helium gas at a flow rate of 1.4 mL/min post target depressurisation directly into a reaction vial containing TBAI (24 mg, 66 µmol), Cs_2CO_3 (21 mg, 66 µmol) and isopropyl alcohol (1.65 µL, 22 µmol) in DMF (400 µL). The mixture was stirred at 100 °C for 5 minutes, benzyl chloride (7.5 µL, 66 µmol) was added and heated for a further 5 minutes before quenching the reaction with H_2O and preforming the HPLC analysis. t_r = 8.45 min; RCC = 82 %.

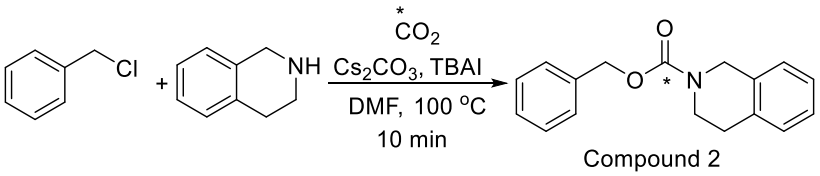

Synthesis of [^{11}C]compound 2: [^{11}C]CO_2 from the cyclotron target was bubbled in a stream of helium gas at a flow rate of 1.4 mL/min post target depressurisation directly into a reaction vial containing TBAI (24 mg, 66 µmol), Cs_2CO_3 (21 mg, 66 µmol) tetrahydroisoquinoline (3 mg, 22 µmol) in DMF (400 µL). The mixture was stirred at 100 °C for 5 minutes, benzyl chloride (7.5 µL, 66 µmol) was added and heated for a further 5 minutes before quenching the reaction with H_2O and preforming the HPLC analysis. t_r = 9.50 min; RCC = 90 %.

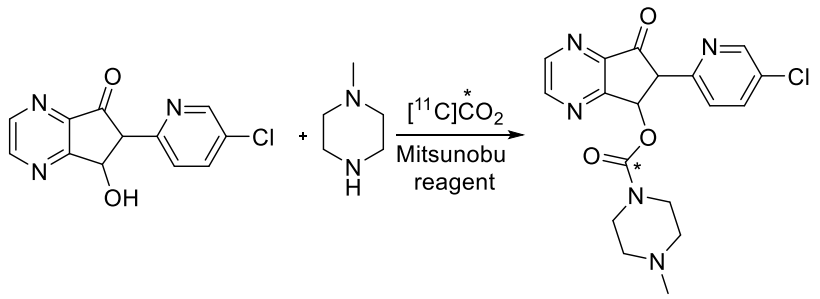

Synthesis of [^{11}C]Zopiclone: [^{11}C]CO_2 from the cyclotron target was bubbled in a stream of helium gas at a flow rate of 1.4 mL/min post target depressurisation directly into a reaction vial containing an an amine (1.89 µL,18.3 µmol), alcohol (7.1 mg, 27.5 µmol) and DBU (0.13 µL, 0.9 µmol) in CH_3CN (300 µL). [^{11}C]CO_2 from the cyclotron was bubbled in the reaction mixture and the resulting solution was stirred, and heated at 50 °C for 1 minute. In a separate vial, tributylphosphine (9 µL, 36.6 µmol) was added to a solution containing di-tert-butyl azodicarboxylate (8 mg, 36.6 µmol) in CH_3CN (100 µL) under argon at room temperature. The resulting solution was transferred into the reaction mixture and stirred for one minute at 50 °C. The reaction was quenching it with water, the crude product was analysed by radio-HPLC. t_r = 25.15 min; RCC = 15 %; RCY = 10 % (uncorrected for decay).

3.5 References

[1] a) K. Miller, B. Neilan, D. M. Y. Sze, *Recent Patents on Anti-Cancer Drug Discovery* **2008**, *3*, 14-19; b) T. Asaka, A. Manaka, H. Sugiyama, *Current Topics in Medicinal Chemistry* **2003**, *3*, 961-989; c) O. Kreye, H. Mutlu, M. A. R. Meier, *Green Chemistry* **2013**, *15*, 1431-1455.

[2] a) S. J. Traub, L. S. Nelson, R. S. Hoffman, *Journal of Clinical Toxicology* **2002**, *40*, 781-787; b) D. L. Zvosec, S. W. Smith, R. Litonjua, R. E. Westfal, *Clinical Toxicology* **2007**, *45*, 261-265; c) K. L. Goa, R. C. Heel, *Drugs* **1986**, *32*, 48-65.

[3] J. G. Kim, D. O. Jang, *Tetrahedron Letters* **2009**, *50*, 2688-2692.

[4] a) A. M. Tafesh, J. Weiguny, *Chemical Reviews* **1996**, *96*, 2035-2052; b) P. G. Jessop, T. Ikariya, R. Noyori, *Chemical Reviews* **1995**, *95*, 259-272; c) J. Sun, S. i. Fujita, M. Arai, *Journal of Organometallic Chemistry* **2005**, *690*, 3490-3497.

[5] a) J. H. Saunders, R. J. Slocombe, *Chemical Reviews* **1948**, *43*, 203-218; b) S. Ozaki, *Chemical Reviews* **1972**, *72*, 457-496; c) F. Paul, *Coordination Chemistry Reviews* **2000**, *203*, 269-323.

[6] J. S. Nowick, D. L. Holmes, G. Noronha, E. M. Smith, T. M. Nguyen, S.-L. Huang, The *Journal of Organic Chemistry* **1996**, *61*, 3929-3934.

[7] A. W. Hofmann, Berichte der Deutschen Chemischen Gesellschaft **1881**, 14, 2725-2736.

[8] a) L. Marinescu, J. Thinggaard, I. B. Thomsen, M. Bols, *The Journal of Organic Chemistry* **2003**, *68*, 9453-9455; b) J. K. Augustine, A. Bombrun, A. B. Mandal, P. Alagarsamy, R. N. Atta, P. Selvam, *Synthesis* **2011**, *2011*, 1477-1483.

[9] P. Dubé, N. F. F. Nathel, M. Vetelino, M. Couturier, C. L. Aboussafy, S. Pichette, M. L. Jorgensen, M. Hardink, *Organic Letters* **2009**, *11*, 5622-5625.

[10] H. Alper, F. W. Hartstock, Journal of the Chemical Society, Chemical Communications **1985**, 1141-1142.

[11] T. W. Leung, B. D. Dombek, Journal of the Chemical Society, Chemical Communications **1992**, 205-206.

[12] L. Ren, N. Jiao, *Chemical Communications* **2014**, *50*, 3706-3709.

[13] J. Paz, C. Pérez-Balado, B. Iglesias, L. Muñoz, *The Journal of Organic Chemistry* **2010**, *75*, 3037-3046.

[14] A. W. Miller, S. T. Nguyen, *Organic Letters* **2004**, *6*, 2301-2304.

[15] M. O. Bratt, P. C. Taylor, *The Journal of Organic Chemistry* **2003**, *68*, 5439-5444.

[16] V. Caló, A. Nacci, A. Monopoli, A. Fanizzi, *Organic Letters* **2002**, *4*, 2561-2563.

[17] a) F. Li, C. Xia, L. Xu, W. Sun, G. Chen, *Chemical Communications* **2003**, 2042-2043; b) K. Kossev, N. Koseva, K. Troev, *Journal of Molecular Catalysis A: Chemical* **2003**, *194*, 29-37; c) M. Antonietta Casadei, S. Cesa, M. Feroci, A. Inesi, *New Journal of Chemistry* **1999**, *23*, 433-436.

[18] R. N. Salvatore, S. I. Shin, A. S. Nagle, K. W. Jung, *The Journal of Organic Chemistry* **2001**, *66*, 1035-1037.

[19] S. Bonnot-Lours, C. Crouzel, C. Prenant, F. Hinnen, *Journal of Labelled Compounds and Radiopharmaceuticals* **1993**, *33*, 277-284.

[20] C. Crouzel, F. Hinnen, E. Maitre, *Applied Radiation and Isotopes* **1995**, *46*, 167-170.

[21] J. P. Holland, P. Cumming, N. Vasdev, American Journal of Nuclear Medicine and Molecular Imaging **2013**, 3, 194-216.

[22] L. Lemoucheux, J. Rouden, M. Ibazizene, F. Sobrio, M. C. Lasne, *The Journal of Organic Chemistry* **2003**, *68*, 7289-7297.

[23] H. Doi, J. Barletta, M. Suzuki, R. Noyori, Y. Watanabe, B. Langstrom, *Organic & Biomolecular Chemistry* **2004**, *2*, 3063-3066.

[24] T. Kihlberg, F. Karimi, B. Långström, *The Journal of Organic Chemistry* **2002**, *67*, 3687-3692.

[25] J. M. Hooker, A. T. Reibel, S. M. Hill, M. J. Schueller, J. S. Fowler, *Angewandte Chemie International Edition* **2009**, *48*, 3482-3485.

[26] A. A. Wilson, A. Garcia, S. Houle, O. Sadovski, N. Vasdev, *Chemistry – A European Journal* **2011**, *17*, 259-264.

[27] a) W. Saba, H. Valette, M. A. Peyronneau, Y. Bramoullé, C. Coulon, O. Curet, P. George, F. Dollé, M. Bottlaender, *Synapse* **2010**, *64*, 61-69; b) A. A. Wilson, A. Garcia, J. Parkes, S. Houle, J. Tong, N. Vasdev, *Nuclear Medicine and Biology* **2011**, *38*, 247-253.

[28] B. H. Rotstein, S. H. Liang, J. P. Holland, T. L. Collier, J. M. Hooker, A. A. Wilson, N. Vasdev, *Chemical Communication* **2013**, *49*, 5621-5629.

[29] P. M. Rusjan, A. A. Wilson, L. Miler, I. Fan, R. Mizrahi, S. Houle, N. Vasdev, J. H. Meyer, *Journal of Cerebral Blood Flow and Metabolism* **2014**, *34*, 883-889.

[30] A. A. Wilson, A. Garcia, S. Houle, N. Vasdev, *Organic and Biomolecular Chemistry* **2010**, *8*, 428-432.

[31] S. L. Peterson, S. M. Stucka, C. J. Dinsmore, *Organic Letters* **2010**, *12*, 1340-1343.

[32] J. R. Atack, Current Drug Targets CNS and Neurological Disorders **2003**, 2, 213-232.

Chapter 4

Radioligand Development

4 Chapter 4

4.1 Introduction

4.1.1 CNS radioligand development

Central nervous system (CNS) radioligands are drug-like molecules that produce a high signal-to-noise ratio for a specific molecular target. Despite the availability of a number of successful PET radioligands (e.g. Table 4.1), there is still lack of radioligands for many CNS receptors and enzymes. The development of further radioligands is of great interest in furthering our understanding of *in vivo* pharmacology and brain function.[1]

Table 4.1. Established CNS radioligands.

radioligand	Chemical structure	Target
[^{11}C]PMP [2]	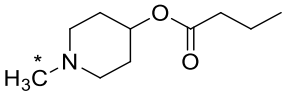	Acetylcholinesterase
[^{11}C]Raclopride [3]	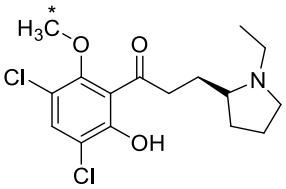	Dopamine D2 receptors
[^{11}C]RO15-4513 [4]	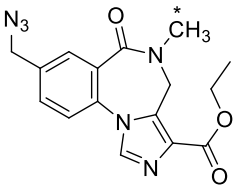	$GABA_A$ receptors
[^{11}C]carfentanil [5]	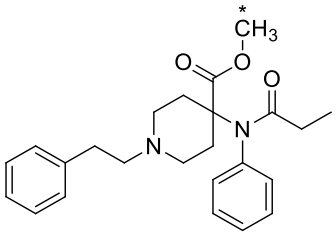	μ-Opioid receptors

There are many similarities between the process of developing a CNS drug and a CNS radioligand, as well as many differences.[6] In drug development, drug candidates can fail for various reasons including low bioavailability, toxicology and inappropriate therapeutic windows. These are not challenges encountered when developing a PET radioligands as the tracer is administrated intravenously in subnanomolar concentrations which allows even toxic or potent compounds to be radiolabelled and administrated into living subjects without producing a pharmacological or toxicological effect.[7] When developing a novel radioligand for PET neuro-imaging, there are some essential design and test parameters that must be considered.[6, 8]

Low Non-specific binding (NSB)

NSB is a major contributing factor for radioligand failure. NSB can be defined as the binding of a radioligand to non-saturable components in tissue.[1] Despite the development of many methods to predict *in vivo* NSB, the phenomenon is poorly understood. The most common methods for predicting *in vivo* NSB are the partition coefficient lipophilicity (Log P) and tissue-section autoradiography.

In PET imaging, it is generally believed that for a successful CNS radioligand, its Log P value should be between 1 and 3.[9] Highly lipophilic compounds are able to cross the blood-brain-barrier but can also bind to the surrounding tissue (non-saturable binding) which results in high NSB. Furthermore, compounds with high Log P values favour binding to plasma proteins which reduces the amount of radioligand available to passively diffuse across the blood-brain-barrier.[1, 10] Conversely, compounds with low log P have limited blood-brain-barrier permeability due to reduced passive diffusion across the membrane.

Kugher *et al.*[11] used *in vitro* autoradiography to study NSB. Although only four different ^{18}F radiolabelled tracers were used, the study showed that the compound with a Log P value of 2.71 had the highest *in vitro* NSB (96 %) while the other compounds with Log P values of 2.45 and 1.81, had NSB of 80 % and 33 %, respectively. Although only 4 sets of compounds were used, the data indicated a linear relationship between Log P and *in vitro* NSB (Figure 4.1).

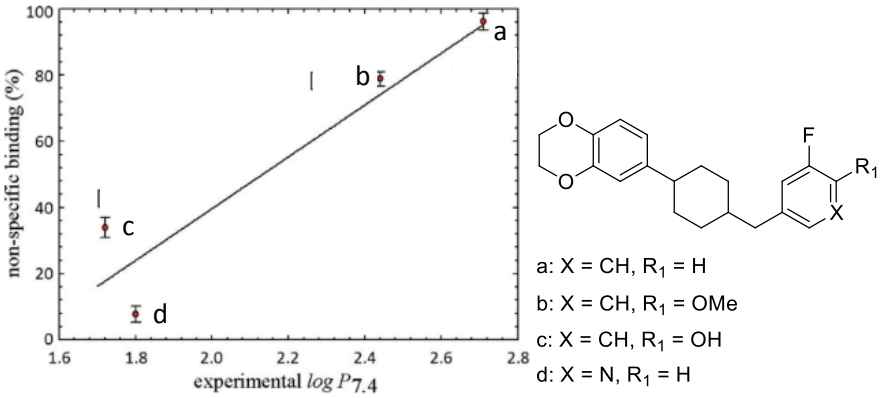

Figure 4.1. The relationship between experimental log P and NSB.[11]

Log P is usually measured using the shake-flask method where the compound is partitioned between a water and *n*-octanol mixture.[12] However, other methods such as the use of reverse-phase HPLC to determine chromatographic hydrophobicity index, (CHI) log D, and, an immobilised artificial membrane column to measure CHI_IAM have been shown to be better predictors of NSB.[12] log D is the value of Log P at physiological pH.

The retention time of compounds exhibiting different retention times on the C18 reverse phase HPLC column are used to determine CHI_logD values. CHI_logD is the HPLC equivalent of Log $D_{oct/wat}$ and can be performed at pH 7.4 to mimic physiological pH. Compounds with high lipophilicity have a long retention times while compounds with low lipophilicity have short retention times.[12]

IAM is a reverse phase HPLC column that has a stationery phase that links a phosphatidylcholine (PC) head group to silica propylamine through a carboxylic acid group (Figure 4.2).[13] CHI_IAM is believed to be a better predictor of *in vivo* NSB as the artificial membrane mimics the biological membrane and hence, gives a more accurate measure of NSB. [13]

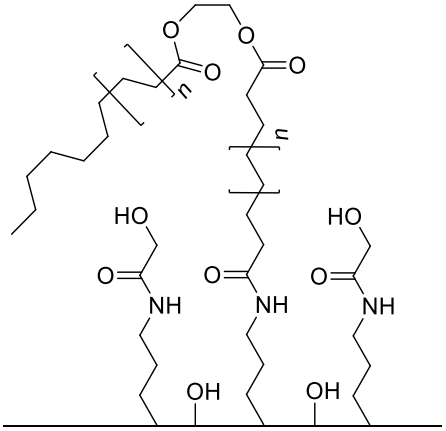

Figure 4.2. The IAM.PC structure containing silica-propylamine and PC group.[13]

Evidence suggests there is a relationship between Log P and NSB.[11] Most radioligands with low NSB have a Log P value in the range of 1 - 3. However, there are compounds such as WAY 100635, which have a high log P (3.28) and have low NSB.[14] If log P alone was used to predict NSB, WAY 100635 may have been excluded from radioligand development studies. This suggests that lipophilicity is not the only parameter that can help predict NSB.[15]

NSB can be estimated using radioligand blocking studies *in vitro*. Autoradiography is a technique that is used to determine tissue localisation of a radioligand. *In vitro* autoradiography involves introducing the radioligand to tissue sections. These tissue sections are generally frozen, sectioned on a cryostat and thaw-mounted onto glass slides. Initially, autoradiography is performed using tracer levels of the radioligand. The overall binding from the first experiment gives the total binding (free radioligand + NSB). The autoradiography study is then repeated but with the addition of a high concentration (over 100 fold) of non-radiolabelled compound that is known to bind specifically to the target site of interest. The second experiment would reveal the extent of the NSB (Equation 4.1). Using estimates for the total binding and the NSB, the specific binding can be calculated. Generally, radioligands require > 90 % *in vitro* specific binding determined by autoradiography, to have a chance of being a successful radioligand *in vivo*.[15]

Equation 4.1. Specific binding = Total binding – Non-specific binding.

NSB and lipophilicity are two of the main parameters that must be considered during radioligand development. Other design and test parameters must also be considered:

Ease of *radiolabelling*

The molecule should be amenable for rapid radiolabelling with a suitable radionuclide. ^{11}C and ^{18}F are the most commonly used radionuclides for PET molecular imaging.[1] There are limited number of radiolabelling methodologies that incorporate these radionuclides into target compounds efficiently. The development of methods that radiolabel compounds with these short-lived radionuclides are therefore important. The overall synthesis time for the radiolabelling reaction should be within 3 half-lives of the radionuclide and produce sufficient quantities of radioligand with a suitable specific activity to collect adequate amounts of data from the PET study.

High Binding potential (BP)

At the early stage of CNS radioligand development, *in vitro* BP measurements help by eliminating radioligand that are likely to fail *in vivo*.[16] In order to calculate *in vitro* BP, the target receptor's density (B_{max}) and the radioligands affinity to the target receptor (K_D) are required (Equation 4.2).

Equation 4.2. $BP = B_{max} / K_D$

High affinity is generally required for a radioligand to successfully bind to the target site. Typically, most successful receptor radioligands have subnanomolar or low nanomolar affinity to the target site of interest. The required affinity for a radioligand is dependent on the density of the target receptor under study i.e. the lower the target density, the higher the affinity required from the radioligand. As a rule-of-thumb, ideal radioligands usually have an *in vitro* BP value of > 10 to produce a good signal-to-noise image *in vivo*.[17] Furthermore, high selectivity to the target receptor over other potential competing binding sites in the region is often desirable.[9]

Tissue *permeability*

For CNS tracers, adequate radioligand entry to the brain is essential to obtain a useful quantitative images. The ability for a CNS radioligand to enter the brain from the plasma depends on at least two factors: its ability to cross blood-brain-barrier and its susceptibility to rejection by efflux pumps.[6, 18]

Most PET tracers are drug-like molecules and therefore, similar factors influence their ability to cross the blood-brain-barrier: Log P (1 to 3), molecular weight (< 500 Da), number of hydrogen bonds (< 10) and lack of formal charge.

The efflux pumps in the blood-brain-barrier (e.g P-glycoprotien (P-gp)) can prevent compounds from accumulating in the brain.[17] To acquire sufficient radioligand signal in the brain, a CNS radioligand should not be a substrate for these proteins. Generally, most compounds that are substrates for P-gp have high lipophilicity, positive charge at physiological pH and multiple aromatic groups.[18]

Metabolism

If a radioligand is metabolised *in vivo*, it is important to exclude radiolabelled metabolites from contaminating the signal of the parent radioligand in the CNS. This is often achieved by the careful choice labelling position whereby hydrophilic metabolites with poor brain penetration are produced.[6]

The above requirements are some of the most important and demanding criteria that must be considered for CNS radioligand development. The subsequent section describes the development of radioligands for the metabotropic glutamate receptor 1 (mGluR1).

4.1.2 Glutamate receptors

There are two different types of glutamate receptors at the synaptic membrane: ionotropic (iGlu) receptors which are ion channel pores that activate upon glutamate binding; and metabotropic (mGlu) receptors which are a family of G-protein coupled receptors.[19] mGlu receptors consist of eight subunits and are divided into three groups based on their signal transduction mechanism, pharmacology and receptor sequence homology (Table 4.2).[20]

Table 4.2. mGluR subunits, their function, synapse site and an example of an agonist.

Group	Receptor types	Function	Synapse site	Agonist
Group 1	mGluR1 and mGluR5	Increase NMDA receptor activity	Postsynaptic	DHPG
Group 2	mGluR2 and mGluR3	decrease NMDA receptor activity	Presynaptic	Eglumegad
Group 3	mGluR4, mGluR6, mGluR7 and mGluR8	decrease NMDA receptor activity	Presynaptic	5 L-AP4

Group one include mGluR1 and mGluR5, group two consists of mGluR2 and mGluR3 and group three includes the other 4 types. Although mGluR are ubiquitous in the brain, the different subtypes are highly expressed in discrete locations. The mGluR1 has shown to play a role in neurological and psychiatric disorders such as anxiety, schizophrenia and other cognition-related disorders.[21] Consequently, mGluR1 has become an important target for the development of radioligands. Developing radioligands to monitor these receptors would subsequently offer a valuable insight into diseases that are associated with mGluR1 dysfunction.

4.1.3 mGluR1 radioligands

In 2004, the first mGluR1 radioligand was developed.[22] The selective radioligand [^{3}H]R214127 was used to determine the densities of mGluR1 in rat brain regions (Table 4.3, Entry 1).

Table 4.3. The mGluR1 densities in different species.[9, 22]

Entry	Species	Regional B_{max} (nM)	
		Cortex	Cerebellum
1	Rat	47.1 ± 6.8	430.2 ± 202.2
2	Rhesus monkey	10 ± 1.9	53 ± 12
3	Human	26 ± 15	82 ± 33

In 2011, Hostetler *et al.*[9] used ^{18}F labelled [^{18}F]MK-1312 to measure the concentration of the receptors in the cerebellum and cortex of humans and primates (Table 4.3, Entries 2 and 3). These B_{max} values enable the minimum affinity requirement for a radioligand to be estimated. In order to obtain a minimum BP value of 10, mGluR1 radioligands require a K_D value of < 5 nM in the cerebellum across all species.[8b] As the mGluR1 B_{max} value in the cortex is lower than the cerebellum, a minimum radioligand K_D of 2.6 nM is required across all species to image the region successfully.

The B_{max} and K_D values differ across species (Table 4.3) and is one of the reasons why a successful *in vitro* radioligand characterised in rodents sometimes fails when it is translated into humans.

^{11}C radiolabelled mGluR1 radioligands

In 2005, [^{11}C]JNJ-16567083 was reported as the first PET radioligand for imaging mGluR1 in rats.[23] The radioligand was synthesised using palladium-mediated Stille coupling with [^{11}C]CH_3I (Scheme 4.1). A radiochemical yield (RCY) of 47 % (decay corrected and based on [^{11}C]CH_3I) and a high affinity for the mGluR1 (K_i = 3.49 ± 0.93 nM) was reported.

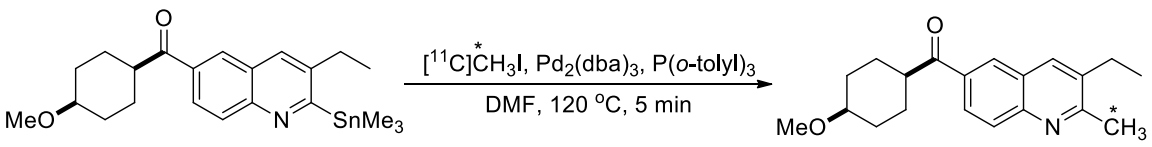

Scheme 4.1. The synthesis of [^{11}C]JNJ-16567083.[23]

Ex vivo studies showed high radioligand uptake in the cerebellum, striatum, hippocampus and frontal cortex; brain regions in which mGluR1 receptors are localised. Subsequently, i*n vivo* studies showed rapid brain entry with peak uptake 10 minutes post intravenous administration and specific mGluR1 binding in rats. When the radioligand was evaluated in non-human primates, high NSB in the brain was observed. Further studies established that the radioligand has lower affinity for cloned human mGluR1 compared to the cloned rat mGluR1 (Table 4.4).[23]

Table 4.4. The affinity of [^{11}C]JNJ-16567083 to mGluR1 in different species.

receptors	K_i (nM)
Cloned rat mGluR1	3.49 ± 0.93
Cloned human mGluR1	13.3 ± 6.49

Due to the species differences in affinity and the high NSB, it was concluded that [^{11}C]JNJ-16567083 was not suitable for imaging of mGluR1 in primates.[23] No further characterisation of the radioligand has been reported.

After a few years of inactivity in the field of mGluR1 PET radioligand development, in 2010, Yanamoto *et al.*[24] reported a novel ^{11}C radiolabelled tracer: [^{11}C]YM-202074. The precursor was labelled using the secondary synthon [^{11}C]CH_3I (Scheme 4.2) with RCY of 7.4 % (based on [^{11}C]CO_2 at the EOB) and a high affinity for the mGluR1 (K_i = 4.8 ± 0.37 nM).[24]

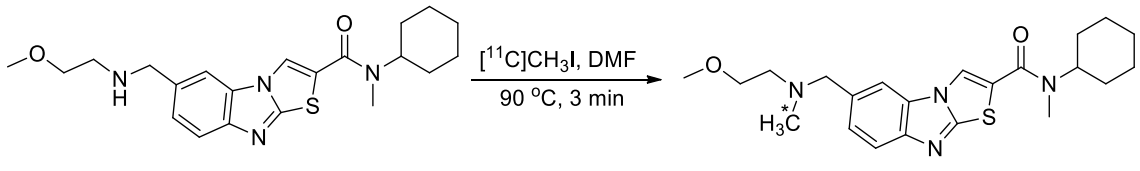

Scheme 4.2. The synthesis of [^{11}C]YM-202074.

In vitro studies showed that the radioligand bound to mGluR1 receptors however, *in vivo* studies revealed low radioligand brain uptake and a high NSB. The results were unexpected as [^{11}C]YM-202074 has high affinity for mGluR1 and an ideal LogD value of 2.7. In mice metabolism studies, only 5 % of the parent radioligand remained in plasma after 30 minutes post-injection, suggesting rapid metabolism of the ligand. Furthermore, [^{11}C]YM-202074 accounted for 50 % of the radioactivity in the cerebellum and 10 % in the rest of the brain which suggests the possible entry of radioactive metabolites into the brain.[24]

In the same year, 2010, another ^{11}C radiolabelled mGluR1 was also established by Prabhakaran *et al.*[25] ([^{11}C]MMTP). The compound was radiolabelled using [^{11}C]CH_3OTf (Scheme 4.3) with a RCY of 30 % (based on [^{11}C]CH_3OTf) and possessed good affinity for mGluR1 (K_i = 7.9 nM).

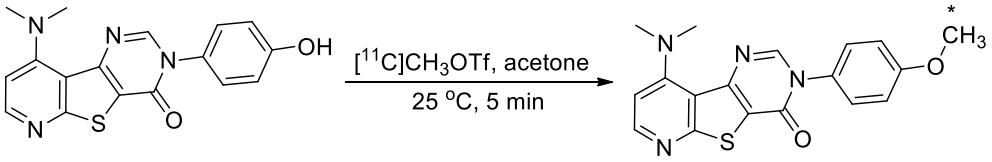

Scheme 4.3. The synthesis of [^{11}C]MMTP.

Fast uptake and clearance from the brain in non-human primates were observed. Further, a high concentration of the radioligand was observed in the cerebellum compared to other regions in the brain, consistent with the known expression levels in non-human primates.[25] No further characterisation of the radioligand has been reported since.

Another mGluR1 radioligand, [^{11}C]ITMM, was also reported.[26] The compound was radiolabelled using [^{11}C]CH_3OTf (Scheme 4.4) with a RCY of 22 % (decay corrected and based on [^{11}C]CO_2). The affinity of the compound was determined with a K_i of 12.6 nM.

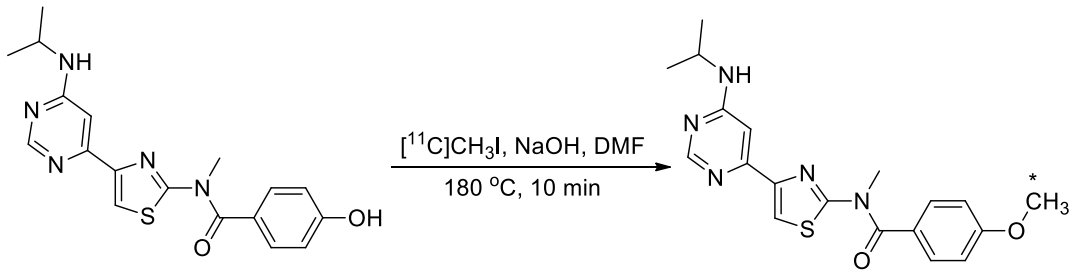

Scheme 4.4. The synthesis of [^{11}C]ITMM

In vivo PET imaging studies in rats showed slow uptake of [^{11}C]ITMM into the brain. But once taken up, high radioligand accumulation was observed in the cerebellum, thalamus and striatum. Further, appreciable washout from the brain was observed within the 90 minutes scan time. Selective binding of the radioligand was confirmed by comparing the binding of the ligand in wild-type mice and mGluR1 knock-out mice. Wild-type mice showed similar regional uptake to that of rats while knock-out mice showed low and uniform uptake.[26]

In 2013, [^{11}C]ITMM was used as the first-in-human radioligand for the molecular imaging of mGluR1.[27] In humans, the radioligand showed slow metabolism in plasma, with 61 % of the parent radioligand remaining at 60 minutes post-injection. Slow and relatively low brain uptake was observed, with continuous accumulation of the radioactivity in the cerebellum. Only a small amount of radioligand washout was observed in other brain regions. Nevertheless, results indicated that [^{11}C]ITMM bound specifically and selectively to mGluR1 receptors in humans.[27]

An analogue of [^{11}C]ITMM where the 4-methoxy group was replaced with 4-methyl group was synthesised using palladium-mediated Stille coupling with [^{11}C]CH_3I (Scheme 4.5).[28] A radiochemical yield (RCY) of 19 % (decay corrected and based on [^{11}C]CO_2) and a good affinity for the mGluR1 (K_i = 13.5 nM) was reported.

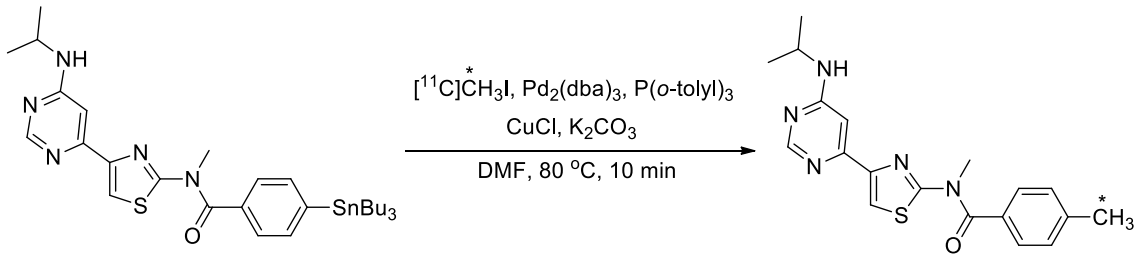

Scheme 4.5. The synthesis of [^{11}C]ITMD

Metabolite studies in rats showed minimal presence of radiometabolites in the brain after 60 minutes (4 – 8 %). Radiometabolites accounted for 66 % of the total radioactivity in the plasma at 60 minutes. This suggested that the radiometabolites do not enter the brain to an appreciable extent.[28] Similar results were observed in monkey brains, however, monkey brain uptake was relatively low compared to [^{11}C]ITMM. Further kinetic studies showed that the radioligand displayed reversible behaviour *in vivo*. Blocking studies with an mGluR1 selective compound (JNJ-1625985) confirmed the specific binding of the new ^{11}C radioligand to mGluR1.

Finally, [^{11}C]LY-2428703 was developed recently as a potential PET mGluR1 radioligand (Scheme 4.6).[29] The radioligand has a good affinity for the mGluR1 (K_i = 8.9 nM) but has a high LogD value of 4.02 ± 0.09.

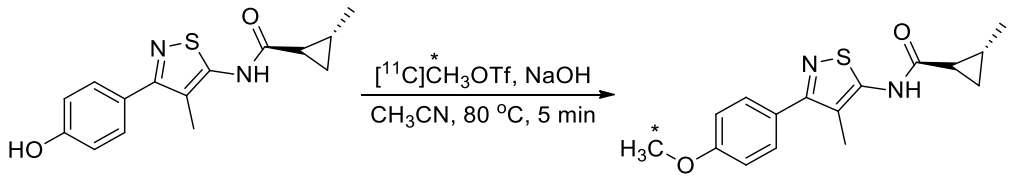

Scheme 4.6. The synthesis of [^{11}C]LY-2428703

Rapid brain uptake and washout were observed in rat brain, with the highest radioligand concentration measured in the cerebellum and cortex. However, low brain uptake was observed in human and non-human primates.[29]

Table 4.5. Examples of mGluR1 PET ligands. (a) The affinity of the radioligand to rat cerebellum homogenate.

Chemical structure	[^{11}C]radioligand	labelling synthon	K_i[a] (nM)
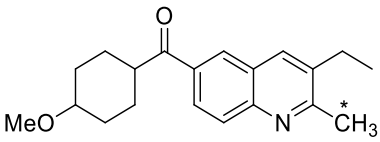	JNJ-16567083 [23]	[^{11}C]CH_3I	4.41
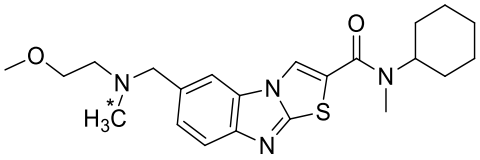	YM-202074 [24]	[^{11}C]CH_3I	4.8
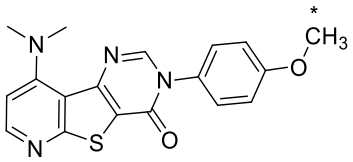	MMTP [25]	[^{11}C]CH_3 OTf	7.9
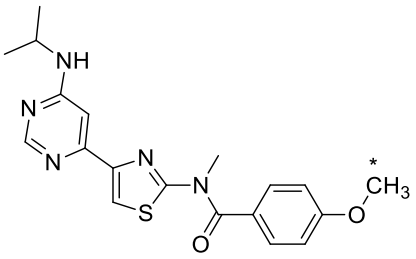	ITMM [26]	[^{11}C]CH_3I	12.6
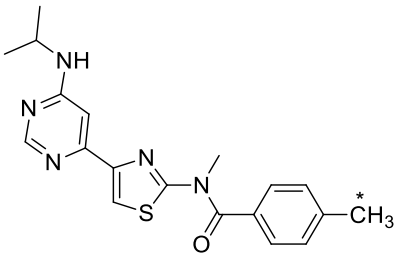	ITMD [28]	[^{11}C]CH_3I	13.6
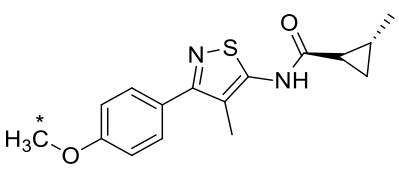	LY2428703 [29]	[^{11}C]CH_3 OTf	0.6

To date, there are no ^{11}C radiolabelled radioligands that can be used to efficiently image mGluR1 in humans.[8b] Furthermore, the available ^{11}C radiolabelled tracers use secondary ^{11}C synthons and therefore, developing mGluR1 radioligands that can be synthesised rapidly and with a good pharmacokinetics is of significant interest.

There are some ^{18}F radioligands (such as MK-1312) that have shown good *in vivo* properties. More examples are found in references 9 and 30.[9, 30]

4.1.4 Summary

Radiolabelling molecules that interact with neurotransmitter systems offer an opportunity to deepen our understanding of brain diseases using molecular imaging techniques.

^{11}C radioligands are useful as they permit repeat studies in the same subject on the same day. There are a number of ^{11}C labelled radioligands available for imaging mGluR1 receptors and although these radioligands are useful, their widespread use is limited by factors such as RCY, slow brain uptake, accumulation and slow clearance of radioactivity from brain. The development of novel ^{11}C radiolabelled mGluR1 radioligands are therefore of considerable interest

4.2 Aims

To use the novel methods developed in chapter 2 and apply them to the development of ^{11}C radiolabelled mGluR1 radioligands. This would demonstrate the utility of the method as a useful rapid radiolabelling reaction for PET molecular imaging.

4.3 Development novel of mGluR1 radioligands

4-[1-(2-fluoropyridin-3-yl)-5-methyl-1H-1,2,3-triazol-4-yl]-N-isopropyl-N-methyl-3,6-dihydropyridine-1(2H)-carboxamide (FTIDC) is a highly potent and selective mGluR1 antagonist with an IC_{50} value of 5.8 nM and a Log P value of 2.1 (Figure 4.3). In 2009, the radiolabelling of the compound was reported in a poster abstract using ^{18}F.[30a] Authors stated that attempts to radiolabel the compound with ^{11}C were unsuccessful. No further characterisation of the radioligand has been reported since. The compound contains a urea structure and therefore, it can in principle be radiolabelled using the novel method developed in chapter 2.

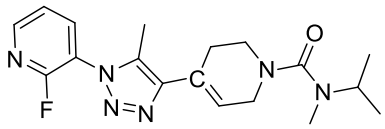

Figure 4.3. The chemical structure of FTIDC.

In this work, a library of three structurally related compounds were synthesised in order to investigate the structural influences on the radiolabelling reaction.

2-chloro-3-(5-methyl-4-(1,2,3,6-tetrahydropyridin-4-yl)-1H-1,2,3-triazol-1-yl)pyridine (compound **1**) was taken as the backbone for all the compounds as this core pharmacophore is found on the established mGluR1 antagonist FTIDC.[31] Furthermore, the synthesis of the compound is established and the Log P value is within the ideal range for PET tracers. The compound has a secondary amine present which enables it to react with various amines, in the presence of CO_2, to form ureas. Aliphatic, aromatic and benzyl amines (Figure 4.4) were selected as the test reagents due to their nucleophilicity and lipophilicity differences.

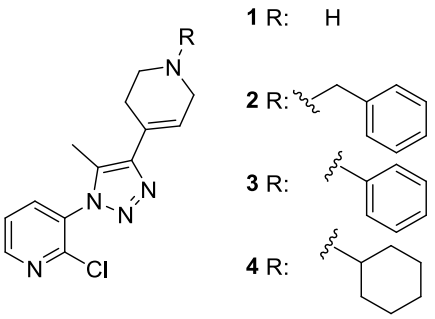

Figure 4.4. Structure of the precursor and the designed compounds.

4.3.1 Synthesis of compound 1

The synthesis of the precursor (compound **1**), reported by Ito *et al.*[32] , is achieved in five steps and includes the formation of an azide from an amine and a subsequent click reaction (Scheme 4.7).

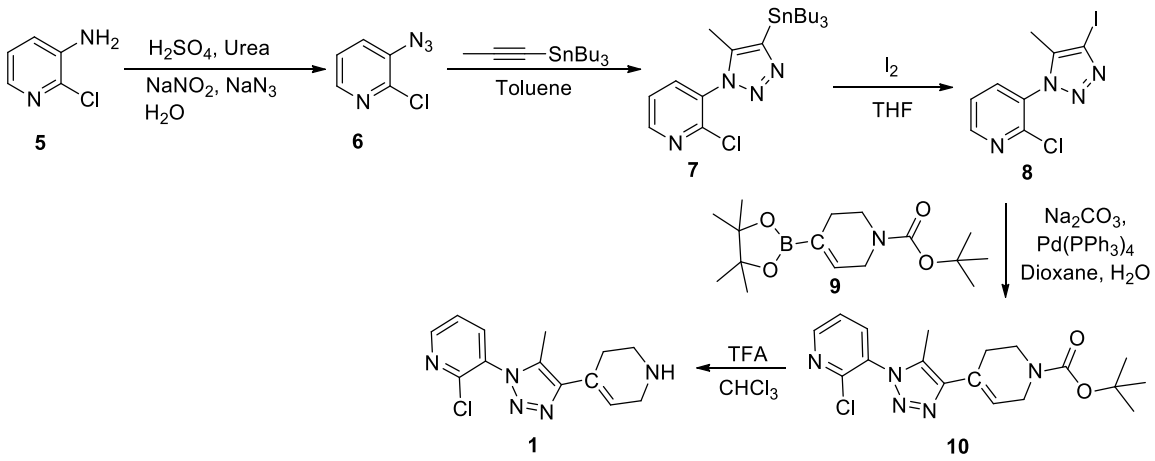

Scheme 4.7. The proposed route for the synthesis of compound **1**.

The synthesis of compounds **6 – 8** proceeded with yields of > 70 %. The click reaction is expected to produce a regioselective product. In the absence of a catalyst, click reactions produce a mixture of two regioisomers, however, due to the steric hindrance effect caused by the bulky $SiBu_3$ group, the reaction is likely to produce a regioselective product. The NMR spectra of compound 7 (Figure 4.5) indicated that the product is produced at a high purity.

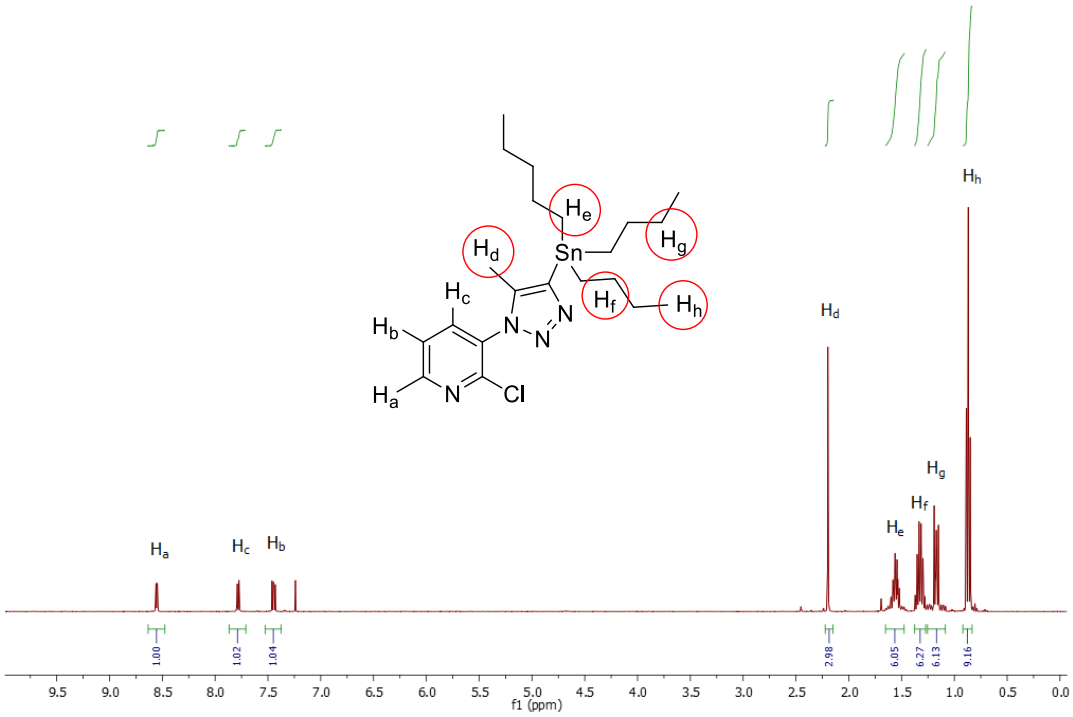

Figure 4.5. The NMR spectra of compound **7**.

The Pd-mediated reaction (the synthesis of compound **10**) was challenging. When the reaction was performed at low concentrations (0.15 mmol of compound **9**), the target product was produced with moderate yields of 20 – 50 %. However, when high concentrations of compound **9** were used (0.15 mmol) the target product was not observed. Although only a small quantity of the precursor is required for each radiolabelling reaction, performing the non-radioactive synthesis in small quantities is time consuming. Furthermore, the reaction yields were in the range of 20 – 50 %. Synthesis of the target compound was subsequently attempted using different Pd-mediated reactions (Scheme 4.8), however, the reaction did not produce the target product.

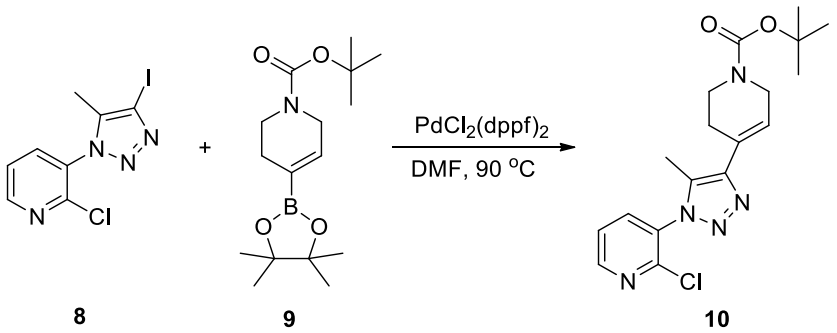

8 9 10

Scheme 4.8. The synthesis of compound **10**.

In order to produce the precursor in sufficient quantities, a different route for the synthesis of the precursor was proposed (Scheme 4.9). A copper-mediated Grignard reaction was used for the synthesis of an internal alkyne (compound **12**). The reaction between the alkyne and azide for the synthesis of compound **10** did not proceed (Scheme 4.9). The reaction was attempted under different conditions and using various catalysts such as $CuSO_4$ and CuI, however, the target product was not observed.

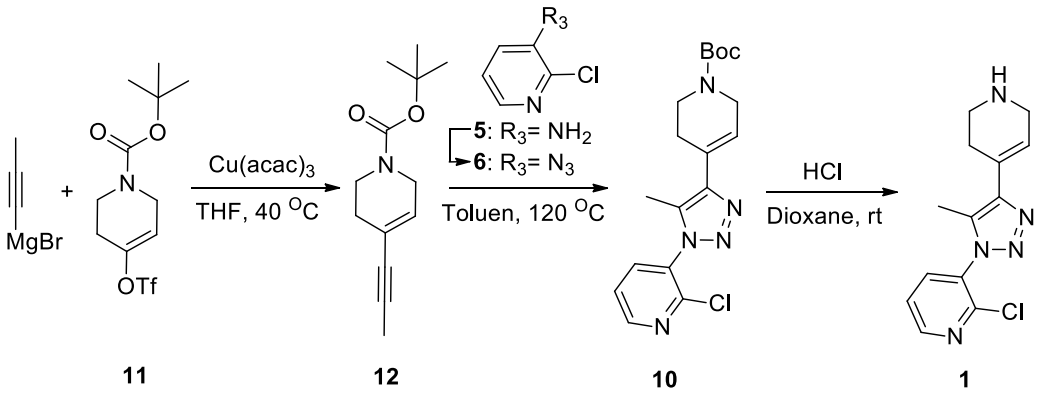

11 12 10 1

Scheme 4.9. The second proposed route for the synthesis of compound **1**.

Literature reviews suggested that there were no reaction methodologies available for the synthesis of compound **10** from **12** due to the alkyne group being internal. However, numerous click reactions with terminal alkynes were available[33] and therefore, the possibility of eliminating the methyl group to form external alkyne was explored.

Ito *et al.*[32] examined the effect of the methyl group on the compound's affinity to mGluR1 receptors. Table 4.6 shows that the methyl group increases the affinity of the compound to mGluR1 receptors (Table 4.6, Entries 1 and 3). However, the selectivity of the compound to mGluR1 versus mGluR5 is higher for un-methylated compounds.

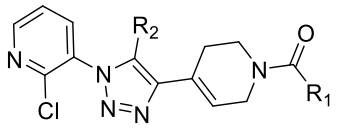

Table 4.6. The effect of a methyl group on compound affinity and selectivity.

Entry	R_1	R_2	IC_{50} ± SEM (nM)	
			mmGluR1	mmGluR5
1	^{t}BuO	H	12 ± 2.2	4300 ± 1600
2	^{t}BuO	Me	1.5 ± 0.15	170 ± 17
3	^{t}PrO	H	180 ± 21	3900 ± 490
4	^{t}PrO	Me	3.3 ± 0.6	40 ± 5.9

As the synthesis of the methylated compound was unsuccessful, it was decided that the synthesis of disubstituted [1,2,3]-triazoles, which is expected to have higher selectivity for mGluR1 over mGluR5, would be pursued (Figure 4.6).

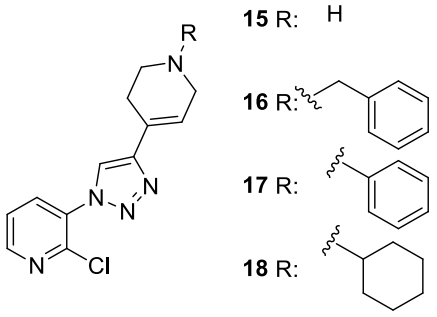

Figure 4.6. Structure of the redesigned mGluR1 radioligand candidates.

4.3.2 Synthesis of compound 15

The synthesis of compound **15** included the nucleophilic substitution reaction with Grignard reagent to form a terminal alkyne and reacting it with an azide to form disubstituted [1,2,3]-triazoles (Scheme 4.10).

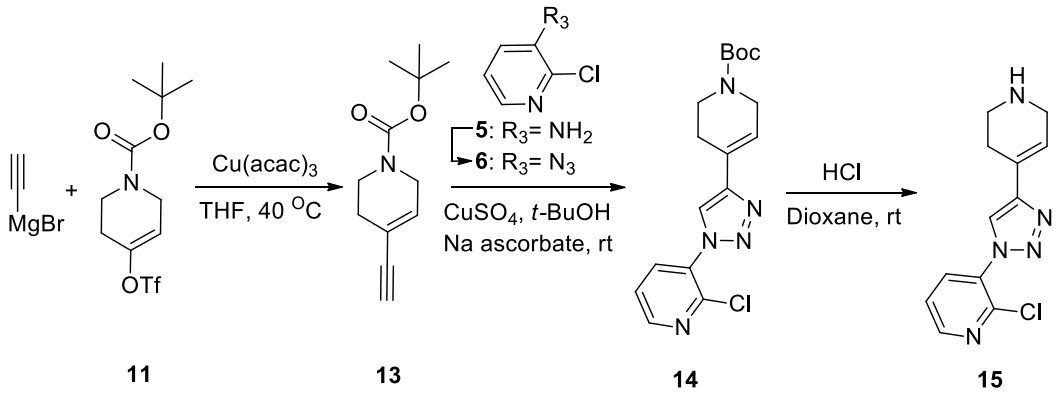

Scheme 4.10. The proposed route for the synthesis of compound 15

The click reaction with a terminal alkyne produced the target product efficiently. Copper was used to catalyse the reaction and therefore, the click reaction product is expected to regioselective. NMR spectra shows that the target product is produced efficiently (Figure 4.7).

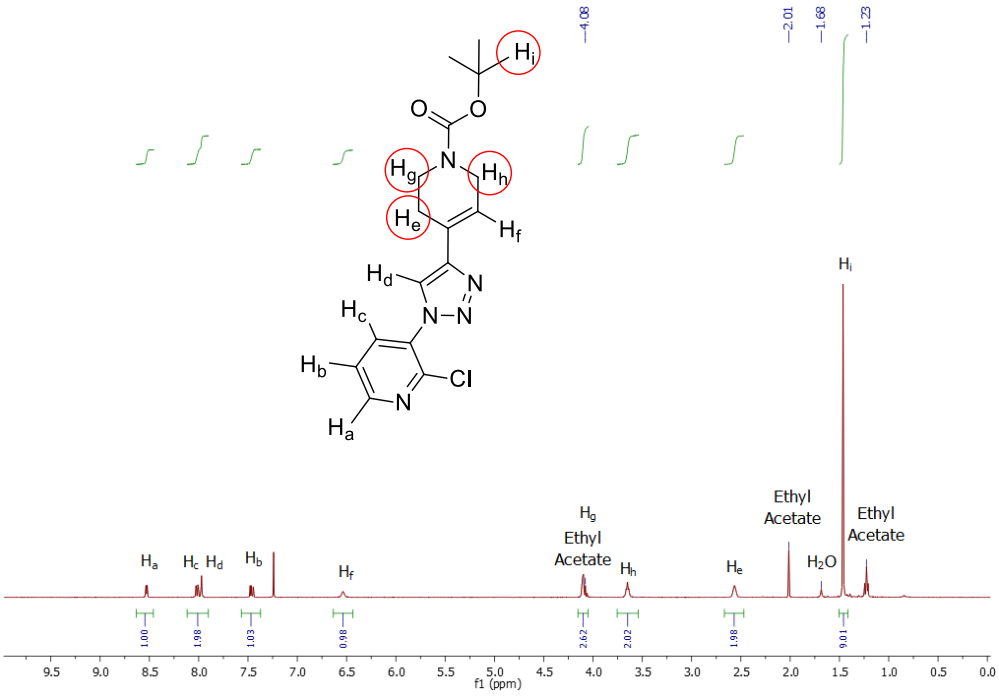

Figure 4.7. The NMR spectra of compound **14**.

The product from the click reaction was protected with a *tert*-Butyloxycarbonyl group (boc) and therefore, the compound was added to an acidic solution to deprotect it and form the secondary amine (compound **15**) in a high yield.

In order to identify the HPLC retention time and characterise the radiolabelled compounds, the synthesised precursor was used for the synthesis of reference compounds. Compound **16** to **18** were successfully produced using a nucleophilic addition reaction. They were purified from the crude products using flash chromatography. The ^{1}H NMR analyses of the compounds are shown in Figures 4.8 to 4.10. The HPLC analysis showed that the purity of the compounds were > 95 % (Figure 4.11).

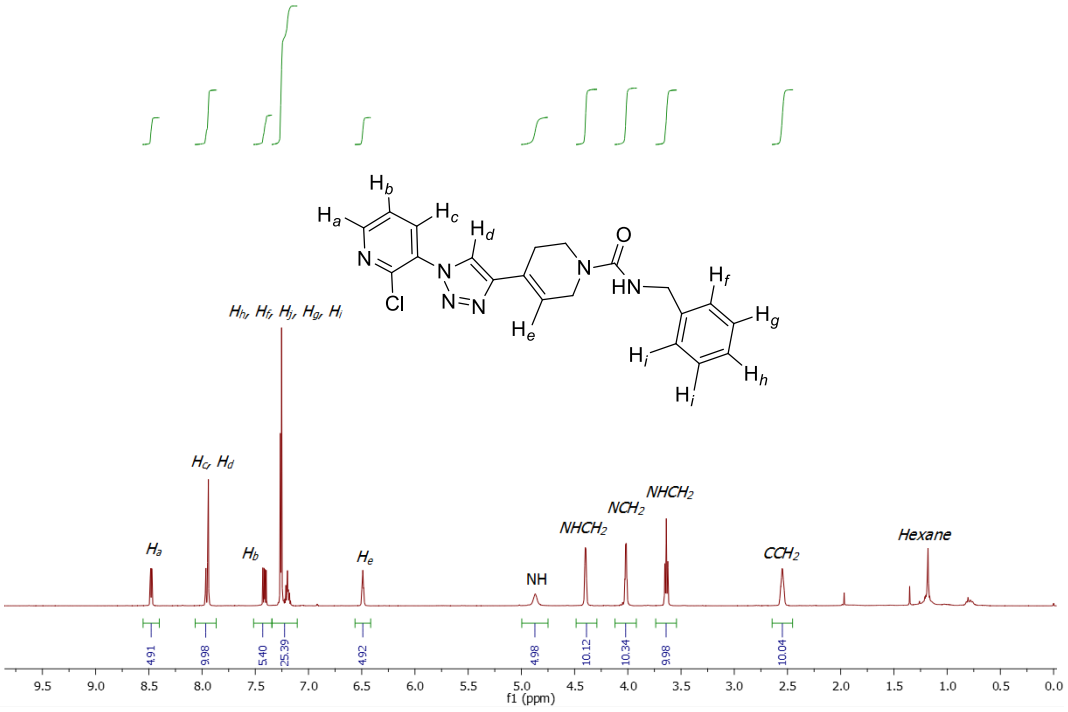

Figure 4.8. The NMR spectra of compound **16**.

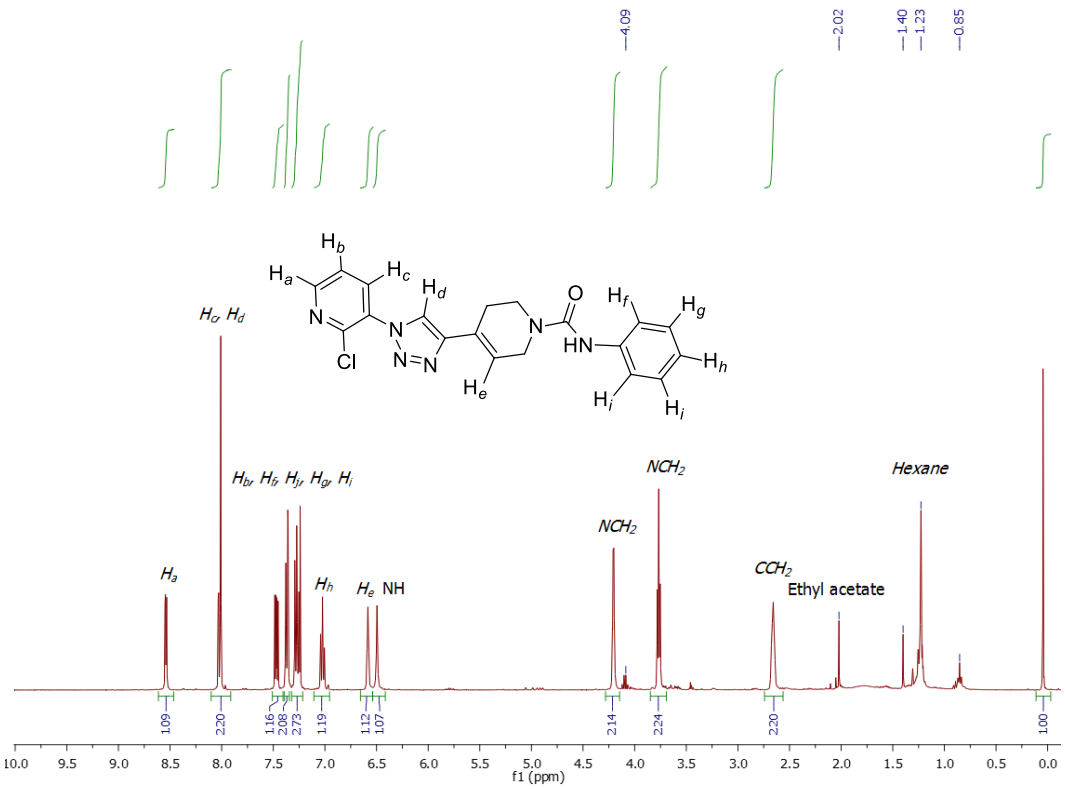

Figure 4.9. The NMR spectra of compound **17**.

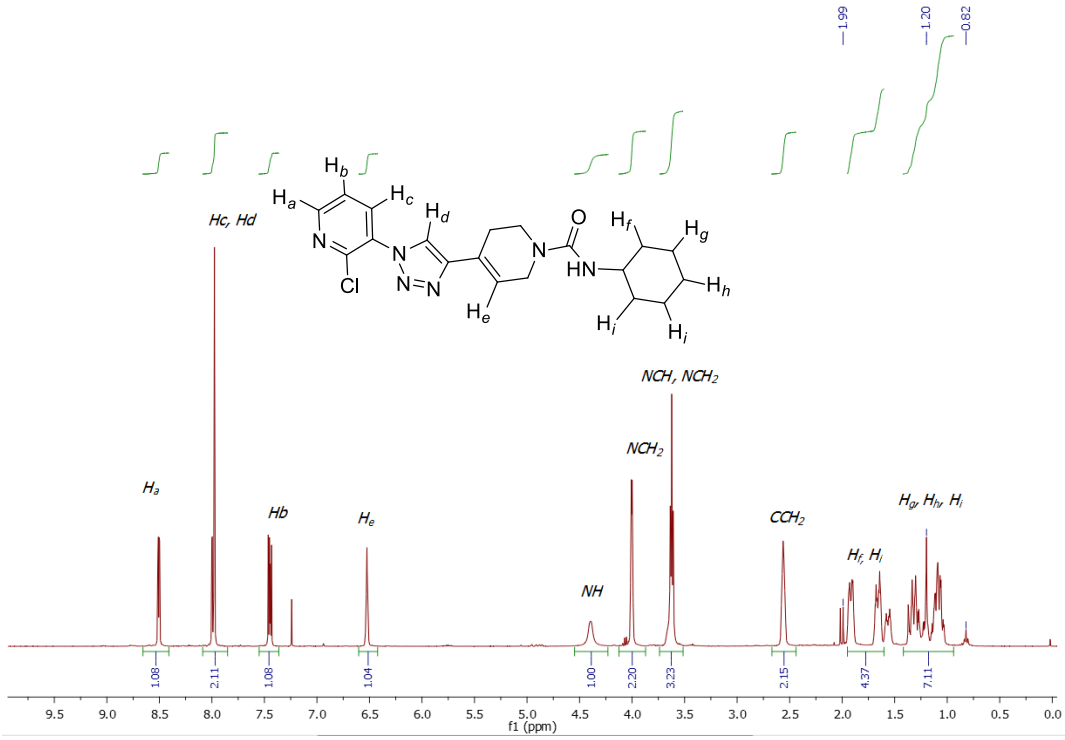

Figure 4.10. The NMR spectra of compound **18**.

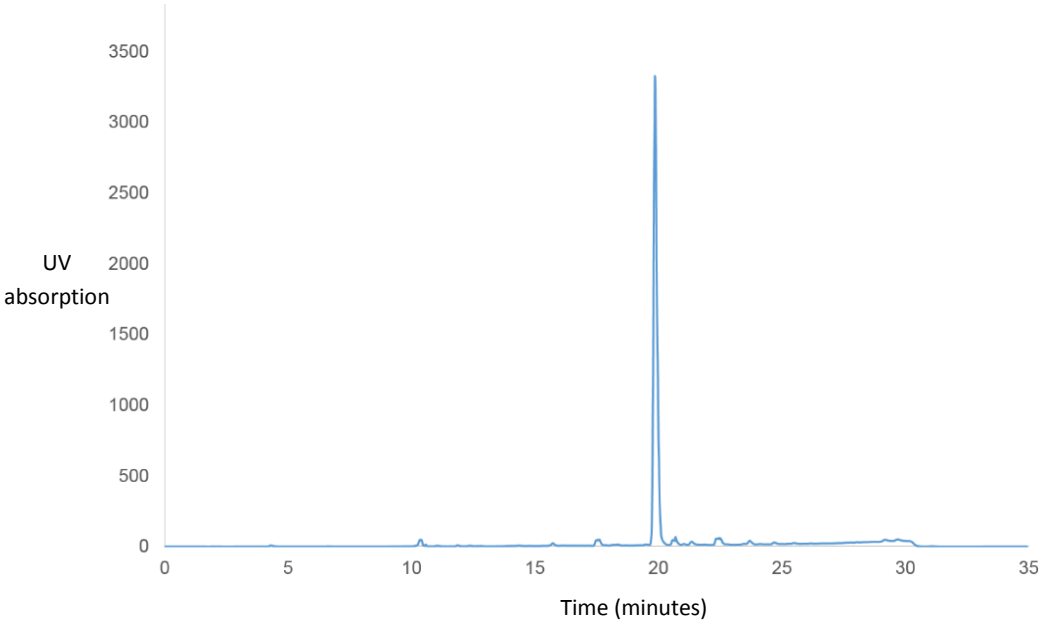

Figure 4.11. The UV-HPLC chromatogram of compound **17**.

4.3.3 Estimation of *in vivo* Partition Coefficients.

The octanol-water Partition Coefficient**,** Log P, is an important parameter that gives an insight into whether the molecule of interest has the ability to cross the blood-brain-barrier. The parameter also gives a prediction of a molecules *in vivo* NSB. As mentioned previously, most successful PET radioligands have a log P value that is in the range of 1 to 3. There are also a number of related measures that have been shown to be better predictors of NSB:

CHI_log$D_{7.4}$

CHI_log$D_{7.4}$ mimics the partition coefficients at physiological pH. In order to obtain the CHI_log$D_{7.4}$ values of compounds **16** - **18**, the retention time of four different standard compounds were initially used to obtain a calibration curve (Figure 4.12). The calibration curve equation was used to convert the HPLC retention times into CHI values. CHI values are usually between 1 and 100 and give an estimate of the percentage organic solvent needed for equal distribution of the compound between the mobile phase and stationary phase. Once CHI values are calculated, equation 4.3 is used to determine the CHI_log$D_{7.4}$ of test compounds. CHI_log$D_{7.4}$ is the value that provides an estimate of NSB.[12]

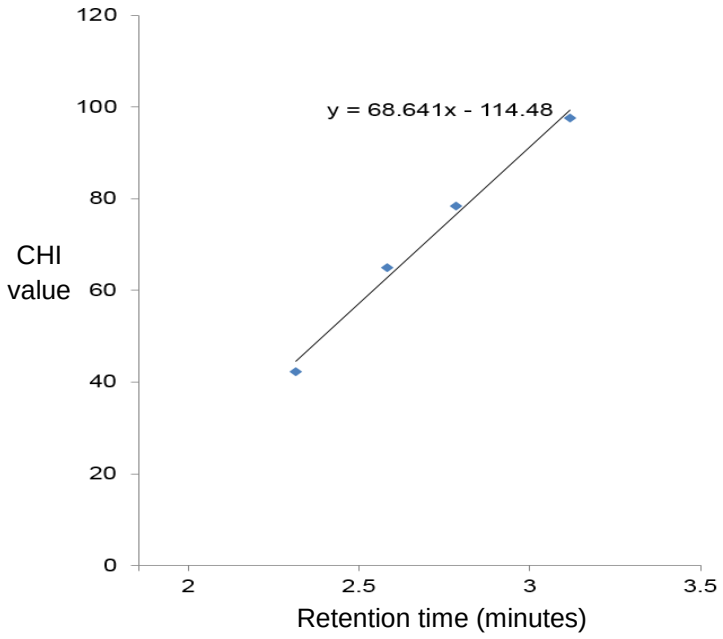

Figure 4.12. The retention time and CHI values of four reference standard compounds.

Equation 4.3 $CHI\_LogD_{7.4} = (0.0525 \times CHI) - 1.476$

Compound **18** had the highest $CHI\_logD_{7.4}$ followed by compound **16** and **17** (Table 4.7). This is to be expected as the addition of unsaturated carbons such as $-CH_2$ increase lipophilicity. Furthermore, benzylamine has a log P value of 1.09 while aniline and cyclohexyl amine have log P values of 0.9 and 1.4 respectively. The addition of a reagent with a high log P value into a molecules back bone increases the overall log P value of the final compound. Results from the $CHI\_logD_{7.4}$ suggested that all three compounds were within the suitable range of successful PET radioligands.

Table 4.7. The CHI and $CHI\_logD_{7.4}$ of the mGluR1 radioligand candidates.

Name	Retention time (minutes)	CHI at pH 7.4	$CHI\_logD_{7.4}$
Compound **16**	1.38	66.2526	2.01
Compound **17**	1.37	65.1079	1.95
Compound **18**	1.40	68.542	2.13

Log K_{IAM}

A HPLC stationary phase composed of an immobilised artificial membrane can be used to mimic the partition of molecules between the cell membrane and its surrounding aqueous environment. Log K_{IAM} is deemed superior to log P and CHI_log$D_{7.4}$ for measuring NSB.[12] The Log KI_{AM} values were obtained by initially measuring the retention time of five different standard compounds (Figure 4.13). A calibration curve was obtained and used to convert retention time to CHI_IAM values using equation 4.4. It is predicted that molecules with higher CHI_IAM values have higher NSB. The outcome values are used as an estimate of NSB.

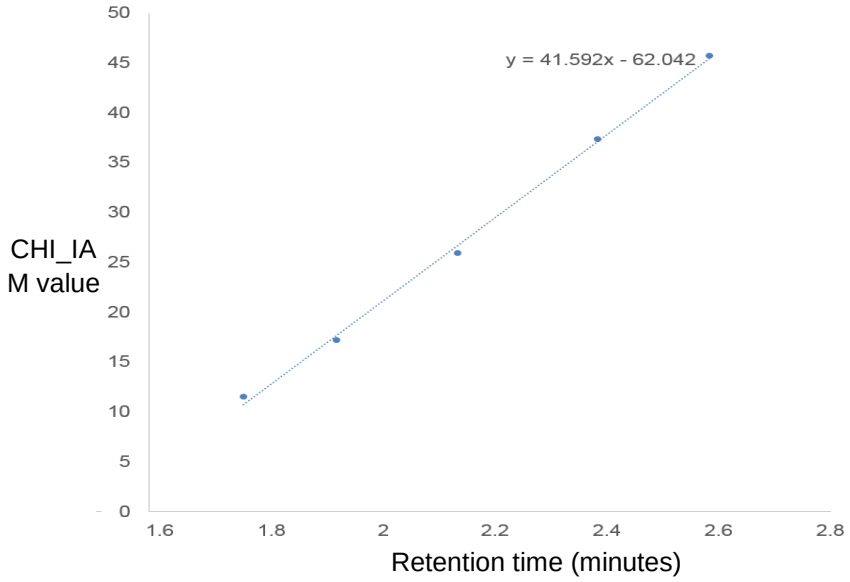

Figure 4.13. The HPLC retention time and CHI_IAM values of reference standard compounds.

Equation 4.4. Log K_{IAM} = (0.046 x CHI IAM) + 0.42

As expected, compound **18** had the highest Log K_{IAM} due to having the highest number of unsaturated carbons (Table 4.8). The difference in Log K_{IAM} values between all three compounds was very small (0.1). Nevertheless, results from the Log K_{IAM} suggested that all of the compounds were within the optimal range.

Table 4.8. The CHI_IAM and Log K_{IAM} of the mGluR1 radioligand candidates

Name	Retention time (minutes)	CHI_IAM	Log K_{IAM}
Compound **16**	2.25	31.54	1.87
Compound **17**	2.27	32.2332	1.90
Compound **18**	2.28	32.9264	1.93

4.3.4 Radiosynthesis

^{11}C is produced by a cyclotron predominantly in the form of $[^{11}C]CO_2$. There are a limited number of methods available that use $[^{11}C]CO_2$ directly for radiolabelling molecules of interest.[34] In chapter 2, a direct and rapid radiolabelling methodology that incorporated $[^{11}C]CO_2$ into amines for the synthesis of ureas was developed. The method was subsequently utilised for the radiolabelling of mGluR1 radioligand candidates. The precursor, compound **15**, was reacted with aliphatic, aromatic and benzylic amines in the presence of $[^{11}C]CO_2$ (Scheme 4.11).

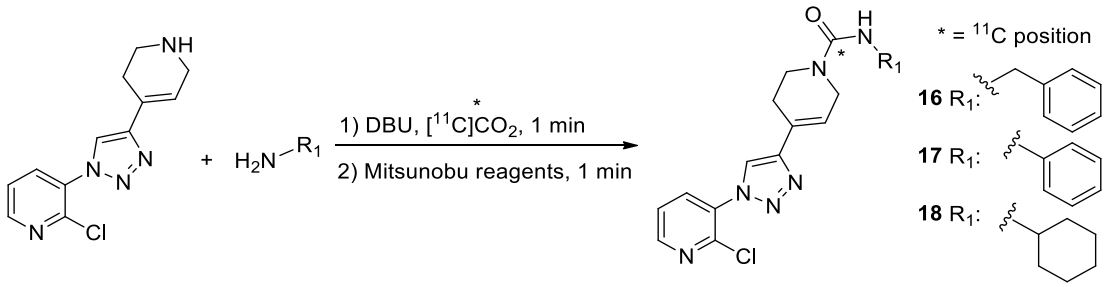

Scheme 4.11. The radiosynthesis of the mGluR1 tracer candidates.

$[^{11}C]CO_2$ was bubbled into a solution containing an amine, compound **15** and DBU in CH_3CN. At the EOB, the solution was stirred at 50 ^oC for one minute. Mitsunobu reagents in CH_3CN were added and the solution was heated for a further minute. The mixture was then purified using semi-preparative HPLC (Table 4.9).

Table 4.9. The radiochemistry reaction steps.

Time (minutes)	Activity
0:00	EOB
1:00	Addition of Mitsunobu reagents
2:00	Start of purification
37:00	End of HPLC purification.

The main by-product from the ^{11}C radiolabelling reaction was unreacted [^{11}C]CO_2 (70 %) which eluted at the solvent front. Other by-products, such as the symmetrical urea, were also observed. Semi-preparative HPLC was used to purify each radioligand. An example of a UV and a radio-chromatogram of the crude product is shown in figure 4.14. A radio-chromatogram of the purified compound is shown in figures 4.15. Although the mass of the product was low (1- 4 µmol), there were small amounts of unknown impurities in the purified product (Figure 4.16).

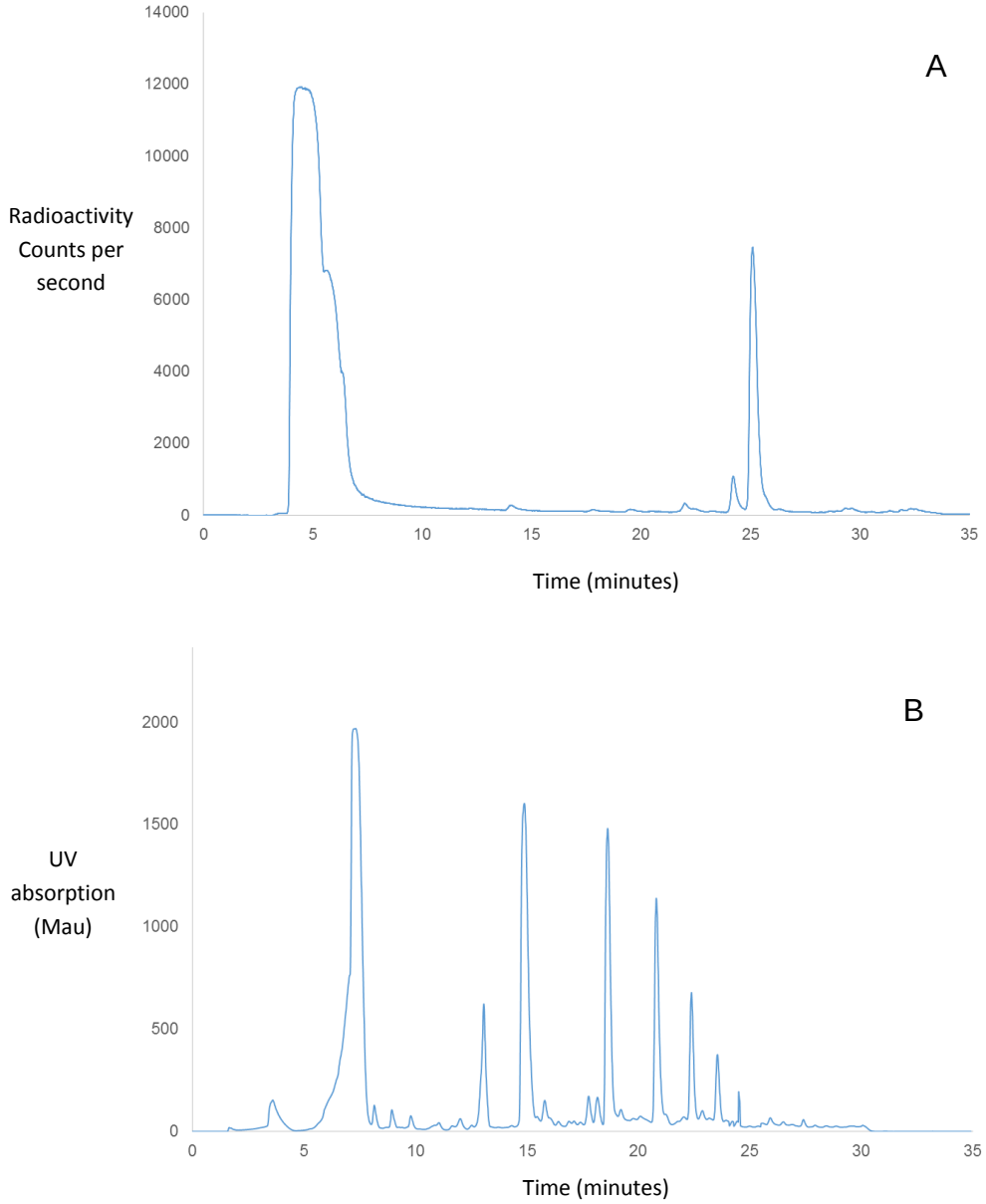

Figure 4.14. The crude (a) radio-HPLC chromatograms (b) UV-HPLC chromatograms radio-HPLC chromatograms of compound **17**.

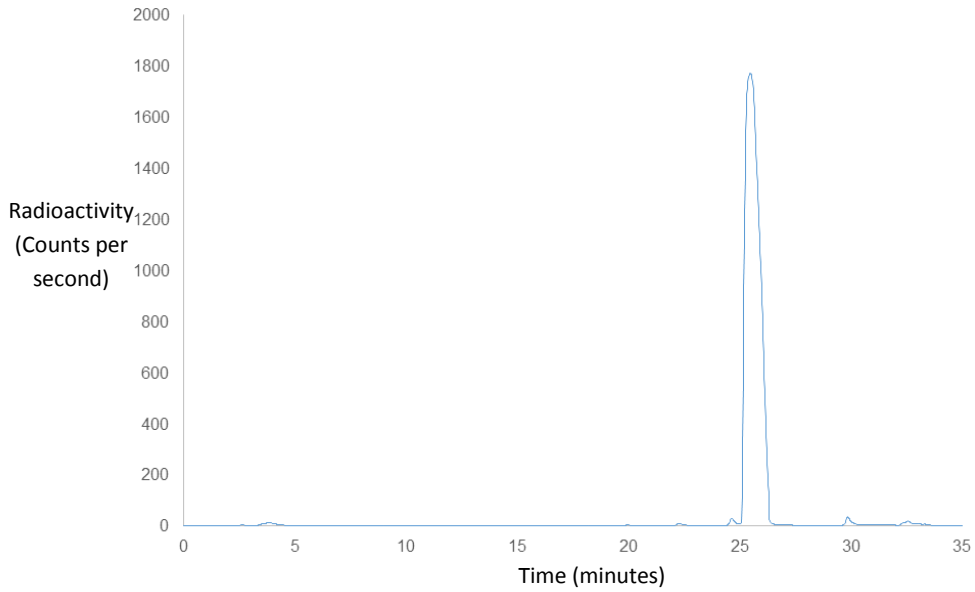

Figure 4.15. The radio-HPLC chromatograms of the purified compound **17**.

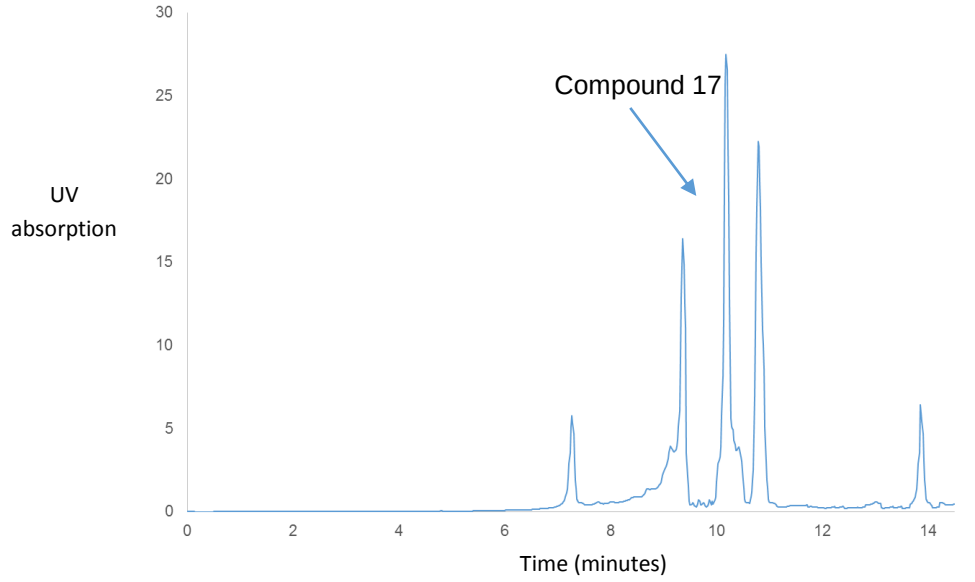

Figure 4.16. The UV-HPLC chromatogram of purified compound **17**.

Compounds 16, 17 and 18 were synthesised with an overall RCYs of 10, 8, and 12 %, respectively (based on starting [^{11}C]CO_2 and uncorrected for decay). A radiochemical purity of > 95 % with an overall synthesis time of 21 minutes from the EOB (including purification) and a specific activity of 2 ± 1.8 GBq/µmol were obtained.

The specific activity of the compounds were relatively low (2 ± 1.8 GBq/µmol) compared to the desired specific activity for imaging applications (> 50 GBq/µmol). This is because short cyclotron bombardments (1 minute) and low

beam currents (5 – 10 µA) were used. In clinical productions at our facility, a cyclotron bombardment times of 50 minutes and beam currents of 30 µA are used to produce higher amounts of radioactivity (typically 60 GBq). The mass of the radiolabelled compounds were in the range of 0.2 – 0.9 µmol. It is therefore estimated that this would increase the specific activity of the purified product to 25 - 50 GBq/µmol at EOS.

4.4 Conclusion

Metabotropic glutamate 1 receptors are linked to many diseases including Alzheimer's disease and autism. Developing radioligands that bind to these receptors would offer a valuable opportunity to deepen our understanding of these diseases by following the fate of these radiolabelled molecules *in vivo*. In this project, a library of candidate compounds were designed and successfully synthesised using traditional organic chemistry. HPLC methods used to predict the NSB of the compounds indicated that candidates CHI_log$D_{7.4}$ and log K_{IAM} are within the ideal range for minimising *in vivo* NSB whilst maintaining sufficient brain penetration.

The candidates were radiolabelled with [^{11}C]CO_2 using the strategy described in chapter 2. The method enables rapid incorporation of [^{11}C]CO_2 into reactive and stable amines for the synthesis of ^{11}C radiolabelled ureas. An isolated RCY of 16.4 % ± 8 (corrected for decay) was obtained. The overall synthesis time including purification was 21 minutes from the EOB and a specific activity of 2 ± 1.8 GBq/µmol was obtained for the radiosynthesis. For imaging applications, it is estimated that specific activity of 25 - 50 GBq/µmol can be obtained for a standard ^{11}C cyclotron bombardment at our facility. *In vitro* autoradiography studies of the radiolabelled compounds are currently in progress.

4.5 Method

4.5.1 General

All purchased chemicals were used without further purification. Chemicals were purchased in highest available purity from Sigma-Aldrich and Alfa Aesar and used as received (> 99 % purity). All solvents were purchased as anhydrous in highest available purity (> 99.8 % purity, water < 50 ppm, extra dry) from Sigma-Aldrich, used as received and stored under argon. Reference compounds were either purchased from Sigma-Aldrich or synthesised using reported procedures. Reactions were carried out under an atmosphere of nitrogen in heat gun dried glassware with magnetic stirring. Reactions were monitored using alumina plate thin-layer chromatography (Merck, silica gel 60, fluorescence indicator F254, or Merck, aluminium oxide neutral, fluorescence indicator F254). Silica gel chromatography was performed using 230-400 Mesh (Grade 60) silica gel. The mobile phase was a mixture of hexane : ethyl acetate in varying ratios and detected by 254 nm UV light. Infra-Red spectra were acquired on a PerkinElmer spectrum 100FTIR. ^{1}H-NMR (400 MHz) and ^{13}C-NMR (100 MHz) spectra were obtained using a BRUKER DRX 400 MHz spectrometer. Chemical shifts are reported in ppm (δ) relative to tetramethylsilane (TMS, d = 0 ppm) and calibrated using solvent residual peaks. Data are shown as follows: Chemical shift, multiplicity (s = singlet, d = doublet, t = triplet, q = quartet, m = multiplet), coupling constant (*J*, Hz) and integration. Calculated mass was determined using PerkinElmer ChemBioDraw Ultra 13.0 program. Mass spectroscopy was performed at King's College London using an Agilent 6520 Accurate-Mass Q-TOF LC/MS connected to an Agilent 1200 HPLC system with UV detector (254 nm) and auto-sampler. [^{11}C]CO_2 was produced by a Siemens RDS112 cyclotron (St Thomas' Hospital, London, United Kingdom) via the ^{14}N(p,α)^{11}C nuclear reaction. Typical irradiation times were 1 minute with a beam current of 10 μA, which yielded a [^{11}C]CO_2 amount of about 300 MBq at end of bombardment. Radiolabelling reactions were performed in a 1.5 mL screw top vial with a "V" internal shape. Analytical HPLC was performed on an Agilent 2060 Infinity HPLC system with a variable wavelength detector (254 nm was used as default wavelength). An Agilent Eclipse XDB-C18 reverse-phase column (4.6 x 150 mm,

5 µm) was used at a flow rate of 1 mL/min and H_2O/MeOH (HPLC grade solvents with 0.1 % TFA) gradient elution (flow rate: 1 mL/min, 0-2 min: 5 % MeOH, 2-11 min: 5 to 95 % MeOH linear gradient, 11-13 min: 90 % MeOH, 13-14 min: 90 % to 5 % MeOH linear gradient, and 14-15 min: 5 % MeOH). An Agilent ZORBAX GF-250 column (9.4 x 250 mm, 4 µm) was used for the purification of the crude product, a flow rate of 5 mL/min and H_2O/MeOH (0.1 % TFA) gradient elution (flow rate: 5 mL/min, 0-5 min: 5 % MeOH, 5-25 min: 5 to 95 % MeOH linear gradient, 25-27 min: 95 % MeOH, 27-32 min: 95 % to 5 % MeOH linear gradient, and 32-35 min: 5 % MeOH). The RCC was estimated by radio-HPLC and defined as the area under the [^{11}C]urea peak expressed as a percentage of the total ^{11}C labelled peak areas observed in the chromatogram. Specific radioactivity was calculated from analytical HPLC sample of 25 µL. A calibration curve of known mass quantity versus HPLC peak area (254nm) was used to calculate the mass concentration of the 25 µL radiolabelled compound. The identity of the radiolabelled compound peak was confirmed by HPLC co-injection of a nonradioactive reference compound and yielded a single peak.

4.5.2 Synthesis of reference compounds

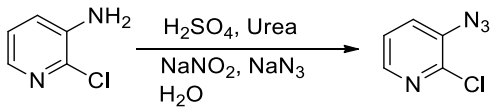

Compound 6

CAUTION: Organic azides are potentially explosive substances and the proposed synthesis needs to be conducted in a well-ventilated exhaust hood. Azides also react with metals and disposal must be highly diluted.

Synthesis of compound 6: H_2SO_4 (1.2 mL) in H_2O (7 mL) was heated at 55 ^oC for 5 minutes, 2-Chloro-3-pyridinamine (0.500 g, 3.89 mmol) was added and heated for further 5 minutes. The solution was cooled to 0 ^oC and $NaNO_2$ (0.55 g, 4.67 mmol) in H_2O (5 mL) was added over 15 minutes. The solution was stirred for 20 minutes at 0 ^oC and urea (0.08 g, 7.70 mmol) was added and stirred for further 20 minutes. NaN_3 (0.55 g, 4.67 mmol) in H_2O (5 mL) was added over 1 hour and mixture was stirred at 0 ^oC for further 20 minutes. The solution was then allowed

to cool to room temperature and stirred for 2 hours. Reaction was quenched with $NaHCO_3$, extracted with diethyl ether, dried over $MgSO_4$, carefully concentrated and purified with silica gel (Hexane/EtOAc). Yellow liquid; 82% yield (0.495 g); IR 2105.81, 1562.19, 1411.77, 1299.37 cm^{-1}; ^1H NMR (400 MHz, $CDCl_3$) δ 8.03 (m, 1H), 7.50 (m, 1H), 7.28 (m, 1H). HPLC-MS m/z: calculated for $[M + H^+]$ = 129.56; found 129.4520.

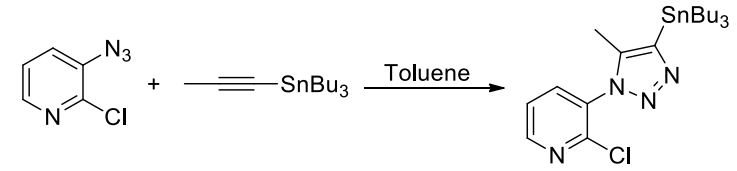

Compound 6 **Compound 7**

CAUTION: Organic azides are potentially explosive substances and the proposed synthesis needs to be conducted in a well-ventilated exhaust hood. Azides also react with metals and disposal must be highly diluted.

Synthesis of compound 7: tributyl(prop-1-yn-1-yl)stannane (0.33 g, 1.63 mmol) was added to compound 6 (0.2 g, 1.29 mmol) in toluene (2 mL) and stirred at 120 ^oC overnight. Reaction was cooled to room temperature and purified with silica gel (Hexane/EtOAc). Yellow liquid; 73% yield (0.593 g); IR 2924.47, 2924.47, 1473.72, 1419.83, 1066.34, cm^{-1}; ^1H NMR (400 MHz, $CDCl_3$) δ 8.40 (m, 1H), 8.00 (m, 1H), 7.40 (m, 1H), 2.30 (s, 3H), 1.55 (t, *J* = 6.4, 6H), 1.20 (m, 12H), 0.90 (t, *J* = 6.6, 9H); HPLC-MS m/z: calculated for $[M + H^+]$ = 484.14; found 484.1620. The spectral data of the synthesised is consistent with reported values.[32]

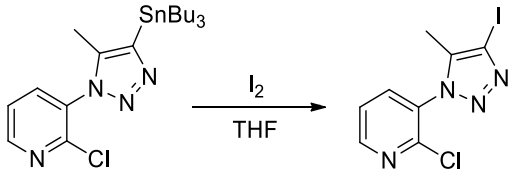

Compound 7 **Compound 8**

Synthesis of compound 8: Compound 7 (0.30 g, 0.622 mmol) in THF (3.5 mL) was added to I_2 (0.20 g, 0.778 mmol) in THF (3 mL) dropwise at 0 ^oC. The reaction was stirred for 5 minutes then allowed to cool to room temperature and stirred for further 3 hours. Mixture was diluted with EtOAc and quenched with $Na_2S_2O_3$.

Organic layer extracted, dried over $MgSO_4$, concentrated and purified with silica gel (Hexane/EtOAc). Yellow liquid; 92 % yield (0.183 g); IR 1507.93, 1472.97, 1415.63 cm^{-1}; ^1H NMR (400 MHz, $CDCl_3$) δ 8.55 (m, 1H), 7.80 (m, 1H), 7.50 (m, 1H), 2.30 (s, 3H); HPLC-MS m/z: calculated for [M + H^+] = 320.93; found 320.9106. The spectral data of the synthesised is consistent with reported values.[32]

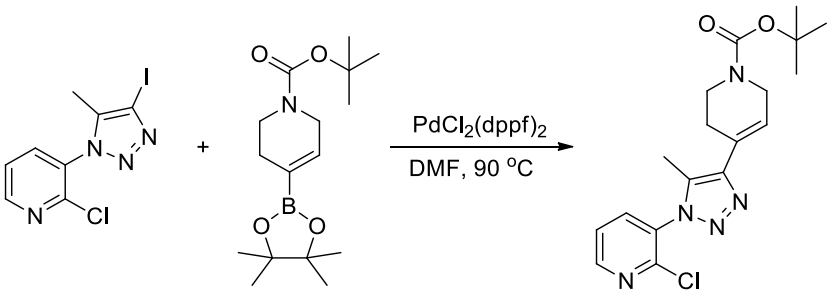

Compound 8 **Compound 9** **Compound 10**

Synthesis of compound 10: Compound 8 (0.040 g, 0.125 mmol), compound 9 (0.046 g, 0.150 mmol) and K_2CO_3 (0.033 g, 0.240 mmol) were added to $PdCl_2(dppf)_2$ (0.010, 0.013 mmol) in DMF (1.5 mL). The reaction mixture was stirred at 90 °C overnight. Mixture was diluted with water (15 mL) and extracted with DCM (x 2) and EtOAc (x 2). The combined organic fractions was dried ($MgSO^4$) and concentrated. ^1H NMR and LCMS of the crude product did not show the target product.

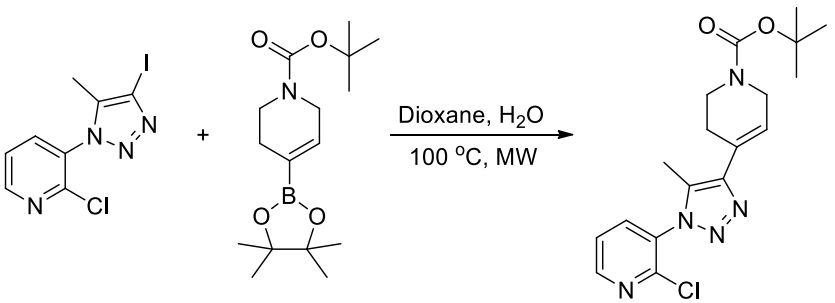

Compound 8 **Compound 9** **Compound 10**

Synthesis of compound 10: Compound 8 (0.040 g, 0.125 mmol), compound 9 (0.046 g, 0.150 mmol) and Na_2CO_3 (0.033 g, 0.375 mmol) were added to Pd $(PPh_3)_4$ (0.022 g, 0.019 mmol) in dioxane (1.5 mL) and H_2O (0.1 mL). The reaction mixture was heated at 100 °C using microwave for 2 hours. Mixture was diluted with water (4 mL) and extracted with DCM (x 2) and EtOAc (x 2). The

organic layer was dried over $MgSO_4$, concentrated and purified using combiflash (Hexane/EtOAc). Yellow solid; 32 % yield (0.047 g); HPLC-MS m/z: calculated for [M + H^+] = 376.15; found 376.1609.

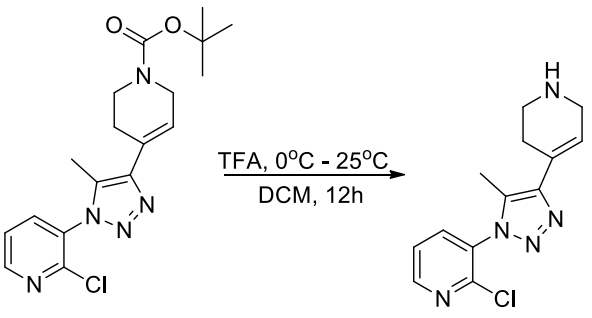

Compound 10 **Compound 1**

Synthesis of compound 1: TFA (192 µL) was added to a solution containing compound 10 (0.028 g, 0.076 mmol) in DCM (0.8 mL) at 0 °C. The reaction was warmed to room temperature and stirred overnight. 1N NaOH (8 mL) was added to the mixture and extracted with DCM (3 x 10 mL). The organic layer was washed with brine, dried with Na_2SO_4, and concentrated. Yellow solid; 100 % yield (0.021 g); HPLC-MS m/z: calculated for [M + H^+]= 276.73; found 276.8230.

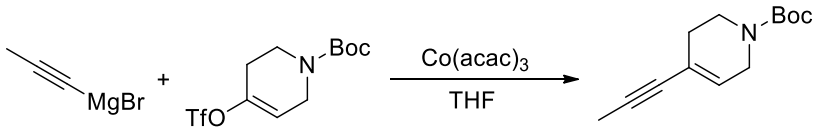

Compound 11 **Compound 12**

Synthesis of compound 12: compound 11 (0.083 g, 0.25 mmol), $Co(acac)_3$ (0.003 g, 0.008 mmol) in THF was added to prop-1-yn-1-ylmagnesium bromide (0.064 g, 0.45 mmol) and stirred at 40 °C overnight. Reaction was quenched with 0.1M HCl (10 mL), extracted with diethyl ether (x 3). The organic layer was washed with brine, dried with $MgSO_4$, and concentrated. No purification was required. Dark yellow liquid; 66 % yield (0.036 g); ^{1}H NMR (400 MHz, $CDCl_3$) δ 5.85 (t, *J* = 9.5, 1H), 3.90 (m, 2H), 3.41 (m, 2H), 2.13 (m, 2H), 1.98 (m, 2H), 1.80 (s, 3H), 1.35 (s, 9H); HPLC-MS m/z: calculated for [M + H^+] = 222.14; found 222.1489.

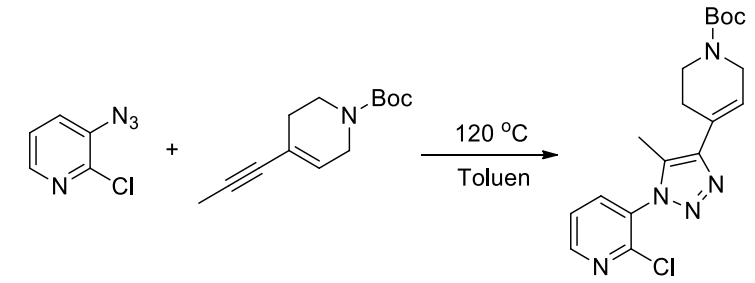

Compound 6 **Compound 12** **Compound 10**

Synthesis of compound 10: compound 12 (0.1 g, 0.45 mmol) was added to compound 6 (0.09 g, 0.585 mmol) in toluene (5 mL) and stirred at 120 °C overnight. ^{1}H NMR and LCMS of the crude product did not show the target product.

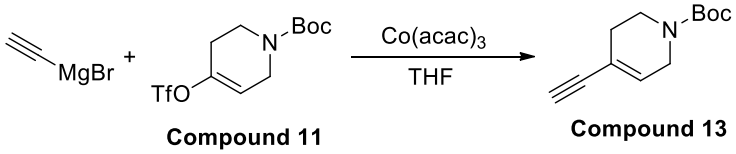

Compound 11 **Compound 13**

Synthesis of compound 13: Compound 11 (0.250 g, 0.755 mmol), $Co(acac)_3$ (0.008 g, 0.022 mmol) in THF (2 mL) was added to ethynylmagnesium bromide (0.195 g, 1.51 mmol) and stirred at 40 °C overnight. Reaction was quenched with 0.1M HCl (10 mL), extracted with diethyl ether (3 x 10 mL). The organic layer was washed with brine, dried with $MgSO_4$, and concentrated. Compound was purified by flash chromatography (Hexane/EtOAc). Colourless solid; 67 % yield (0.104 g); IR 3289, 3240, 2974, 2929, 2838, 1658, 1413 cm^{-1}; ^{1}H NMR (400 MHz, $CDCl_3$) δ 6.10 (t, *J* = 9.7, 1H), 3.97 (m, 2H), 3.50 (m, 2H), 2.90 (s, 1H), 2.26 (m, 2H), 1.47 (s, 9H); ^{13}C NMR (100 MHz, $CDCl_3$) δ 154.9, 132.4, 119.0, 84.0, 80.1, 76.5, 43.8 29.4, 28.7.

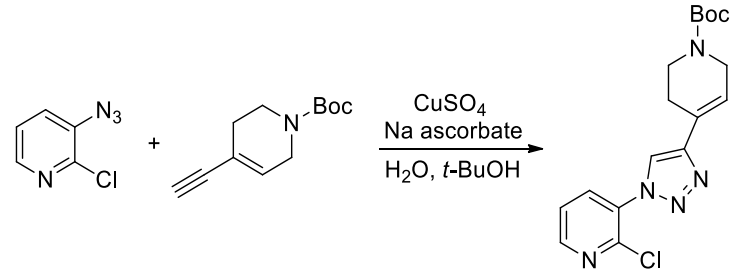

Compound 6 **Compound 13** **Compound 14**

CAUTION: Organic azides are potentially explosive substances and the proposed synthesis needs to be conducted in a well-ventilated exhaust hood. Azides also react with metals and disposal must be highly diluted.

Synthesis of compound 14: compound 6 (0.212 g, 1.37 mmol) and compound 13 (0.237 g, 1.14 mmol) were added to a round bottom flask containing H_2O (2.3 mL) and *t*-BuOH (2.3 mL). Reaction mixture was stirred at room temperature for 5 minutes before adding $CuSO_4$ (17.5 µL, 1 M) and sodium ascorbate (175 µL, 1 M). The mixture was stirred at room temperature overnight. H_2O was added to the mixture and extracted with DCM. The organic layer was washed with brine, saturated $NaHCO_3$, dried with $MgSO_4$ and concentrated. Compound was purified by flash chromatography (Hexane/EtOAc). Yellow solid; 67 % yield (0.280 g); ^{1}H NMR (400 MHz, $CDCl_3$): δ 8.56 (m, 1H), 8.04 (m, 1H), 8.00 (s, 1H), 7.50 (m, 1H), 6.57 (t, *J* = 4.9, 1H), 4.14 (m, 2H), 3.67 (m, 2H), 2.59 (m, 2H), 1.49 (s, 9H).

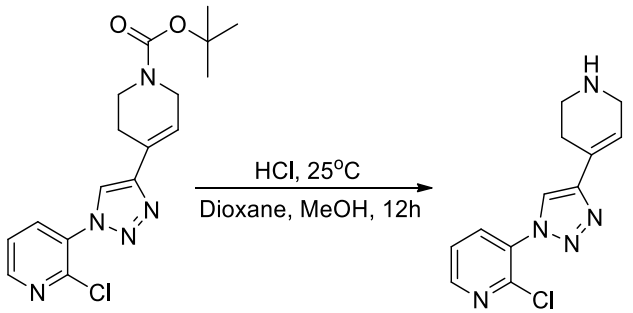

Compound 14 **Compound 15**

Synthesis of compound 15: HCl (8.5 mL, 4 M) was added to a solution containing compound 14 (0.615 g, 1.70 mmol) in dioxane (5 mL) and H_2O (5 mL). The reaction was stirred at room temperature overnight and concentrated. Yellow solid; 61 % yield (0.374 g);. ^{1}H NMR (400 MHz, CD_3OD) δ 8.56 (m, 1H), 8.39 (s, 1H), 8.09 (m, 1H), 7.61 (m, 1H), 6.57 (s, 1H),4.48 (m, 2H), 3.04 (m, 2H), 2.51 (s,

2H). ^{13}C NMR (100 MHz, CD_3OD): 152.1, 149.9, 147.3, 138.4, 133.6, 127.1, 125.3, 125.0, 123.5, 45.2, 43.2, 27.1. HPLC (linear gradient from 20 % to 100 % ACN over 15 min): t_r = 8.17 min, purity = 95 %. HPLC-MS m/z: calculated for [M + H^+] = 362.08; found 362.1003.

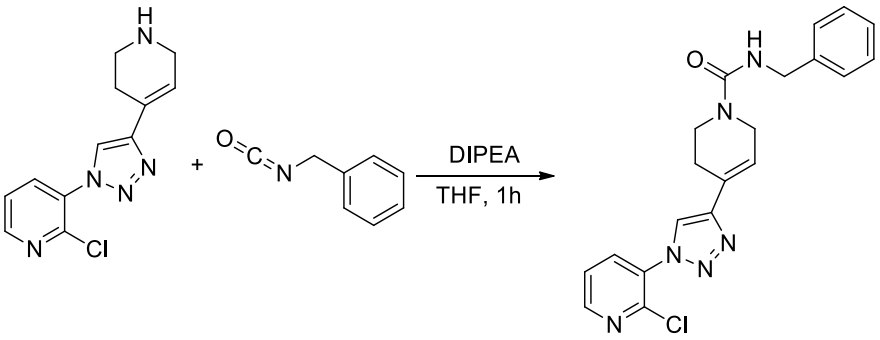

Compound 15 **Compound 16**

Synthesis of compound 16: Compound 15 (40 mg, 0.152 mmol) in THF (10 mL) was added to (isocyanatomethyl)benzene (128 µL, 1.04 mmol) and stirred at room temperature for 1 hour. The mixture was concentrated and purified by flash chromatography (EtOAc to 10 % MeOH/EtOAc). White solid; Yield = 81 % (44 mg); IR 3377, 3265, 3062, 2921, 1637, 1593, 1535, 1235 cm^{-1}; ^{1}H NMR (400 MHz, $CDCl_3$) δ 8.49 (m, 1H), 7.97 (m, 1H), 7.96 (s, 1H), 7.43 (m, 1H), 7.26 (m, 5H), 6.51 (m, 1H), 4.8 (s, 1H), 4.41 (m, 2H), 4.04 (m, 2H), 3.67 (m, 2H), 2.56 (m, 2H). ^{13}C NMR (100 MHz, CDCl3): 157.4, 150.2, 147.9, 144.8, 139.3, 135.8, 132.0, 128.6, 127.7, 127.3, 126.6, 123.4, 121.3, 120.5, 44.9, 43.5, 26.4. HPLC (linear gradient from 20 % to 100 % ACN over 15 min): t_r = 9.11 min, purity = 98.5%. HPLC-MS m/z: calculated for [M + H^+] 395.13, found 395.1368 (M + H^+, ^{35}Cl), 397.1342 (M + H^+, ^{37}Cl), 417.1189 (M + Na^+, ^{35}Cl), 419.118 (M + Na^+, ^{37}Cl).

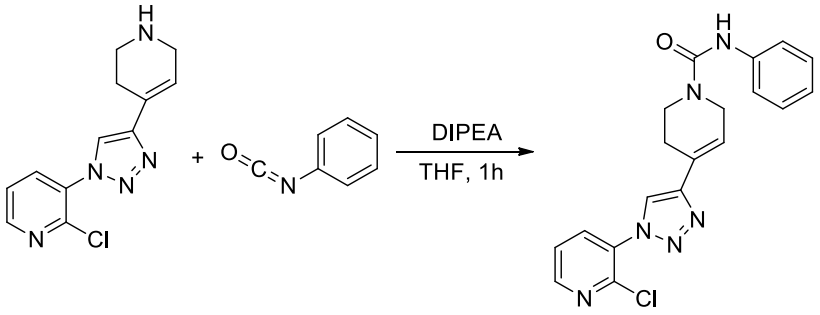

Compound 15 **Compound 17**

Synthesis of compound 17: Compound 15 (40 mg, 0.152 mmol) in THF (10 mL) was added to isocyanatobenzene (128 µL, 1.04 mmol) and stirred at room temperature for 1 hour. The mixture was concentrated and purified by flash chromatography (EtOAc to 10 % MeOH/EtOAc). Pale yellow solid; Yield = 82 % (47 mg); IR 3325, 3131, 2922, 1624, 1527, 1476, 1387 cm^{-1}; ^{1}H NMR (400 MHz, $CDCl_3$) 8.49 (m, 1H), 7.97 (m, 1H), 7.96(s, 1H), 7.43 (m, 1H), 7.31 (m, 2H), 7.21 (m, 2H), 6.98 (m, 1H), 6.54 (s, 1H), 6.45 (s, 1H), 4.15 (m, 2H), 3.71 (m, 2H), 2.61 (m, 2H). ^{13}C NMR (100 MHz, CDCl3): 154.4, 150.2, 147.8, 144.8, 138.8, 135.8, 128.9, 126.2, 123.4, 123.2, 121.1, 120.6, 120.1, 43.9, 40.0, 26.4. HPLC (linear gradient from 20% to 100% ACN over 15 min): t_r = 9.15 min, purity = 98.1%. HPLC-MS m/z: calculated for [M + H^+] 381.12, found 381.1209 (M+H^+, ^{35}Cl), 383.1200 (M+H^+, ^{37}Cl), 403.1034 (M+Na^+, ^{35}Cl), 405.1025 (M+Na^+, ^{37}Cl).

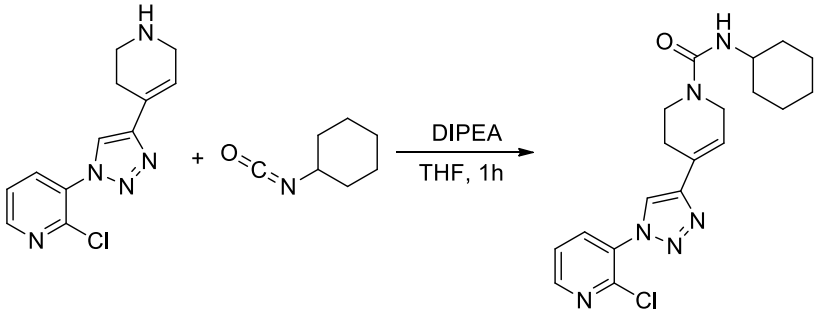

Compound 15 **Compound 18**

Synthesis of compound 18: Compound 15 (40 mg, 0.152 mmol) in THF (10 mL) was added to isocyanatocyclohexane (128 µL, 1.04 mmol) and stirred at room temperature for 1 hour. The mixture was concentrated and purified by flash chromatography (EtOAc to 10 % MeOH/EtOAc). white solid; Yield = 84 % (49

mg); IR 3342, 3153, 2926, 2852, 1615, 1528, 1228 cm^{-1}; ^{1}H NMR (400 MHz, $CDCl_3$) 8.54 (m, 1H), 8.01(m, 2H), 7.48 (m, 1H), 6.56 (m, 1H), 4.42 (s, 1H), 4.02 (m, 2H), 3.64 (m, 3H), 2.57 (m, 2H), 1.93 (m, 2H), 1.66 (m, 2H), 1.16 - 1.57 (m, 6H). ^{13}C NMR (100 MHz, $CDCl_3$): 156.8, 150.1, 147.9, 144.8, 135.8, 131.9, 126.0, 123.4, 121.4, 120.5, 49.4, 43.4, 39.4, 33.9, 26.4, 25.5, 25.0. HPLC (linear gradient from 20 % to 100 % ACN over 15 min): t_r = 9.58 min, purity = 98.5%. HPLC-MS m/z: calculated for [M + H^+] 387.13, found 387.1699 (M+H^+, ^{35}Cl), 389.1667 (M+H^+, ^{37}Cl).

4.5.3 Lipophilicity

CHI_log$D_{7.4}$

HPLC was performed on an Agilent 1200 system with a UV wavelength detector (254 nm) and radio-detector. Luna C18 column (50 x 30 mm, 25µm) was used with the following mobile phase condition: Solvent A: 50 mM ammonium acetate buffer (pH 7.4); solvent B: acetonitrile. The HPLC was performed at a flow rate of 1 mL/min. four different compounds were used to create a calibration curve (acetophenone, propiophenone, valerophenone and acetanilide). All samples were prepared on 1 mL/mg solution using 50:50 solvent A and B, and 20 um was used for HPLC. Retention time of all reagents were converted to Log $D_{7.4}$ using equation 4.3 where CHI is the obtained from the calibration curve.

Equation 4.3: CHI_Log$D_{7.4}$ = (0.525 x CHI) - 1.476

logK_{IAM}

HPLC was performed on an Agilent 1200 system with a UV wavelength detector (254 nm) and radio-detector. Immobilised artificial membrane PC2 HPLC column (150 x 4.6 mm, 12 µm) was used with the following mobile phase conditions: Solvent A: 50 mM ammonium acetate buffer (pH 7.4); solvent B: acetonitrile. The HPLC was performed at a flow rate of 2 mL/min. Five different compounds were used to create a calibration curve (acetophenone, propiophenone, butrophenone, valerophenone and acetanilide). All samples were prepared on 1 mL/mg solution

using 50:50 solvent A and B, and 20 um was used for HPLC. Retention time of all reagents were converted to CHI_IAM using equation X where CHI_IAM is the obtained from the calibration curve.

Equation 4.4: Log K_{IAM} = (0.046 x CHI IAM) + 0.42

4.5.4 Radiolabelling procedure

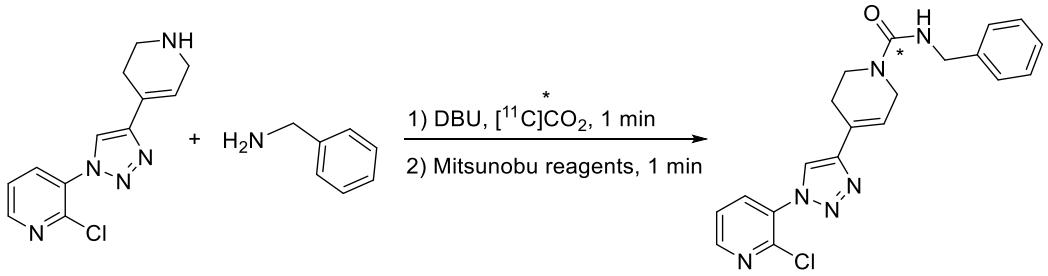

Compound 15 **[^{11}C]Compound 16**

Synthesis of [^{11}C]compound 16: Compound 15 (10 mg, 27.5 µmol) was added to a vail containing benzylamine (2 µL, 18.3 µmol) and DBU (0.13 µL, 0.9 µmol) in CH_3CN (300 µL). [^{11}C]CO_2 from the cyclotron was bubbled into the reaction mixture and the resulting solution was stirred, and heated at 50 ^{o}C for 1 minute. In a separate vial, tributylphosphine (9 µL, 36.6 µmol) was added to a solution containing di-*tert*-butyl azodicarboxylate (8 mg, 36.6 µmol) in CH_3CN (100 µL) under argon. The resulting solution was transferred into the reaction mixture and stirred for one minute at 50 ^{o}C and purified by HPLC. t_r = 25.15 min; RCC = 16 %; RCY = 10 % (uncorrected for decay); RCP = > 95 %; specific activity = 2 ± 1.8 GBq/µmol.

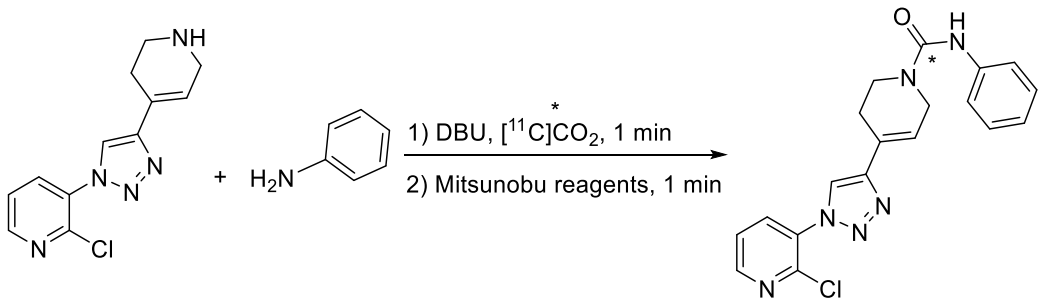

Compound 15 **[^{11}C]compound 17**

Synthesis of [^{11}C]compound 17: Compound 15 (10 mg, 27.5 µmol) was added to a vail containing cyclohexylamine (1.67 µL, 27.5 µmol) and DBU (0.13 µL, 0.9 µmol) in CH_3CN (300 µL). [^{11}C]CO_2 from the cyclotron was bubbled into the reaction mixture and the resulting solution was stirred and heated at 50 ^{o}C for 1 minute. In a separate vial, tributylphosphine (9 µL, 36.6 µmol) was added to a solution containing di-*tert*-butyl azodicarboxylate (8 mg, 36.6 µmol) in CH_3CN (100 µL) under argon. The resulting solution was transferred into the reaction mixture and stirred for one minute at 50 ^{o}C and purified by HPLC. t_r = 25.43 min; RCC = 13 %; RCY = 8 % (uncorrected for decay); RCP = > 95 %; specific activity = 2 ± 1.8 GBq/µmol.

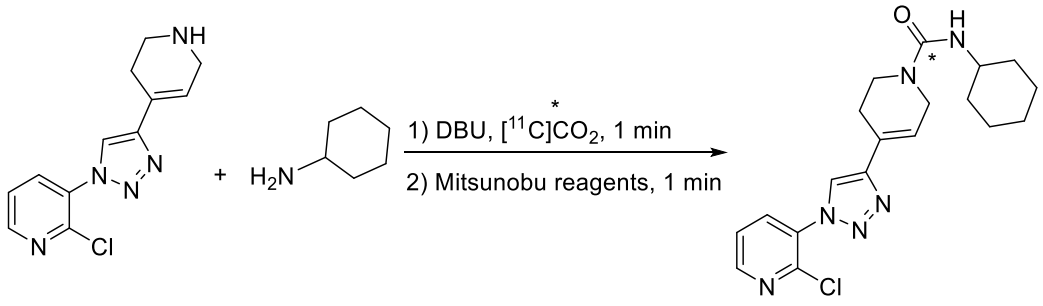

Compound 15 **[^{11}C]compound 18**

Synthesis of [^{11}C]compound 18: Compound 15 (10 mg, 27.5 µmol) was added to a vail containing cyclohexylamine (2.1 µL, 27.5 µmol) and DBU (0.13 µL, 0.9 µmol) in CH_3CN (300 µL). [^{11}C]CO_2 from the cyclotron was bubbled into the reaction mixture and the resulting solution was stirred and heated at 50 ^{o}C for 1 minute. In a separate vial, tributylphosphine (9 µL, 36.6 µmol) was added to a solution containing di-*tert*-butyl azodicarboxylate (8 mg, 36.6 µmol) in CH_3CN (100 µL) under argon. The resulting solution was transferred into the reaction mixture and stirred for one minute at 50 ^{o}C. The reaction was quenched with H_2O

(0.5 mL) and purified by HPLC. t_r = 27.05 min; RCC = 12 %; RCY = 6.5 % (uncorrected for decay); RCP = > 95 %; specific activity = 2 ± 1.8 GBq/µmol.

4.6 References

[1] P. W. Miller, N. J. Long, R. Vilar, A. D. Gee, *Angewandte Chemie International Edition* **2008**, *47*, 8998-9033.

[2] S. E. Snyder, L. Tluczek, D. M. Jewett, T. B. Nguyen, D. E. Kuhl, M. R. Kilbourn, *Nuclear Medicine and Biology* **1998**, *25*, 751-754.

[3] C. Muhr, M. Bergström, P. O. Lundberg, K. Bergström, B. Långström, *Acta Radiologica, Supplement* **1986**, *369*, 406-408.

[4] O. Inoue, T. Suhara, T. Itoh, K. Kobayashi, K. Suzuki, Y. Tateno, *Neuroscience Letters* **1992**, *145*, 133-136.

[5] B. Bencherif, P. N. Fuchs, R. Sheth, R. F. Dannals, J. N. Campbell, J. J. Frost, *Pain* **2002**, *99*, 589-598.

[6] V. W. Pike, *Trends in Pharmacological Sciences* **2009**, *30*, 431-440.

[7] A. H. Jacobs, H. Li, A. Winkeler, R. Hilker, C. Knoess, A. Rüger, N. Galldiks, B. Schaller, J. Sobesky, L. Kracht, P. Monfared, M. Klein, S. Vollmar, B. Bauer, R. Wagner, R. Graf, K. Wienhard, K. Herholz, W. D. Heiss, *European Journal of Nuclear Medicine and Molecular Imaging* **2003**, *30*, 1051-1065.

[8] a) A. D. Gee, *British Medical Bulletin* **2003**, *65*, 169-177; b) S. Li, Y. Huang, *Current Medicinal Chemistry* **2014**, *21*, 113-123.

[9] E. D. Hostetler, W. Eng, A. D. Joshi, S. Sanabria Bohórquez, H. Kawamoto, S. Ito, S. O'Malley, S. Krause, C. Ryan, S. Patel, M. Williams, K. Riffel, G. Suzuki, S. Ozaki, H. Ohta, J. Cook, H. D. Burns, R. Hargreaves, *Synapse* **2011**, *65*, 125-135.

[10] R. N. Waterhouse, *Molecular Imaging and Biology* **2003**, *5*, 376-389.

[11] F. Kügler, W. Sihver, J. Ermert, H. Hübner, P. Gmeiner, O. Prante, H. H. Coenen, *Journal of Medicinal Chemistry* **2011**, *54*, 8343-8352.

[12] C. Pidgeon, S. Ong, H. Liu, X. Qiu, M. Pidgeon, A. H. Dantzig, J. Munroe, W. J. Hornback, J. S. Kasher, L. Glunz, *Journal of Medicinal Chemistry* **1995**, *38*, 590-594.

[13] A. Taillardat Bertschinger, P. A. Carrupt, F. Barbato, B. Testa, *Journal of Medicinal Chemistry* **2003**, *46*, 655-665.

[14] a) S. Marchais, B. Nowicki, H. Wikström, L. T. Brennum, C. Halldin, V. W. Pike, *Bioorganic & Medicinal Chemistry* **2001**, *9*, 695-702; b) S. Marchais

Oberwinkler, B. Nowicki, V. W. Pike, C. Halldin, J. Sandell, Y. H. Chou, B. Gulyas, L. T. Brennum, L. Farde, H. V. Wikström, *Bioorganic & Medicinal Chemistry* **2005**, *13*, 883-893.

[15] A. M. Seddon, D. Casey, R. V. Law, A. Gee, R. H. Templer, O. Ces, *Chemical Society Reviews* **2009**, *38*, 2509-2519.

[16] W. D. Heiss, K. Herholz, *Journal of Nuclear Medicine* **2006**, *47*, 302-312.

[17] T. G. Hamill, S. Krause, C. Ryan, C. Bonnefous, S. Govek, T. J. Seiders, N. D. P. Cosford, J. Roppe, T. Kamenecka, S. Patel, R. E. Gibson, S. Sanabria, K. Riffel, W. Eng, C. King, X. Yang, M. D. Green, S. S. O'Malley, R. Hargreaves, H. D. Burns, *Synapse* **2005**, *56*, 205-216.

[18] T. J. Raub, *Molecular Pharmaceutics* **2006**, *3*, 3-25.

[19] B. S. Meldrum, *The Journal of Nutrition* **2000**, *130*, 1007S-1015S.

[20] K. Yanamoto, F. Konno, C. Odawara, T. Yamasaki, K. Kawamura, A. Hatori, J. Yui, H. Wakizaka, N. Nengaki, M. Takei, M. R. Zhang, *Nuclear Medicine and Biology* **2010**, *37*, 615-624.

[21] J. Toyohara, M. Sakata, M. Fujinaga, T. Yamasaki, K. Oda, K. Ishii, M. R. Zhang, C. M. Moriguchi Jeckel, K. Ishiwata, *Nuclear Medicine and Biology* **2013**, *40*, 214-220.

[22] H. Lavreysen, S. N. Pereira, J. E. Leysen, X. Langlois, A. S. J. Lesage, *Neuropharmacology* **2004**, *46*, 609-619.

[23] P. Zanotti Fregonara, V. N. Barth, S. S. Zoghbi, J. S. Liow, E. Nisenbaum, E. Siuda, R. L. Gladding, D. Rallis Frutos, C. Morse, J. Tauscher, V. W. Pike, R. B. Innis, *European Journal of Nuclear Medicine and Molecular Imaging Research* **2013**, *3*, 47-47.

[24] K. Yanamoto, F. Konno, C. Odawara, T. Yamasaki, K. Kawamura, A. Hatori, J. Yui, H. Wakizaka, N. Nengaki, M. Takei, M. R. Zhang, *Nuclear Medicine and Biology* **2010**, *37*, 615-624.

[25] J. Prabhakaran, V. J. Majo, M. S. Milak, S. A. Kassir, M. Palner, L. Savenkova, P. Mali, V. Arango, J. J. Mann, R. V. Parsey, J. S. D. Kumar, *Bioorganic and Medicinal Chemistry Letters* **2010**, *20*, 3499-3501.

[26] M. Fujinaga, T. Yamasaki, J. Yui, A. Hatori, L. Xie, K. Kawamura, C. Asagawa, K. Kumata, Y. Yoshida, M. Ogawa, N. Nengaki, T. Fukumura, M. R. Zhang, *Journal Medicinal Chemistry* **2012**, *55*, 2342-2352.

[27] J. Toyohara, M. Sakata, M. Fujinaga, T. Yamasaki, K. Oda, K. Ishii, M. R. Zhang, C. M. Moriguchi Jeckel, K. Ishiwata, *Nuclear Medicine and Biology* **2013**, *40*, 214-220.

[28] T. Yamasaki, J. Maeda, M. Fujinaga, Y. Nagai, A. Hatori, J. Yui, L. Xie, N. Nengaki, M. R. Zhang, *American Journal of Nuclear Medicine and Molecular Imaging* **2014**, *4*, 260-269.

[29] P. Zanotti Fregonara, V. N. Barth, J. S. Liow, S. S. Zoghbi, D. T. Clark, E. Rhoads, E. Siuda, B. A. Heinz, E. Nisenbaum, B. Dressman, E. Joshi, D. Luffer Atlas, M. J. Fisher, J. J. Masters, N. Goebl, S. L. Kuklish, C. Morse, J. Tauscher, V. W. Pike, R. B. Innis, *European Journal of Nuclear Medicine and Molecular Imaging* **2013**, *40*, 245-253.

[30] a) H. T. Ohgami M, Takai N, Zhang MR, Kawamura K, Yamaski T, Yanamoto K., *European Journal of Nuclear Medicine and Molecular Imaging* **2009**, *36*; b) M. Fujinaga, J. Maeda, J. Yui, A. Hatori, T. Yamasaki, K. Kawamura, K. Kumata, Y. Yoshida, Y. Nagai, M. Higuchi, T. Suhara, T. Fukumura, M. R. Zhang, *Journal of Neurochemistry* **2012**, *121*, 115-124.

[31] G. Suzuki, T. Kimura, A. Satow, N. Kaneko, J. Fukuda, H. Hikichi, N. Sakai, S. Maehara, H. Kawagoe Takaki, M. Hata, T. Azuma, S. Ito, H. Kawamoto, H. Ohta, *Journal of Pharmacology and Experimental Therapeutics* **2007**, *321*, 1144-1153.

[32] S. Ito, A. Satoh, Y. Nagatomi, Y. Hirata, G. Suzuki, T. Kimura, A. Satow, S. Maehara, H. Hikichi, M. Hata, H. Kawamoto, H. Ohta, *Bioorganic and Medicinal Chemistry* **2008**, *16*, 9817-9829.

[33] a) V. V. Rostovtsev, L. G. Green, V. V. Fokin, K. B. Sharpless, *Angewandte Chemie International Edition* **2002**, *41*, 2596-2599; b) B. C. Boren, S. Narayan, L. K. Rasmussen, L. Zhang, H. Zhao, Z. Lin, G. Jia, V. V. Fokin, *Journal of the American Chemical Society* **2008**, *130*, 8923-8930; c) J. A. Shin, Y. G. Lim, K. H. Lee, *The Journal of Organic Chemistry* **2012**, *77*, 4117-4122.

[34] B. H. Rotstein, S. H. Liang, J. P. Holland, T. L. Collier, J. M. Hooker, A. A. Wilson, N. Vasdev, *Chemical Communication* **2013**, *49*, 5621-5629.

Chapter 5

Conclusions and Future work

5.1 Conclusions

PET is a non-invasive molecular imaging technique that provides quantitative data on the biodistribution and kinetics of radiolabelled molecules *in vivo*. The use of the technique has increased over the last decades due to the high sensitivity of PET which makes it ideal for *in vivo* medical diagnosis, medical research and drug studies. Carbon-11 (^{11}C) is one of the most commonly used radionuclides for PET molecular imaging. The presence of carbon in all naturally occurring organic molecules makes ^{11}C an attractive positron emitter: substituting the naturally abundant carbon-12 in biological molecules with radioactive ^{11}C has no effect on its biological activity. ^{11}C is produced by a cyclotron, most commonly in the form of $[^{11}C]CO_2$ and it is usually converted into more reactive species such as [^{11}C]methyl iodide and [^{11}C]carbon monoxide for radiolabelling. Although these reactive species are useful for radiolabelling, ^{11}C has a half-life of 20.4 minutes and therefore, avoiding the conversion of $[^{11}C]CO_2$ to other forms provides a strategy to shorten synthesis times.

There are a limited number of methods that incorporate $[^{11}C]CO_2$ directly into target molecules of interest.[1]

In this thesis, a novel radiolabelling reaction that efficiently incorporates $[^{11}C]CO_2$ directly into [^{11}C]carbamates and [^{11}C]carbonates has been developed. The rapid methodology produced target radiolabelled products in high radiochemical yields (> 80 %) and in a short reaction times (10 minutes). The strategy enables the radiolabelling of carbonates which were previously inaccessible for ^{11}C radiolabelling. This reaction is therefore a useful addition to the arsenal of methodologies available for ^{11}C radiolabelling. However, due to the presence of carbonate (from Cs_2CO_3), the reaction resulted in specific activities in the range of 1 - 10 GBq/µmol (mass range: 10 - 50 µmol). Although this is undesirable for imaging receptors or enzymes expressed at very low concentrations, the method can be used for other purposes including the study of the biodistribution and kinetics of drugs *in vivo*.

Ureas are functional groups found in numerous drugs (e.g. phenacedine and ZJ43). Although there are methods available to radiolabel ureas with $[^{11}C]CO_2$, these methods are limited to radiolabelling aliphatic and benzylic compounds and

therefore, developing robust methods to radiolabel aromatic amines is of considerable interest. A rapid radiolabelling methodology that incorporates [^{11}C]CO_2 directly into amines for the synthesis of ^{11}C labelled ureas was developed. The new radiolabelling reaction produced high radiochemical yields similar to that reported in the literature (up to 95 %) when aliphatic and benzylic amines were synthesised. However, in contrast to existing reactions, the new methodology produced much higher radiochemical yields for unreactive amines such as aniline (up to 91 %) compared to the methods described in the literature (6 %).[1b] The synthetic method can be carried out in less than 5 minutes from the end of bombardment and is robust.

Reaction mechanism studies suggest that 1,8-diazabicycloundec-7-ene (DBU) and an amine are required in order to trap the [^{11}C]CO_2 within the solution. The trapping method is reversible: ^{11}C is released from the mixture when the reaction mixture is heated to 60 ^{o}C. When Mitsunobu reagents are added to the reaction mixture, a phosphine oxonium ion intermediate is formed which undergoes nucleophilic attack to produce the target [^{11}C]urea.

The developed method was used in the proof-of-concept for the radiolabelling of three urea-containing target molecules. These molecules had different structural features including aliphatic, aromatic and benzylic amines and were designed as potential mGluR1 radiotracers. Design parameters for the molecules predicted good biological activity and low non-specific binding (radiotracers have a CHI_log$D_{7.4}$ and Log K_{AIM} value that is in the range of 1 – 3). All of the molecules were successfully radiolabelled with an isolated radiochemical yield of 8.2 % ± 4 based on the starting [^{11}C]CO_2 (uncorrected for decay), > 95 % radiochemical purity, total synthesis time of 21 minutes from the end of bombardment (including purification) and specific activity of 2 ± 1.8 GBq/µmol. The experiments were performed with short cyclotron bombardment times, so the low specific activity can be improved by increasing the cyclotron bombardment time from 1 minute to 50 minutes. The amount of target compounds produced was in the range of 0.2 – 0.9 µmol. It is estimated for an extended ^{11}C target bombardment that specific activities in the range of 25 – 50 GBq/µmol are easily achievable. The radiolabelled candidate's binding to mGluR1 receptors are currently being evaluated using autoradiography and homogenate binding assays.

It has been shown that in some cases, similar reaction conditions can be used for the synthesis of ureas and carbamates.[1b, 2] The method for the synthesis of [^{11}C]ureas was used for radiolabelling Zopiclone, a carbonate-containing compound that binds to GABA receptors. Reaction optimisation was required in order to obtain a RCY of 28 % (determined by HPLC). Purification and *in vitro* studies to determine affinity and selectivity are in progress.

5.2 Future work

5.2.1.mGluR1 radiotracer development

Purification

HPLC was chosen as the purification method for the radiolabelling reactions. Isolated compounds with a radiochemical purity of > 95 % were obtained for the potential mGluR1 radiotracers which is usually suitable for *in vivo* and *in vitro* imaging applications. However, small amounts of non-radioactive impurities were observed on the UV-HPLC of the isolated compound. Although these unknown impurities are only present in small quantities and may not affect the biological studies, highly pure radiotracers are important to obtain reliable results. Water and methanol were used as the HPLC solvents in the described experiments. Choosing different HPLC eluents, buffers and columns might improve the efficiency of the existing purification method. Solid-phase extraction (SPE) might also be a method to increase the chemical purity further.

Specific activity

A specific activity of 2 ± 1.8 GBq/µmol was obtained when the potential mGluR1 radiotracers were radiolabelled in chapter 4. The specific activity of the compounds are relatively low compared to the desired specific activity (> 50 GBq/µmol). There are several ways that the specific activity could be increased:

1. As the mass of the radiolabelled compounds was suitable for *in vivo* imaging (10 – 40 µmol), increasing the cyclotron bombardment time from 1 minute to 50 minutes will increase the specific activity. It is estimated that this would result in specific activities of 30 – 50 GBq/µmol, a similar specific activity value routinely obtained for other 11C compounds in our laboratory.

2. Automating the labelling procedure. One of the main disadvantages of using [^{11}C]CO_2 directly is the potential for isotopic dilution from

atmospheric CO_2. Developing an automated system may reduce isotopic dilution from atmospheric CO_2 and hence, increase the specific activity.

The development of an automated system for direct [^{11}C]CO_2 labelling is currently in progress (Figure 5.1).

[^{11}C]CO_2 is delivered into the automated system in a stream of helium gas. The gas passes through valves 1 (Figure 1) and bubble into the reaction mixture. Any gases that are not trapped within the reaction mixture will escape through valve 2 into a waste bag. The reaction mixture is heated at 50 ^{o}C for a minute and the Mitsunobu reagents are added to the reaction mixture *via* valve 2. The reaction mixture is heated for a further minute before being transferred to a HPLC column *via* valves 3. The HPLC fraction containing the pure compound will be sent through valves 4, and collected. Nitrogen gas will be used to transfer reagents to minimise atmospheric CO_2 contamination.

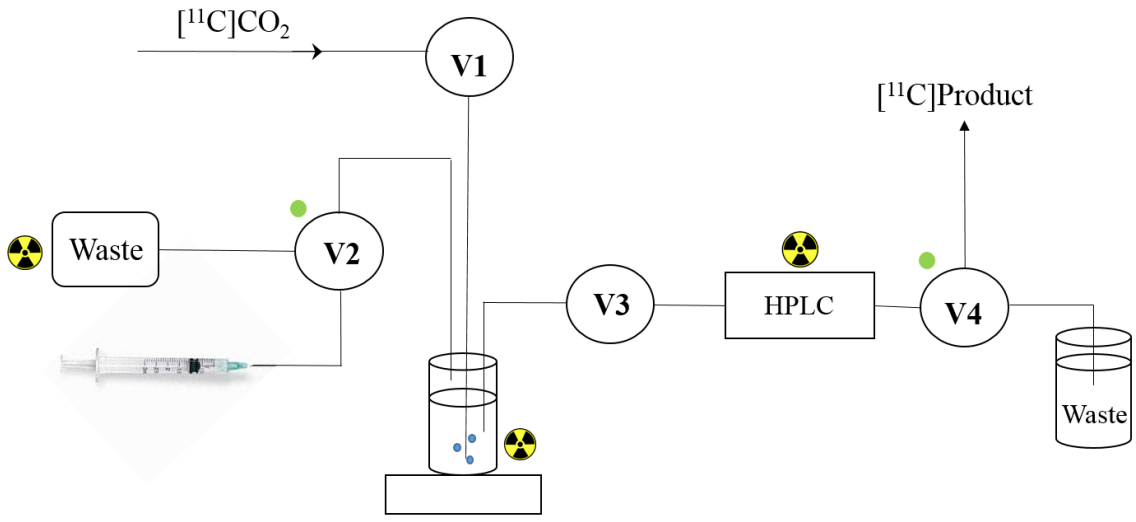

Figure 5.1. Schematic diagram of the proposed automated system.

Non-specific binding

In vitro autoradiography is an experimental technique that is used to estimate NSB. Autoradiography experiments will be carried out using the tracers radiolabelled in chapter 4. The experiments will determine whether the compounds specifically bind to mGluR1 receptors.

Male Wistar rat tissue sections will be used during the autoradiography experimental procedure. Tissue sections will be prepared by isolating the brain from a rat and rapidly freezing it in isopentane (- 40 ^{o}C) and stored at - 80 ^{o}C until required. The rat brain will be sectioned using cryostat in the sagittal plane (20 µm thickness) and will be thaw-mounted on superfrost glass slides. The slides will be stored in – 80 ^{o}C until required for use.

Initially, autoradiography studies will be performed using different radiotracer concentrations and different incubation times. Once an optimal time and concentration is determined, competition binding studies to calculate NSB will be carried out. In competition binding experiments, the specific binding of a radiotracer will be determined in the presence of a competing unlabelled compound. An unlabelled compound with high affinity for mGluR1 should be chosen for use in competition binding studies.

Affinity

Appropriate affinity is one of the essential design and test parameters that must be considered during radiotracer development. The most promising *in vivo* mGluR1 radiotracers (e.g. [^{11}C]ITMM and [^{11}C]MMTP) have K_i values < 15 nM. mGluR1 are predominantly found in the cerebellum, which can be homogenised mechanically in buffer and used to determine the K_i value of the test compounds.

Binding studies will be performed using non-radioactive candidate compounds and a known selective mGluR1 tritium labelled compound ([^{3}H]YM-202074).

5.2.2. [^{11}C]CO_2 method development

As previously mentioned in this thesis, there are many traditional organic syntheses that incorporate CO_2 into target structures. These methods can be used as a starting point to develop [^{11}C]CO_2 radiolabelling methodologies.

Carboxylic acids are found in a plethora of biologically active molecules and although there is an existing method to radiolabel carboxylic acids using [^{11}C]CO_2, it requires the use of boronic esters (Scheme 5.1).[1a]

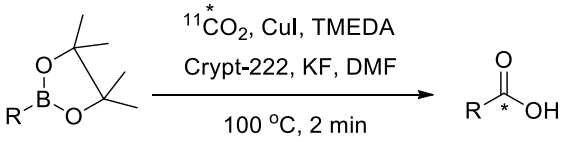

Scheme 5.1: The developed method to radiolabel carboxylic acids with [^{11}C]CO_2

Developing methods that avoid the requirement for boronic esters would be attractive. Unlike boronic esters, organohalides are widely commercially available, therefore, developing methods that carboxylate halides are of interest. We propose a simple methodology[3] that uses nickel (II) and [^{11}C]CO_2 directly from the cyclotron to radiolabel organohalides (Scheme 5.2).

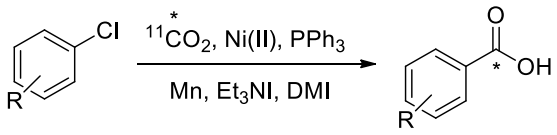

Scheme 5.2. The proposed method for the synthesis of [^{11}C]carboxylic acids using [^{11}C]CO_2

Results from this project are not covered in this thesis however, preliminary results indicate that [^{11}C]CO_2 is not trapped within the reaction mixture. Future work will include screening the reaction mixture with various trapping reagents such as DBU, BEMP and tetramethylethylenediamine. Once a high trapping efficiency is achieved, experiments will then be performed in several polar solvents with the aim to identify the best solvent for the reaction. Reactions will also be performed at different temperatures, times and reagent concentrations as part of reaction optimisation.

5.3 References

[1] a) P. J. Riss, S. Lu, S. Telu, F. I. Aigbirhio, V. W. Pike, *Angewandte Chemie International Edition* 2012, 51, 2698-2702; b) A. A. Wilson, A. Garcia, S. Houle, O. Sadovski, N. Vasdev, *Chemistry – A European Journal* 2011, 17, 259-264; c) A. K. Haji Dheere, N. Yusuf, A. Gee, *Chemical Communications* 2013, 49, 8193-8195; d) A. K. H. Dheere, A. Gee, J. Label. Compd. Radiopharm. 2013, 56, S90-S90; e) J. M. Hooker, A. T. Reibel, S. M. Hill, M. J. Schueller, J. S. Fowler, *Angewandte Chemie International Edition* 2009, 48, 3482-3485; f) B. H. Rotstein, S. H. Liang, J. P. Holland, T. L. Collier, J. M. Hooker, A. A. Wilson, N. Vasdev, *Chemical Communications* 2013, 49, 5621-5629.

[2] R. N. Salvatore, S. I. Shin, A. S. Nagle, K. W. Jung, *Journal of Organic Chemistry* 2001, 66, 1035-1037.

[3] T. Fujihara, K. Nogi, T. Xu, J. Terao, Y. Tsuji, *Journal of the American Chemical Society* 2012, 134, 9106-9109.